COMPUTED TOMOGRAPHY TECHNIQUE FOR THE MEASUREMENT OF BONE DEFECTS ADJACENT TO UNCEMENTED ACETABULAR COMPONENTS OF TOTAL HIP REPLACEMENT

DEVELOPMENT, VALIDATION AND CLINICAL APPLICATION

Roumen Botev Stamenkov, MD (Sofia)

Discipline of Orthopaedics and Trauma

The University of Adelaide

Thesis submitted for the degree of Master of Surgery

In The University of Adelaide

2009

Table of Contents

ABSTRACT

This thesis describes work, the aim of which was to develop a computed tomography (CT) technique that provides accurate and reliable volumetric measurement of bone defects adjacent to uncemented metal-backed acetabular components of total hip replacement (THR).

Periprosthetic osteolysis (PO) around THR is a major clinical problem in the mid-to long term post-operative period. Some implants remain well fixed in the presence of significant bone loss, and the hips may also be asymptomatic. However, undetected, the PO can lead to dramatic implant failure, or periprosthetic fracture, requiring complex and expensive revision surgery, with associated morbidity. Clinical assessment of THR for PO has relied on plain radiographs. However, numerous studies have shown that there are major limitations of this method in detecting the presence and extent of osteolysis and the volume of the defects cannot be quantified. Therefore, clinical management decisions regarding the need to revise prostheses for PO have been based on this unreliable diagnostic tool. Until recently, the use of CT to detect and measure defects was not effective because of the resulting artifact from the metallic components of the THR prostheses.

The studies described in this thesis represent the development, validation and the clinical application of a CT technique for quantification of acetabular periprosthetic osteolysis after THR.

In the first in-vitro validation study, a CT protocol was developed using a conventional CT scanner with limited CT scale (up to 4,000 Hounsfield units [HU]). The CT operating conditions were determined that enabled volumetric measurements that were accurate to within 96% for small and large defects and precise to greater than 98% for small and large defects. Since the ilium is the most commonly affected site by PO, and is an area almost free of metallic artifact, this technique is applicable for use with conventional CT scanners with limited CT scale.

In the second in-vitro validation study, a CT protocol was developed to use a multi-slice spiral CT scanner with an extended CT scale (up to 40,000 HU) for the measurement of acetabular periprosthetic bone defects. This technique enabled volumetric measurements of bone defects in all acetabular and periacetabular areas.

In the third study, the clinical application of the developed CT technique was investigated in two sub-studies.

The aim of the first clinical study was to determine, using quantitative CT, the distribution, volume and rate of progression of PO lesions around 46 cementless THR prostheses in 33 patients. The findings showed that, in the long term, there were differences in the distribution of osteolytic lesions between different designs of cementless acetabular components. In particular, osteolysis commonly involved sites of access of the joint fluid- the peripheral region of the components, where prosthesis fixation is important, and fixation screw holes.

The aim of the second clinical study was to use quantitative CT to determine the progression of osteolysis and the factors that may associate with it, including component migration, liner polyethylene wear, and patient variables, in 30 patients with 38 cementless acetabular components. The data provided the first reliable information on the progression of osteolytic lesions around uncemented THR prostheses and suggested that, for THR, the rate of polyethylene wear is a strong predictor of PO progression.

The results from in-vitro studies and the findings from the clinical studies suggest that the use of this CT technique allows investigation of the natural history of osteolytic lesions, and will enhance preoperative planning, improve monitoring of THR patients, and enable measurement of the outcomes of new ways to manage PO.

Declaration

NAME: ROUMEN BOTEV STANEKOV PROGRAM: MASTERS BY RESEARCH

This work contains no material which has been accepted for the award of any other degree or diploma in any university or other tertiary institution and, to the best of my knowledge and belief, contains no material previously published or written by another person, except where due reference has been made in the text.

I give consent to this copy of my thesis, when deposited in the University Library, being made available for loan and photocopying, subject to the provisions of the Copyright Act 1968.

I also give permission for the digital version of my thesis to be made available on the web, via the University's digital research repository, the Library catalogue, the Australasian Digital Theses Program (ADTP) and also through web search engines, unless permission has been granted by the University to restrict access for a period of time.

SIGNATURE:

DATE: 09/10/2009

ACKNOWLEDGMENTS

I would like to acknowledge the help I received from the following staff:

Professor Donald Howie, who gave me the unique chance to work on this interesting and challenging area of orthopaedic research. He also gave me a great number of English grammar lessons and taught me how to be better organised.

Professor David Findlay, an uncompromising editor, who gave me inspiration, motivation and valuable advice.

Ms Margaret McGee, senior medical scientist, for her understanding, endless support and help with the study design and statistics.

Dr Oksana Holubowycz, postgraduate coordinator, who provided me with valuable information on statistics, and organised my attendance at various courses, including the Integrated Bridging Program at the University of Adelaide.

Mrs Susan Neale, research officer, for her help with statistical issues, and hard work as a second observer in the in-vitro validation study.

Mr Stuart Callary, research assistant, for his precise and hard work as a third observer in the in-vitro validation study.

Dr James Taylor, head of Department of Radiology, Royal Adelaide Hospital for providing great administrative and technical support.

Mr George Kourlis, senior radiographer, Royal Adelaide Hospital, for special technical advice, and help with the development of CT protocols.

Perrett Imaging Centre staff at the Calvary and Memorial Hospitals, Adelaide, SA, for their collaboration in this study.

Ms Michelle Koarlet, senior radiographer for her enthusiastic work in the development of CT protocols.

Mr Angelo Carbone, technical officer for his help with instruments and specimen delivery.

Department of Orthopaedics and Trauma staff at the Royal Adelaide Hospital for their support provided to the CT program.

The staff of the Department of Radiology, Royal Adelaide Hospital for their hospitality.

Mrs Margaret Cargill and Mrs Karen Adams from the Integrated Bridging Program, University of Adelaide for teaching me how to write scientific papers.

And last, but not the least, I thank my wife Maria and our son Stefan for giving me love and inspiration.

Dedication

To my family for their endless love, understanding and support.

PUBLICATIONS ARISING

The work of this thesis has resulted in the publication of the following papers:

PUBLISHED PAPERS

1. **Stamenkov R,** Howie D, Taylor J, Findlay D, McGee M, Kourlis G, Carbone A, Burwell M. Measurement of bone defects adjacent to acetabular components of hip replacement. Clin Orthop Relat Res 412: 117-124, 2003.

2. Holding C, Findlay D, **Stamenkov R**, Neale S, Helen L, Dharmapatni A, Callary S, Shrestha K, Atkins G, Howie D, Haynes D. The correlation of RANK, RANKL and TNFα expression with bone loss volume and polyethylene wear debris around hip implants. Biomaterials 27 (30): 5212-5219, 2006.

3. Howie D, Neale S, **Stamenkov R**, McGee M, Taylor D, Findlay D. Progression of acetabular periprosthetic osteolytic lesions measured with computed tomography. J Bone Joint Surg 89-A: 1818-1825, 2007.

ARTICLES IN PRESS

1. **Stamenkov R,** Howie D, Neale S, McGee M, Taylor D, Findlay D. Distribution of periacetabular osteolytic lesions varies according to component design. J Arthroplasty, Article in Press, 2009.

ABBREVIATIONS

AP	Antero-Posterior
ARPANSA	Australian Radiology Protection and Nuclear Safety Agency
BMD	Bone Mineral Density
CoCr	Cobalt Chrome
CT	Computed Tomography
$CTDI_w$	Weighted Computed Tomography Dose Index
CV	Coefficient of Variation
DEXA	Dual Energy X-ray Absorptiometry
DICOM	Digital Imaging and Communication in Medicine
DLP	Dose-Length Product
EBRA	Ein Bild Roentgen Analyse
FOV	Field Of View
HHS	Harris Hip Score
HU	Hounsfield Unit
ICRP	International Commission on Radiological Protection
ICC	Intra-class Correlation Coefficient
JR	Joint Replacement
kV	Kilovolts
MMP-1	Matrix Metalloprotease
mAs	Milliamperes
mGy	Milligray
MRI	Magnetic Resonance Imaging
mSv	Millisieverts
OPG	Osteoprotegerin
PO	Periprosthetic Osteolysis

PE	Polyethylene
PMMA	Polymethylmethacrylate
ROI	Region of Interest
RSA	Radiostereophotogrametric Analysis
SD	Standard Deviation
THR	Total Hip Replacement
TKR	Total Knee Replacement
TNF	Tumour Necrosis Factor
TNFα	Tumor Necrosis Factor α

LIST OF FIGURES

LIST OF TABLES

Chapter 1

The Clinical Problem of Periprosthetic Osteolysis: A Literature Review

1.1 Introduction

Total hip replacement (THR) is a highly successful and widely utilised procedure for treatment of the symptomatic hip joint in individuals suffering from conditions such as osteoarthritis and rheumatoid arthritis. The aim of THR is to eliminate pain and to re-establish normal hip mobility and function in individuals who would otherwise be substantially disabled. THR is an operation designed to replace the damaged hip joint with a cup inserted into the acetabulum to provide a bearing surface and a stem attached to a ball inserted into the femur to replace the head of the femur. There are many makes and models of these prostheses, made of a number of different materials and with the acetabular and femoral components designed to attach to bone with or without the use of cement. The most commonly used bearing combinations in THR today are metal or ceramic “heads” against cup liners manufactured from ultra high molecular weight polyethylene (PE).

THR greatly improves quality of life and is in the short to medium term a cost-effective intervention in end-stage arthritis (Lapaucis et al., 1993). Joint replacement (JR) is one of the largest single items of recurrent health services expenditure, accounting for about 1.4% of all Australian health dollars. Approximately 65,000 JR were under taken in Australia in the 2006/2007 financial year, with acute care costs of nearly $1 billion annually (AOA NJRR, Annual Report. Adelaide: AOA; 2008). The number of primary JR is increasing, primarily because of increased life expectancy and expectation of continued activity within ageing Western populations.

Despite the success of JR, long-term failure of the THR, leading to the need for revision surgery is a concern. The published results suggest that for most THR

prosthesis designs, the incidence of revision is about 10% at ten years (Swedish Hip Arthroplasty Register, Annual Report, 2006) (Fig.1.1). Some designs of THR demonstrate good results at five years but may develop a high failure rate by ten years (Malchau et al., 2002).

According to the Australian Orthopaedic Association National Joint Replacement Registry, 32.092 hip replacements were performed in Australia in the financial year ending June 2007, with the number increasing between 5%-10% each year for the past 10 years (Graves et al., 2008). The number of hip joint replacements in 2007 was 19.8% higher than 2003 (AOA NJRR Annual Report 2008). Approximately 75% of hip replacements in Australia are THR (the remainder are partial, largely for fractures), the majority of which were 'standard' metal-on-polyethylene design (AOA NJRR Annual Report 2008). It is estimated that 20-24% of the patients with THR will require THR revision surgery during the life of their implants. The eventual failure of total hip and other arthroplasties is of significant concern. Younger, more active individuals are now receiving JR surgery to improve their quality of life. This, combined with the fact that life expectancy is increasing, means that the number of implants that need to be replaced will become an escalating health issue, with major financial impact upon our health budget. The current average acute cost of a revision THR is $15000-$25000, which does not include rehabilitation and other costs. It is now vital that we obtain better understanding of the causes of implant failure in order to extend the life of implants.

The known causes of implant failure include patient factors, such as infection and fracture, and additional factors, such as implant and fixation failure and poor surgical technique. Stress shielding can also result in significant loss of bone from around prostheses, largely in the early post-operative period.

Incidence of Revision THR

Fig.1.1 Incidence of revision THR (Swedish Hip Arthroplasty Register, Annual Report 2006).

The National Joint Replacement Registry identified aseptic periprosthetic bone loss as the most common reason for revision surgery (Graves et al., 2004). Periprosthetic bone loss, or osteolysis, is an important mode of implant failure (Harris, 1995). It reduces bone stock around prostheses, which can make revision of joint implants a difficult clinical problem, with complicated and expensive surgery, frequently associated with considerable patient morbidity, and even mortality. There is convincing evidence that Periprosthetic Osteolysis (PO) is associated with wear particles liberated from the bearing surfaces of the prosthesis (Howie, 1990) that stimulate a chronic cellular response dominated by macrophages. Aggressive granulomatous lesions, consisting of large numbers of macrophages that have engulfed wear particles, are often associated with the ingrowth of a synovial-like membrane at the bone-cement or bone-prosthesis interface in loose implants (Santavirta et al., 1990). Macrophages are also thought to participate in osteolysis by producing pro-inflammatory mediators that enhance osteoclast formation. Moreover, osteoclasts arise from cells of the monocyte/macrophage lineage (Quinn et al., 1998) and cells isolated from revision tissue readily form osteoclast-like cells capable of resorbing bone in culture.

Osteolysis is a recognized consequence of uncemented THR (Nayak, 1996). This has been well documented on the femoral side (Xenos et al., 1999, Bono et al., 1994, Burt et al., 1998, Engh et al., 2000) and is increasingly being observed in peri-acetabular sites. Various studies have cited the prevalence of pelvic osteolysis to be 7% to 37% (7.4% at 9 years, Berger et al., 1997), (17% at 5 years, Schmalzried et al., 1994), (37% at 9 years, Zikat et al., 1996). These studies have identified the presence of OL of the pelvis based on a single anteroposterior (AP) X-ray view. The rise in cases of pelvic osteolysis may be attributable to several factors. The now common usage of non cemented metal-backed acetabular components, many of

which have unfilled screw holes, may provide a conduit, by which debris can gain access to the underlying pelvic bone. Micromotion of the liner shell acetabular construct may accentuate this problem in components with poorly designed locking mechanisms (Smith 1996 et al., Perez et al., 1998). The use of thin (6–8 mm) or inferior PE, often in combination with a large-diameter femoral head, may also provide a source of PE debris (Bartel et al., 1986). Routine follow-up radiographic examinations are recommended by most joint reconstructive surgeons to detect problems with the THR that may not be symptomatic. The goal of this type of evaluation is to identify THR-related bone loss, which may make secondary reconstruction difficult. Bone loss secondary to pelvic osteolysis is less commonly detected because, depending on the site, a significant amount of bone must be absent for a lesion to present on radiographs. The presence of radio-opaque components in THR can make identification of early lesions even more difficult. Usual follow-up radiographs consist of an AP pelvic and a lateral view of the involved hip. In contrast to femoral osteolysis, peri-acetabular pelvic osteolysis is not well defined on a single AP radiograph of the pelvis. Lateral radiographs of the hip frequently do not give specific information about the pelvis unless taken in a specific fashion.

The presence and treatment of OL of the pelvis has been reported by various authors (Schmalzried et al., 1994, Maloney et al., 1997, Fowble et al., 1997, Maloney et al., 1993, Hozack et al., 1996). Before an effective treatment protocol can be established, the pelvic lesions first must be identified and graded as to their degree of involvement, based on extent and anatomic location. As mentioned, until recently, plain radiographs have been the most common method for the detection of acetabular osteolysis. However, based on human cadaver studies, plain radiography is not sufficiently sensitive for the reliable detection and measurement of peri-acetabular osteolysis (Claus et al., 2003, Walde et al., 2005), particularly in hips with

large metal-backed cups. Even with the inclusion of multiple radiographic views, plain radiographs have been shown to underestimate significantly the extent and size of OL. This is particularly the case for small lesions and lesions in the ischium and acetabular rim (Claus et al., 2003, Puri et al., 2002). The identification of early pelvic osteolysis is essential to prevent the progression of these lesions into uncontained segmental deficiencies.

CT can reveal osteolysis that may not be detectable on plain radiographs and also CT gives much more information about the extent and anatomical localisation of the OL (Robertson et al., 1998). However, attempts to extend this application of CT to the measurement of OL adjacent to THR prostheses have been limited until recently because of the artifact produced by the metallic components and fixation screws.

This chapter will review the clinical and experimental studies that identify the current problems related to the radiographic detection and analysis of bone defects due to PO adjacent to THR components, and will review the methods of metal artifact reduction and radiation dose reduction in CT.

1.2 Periprosthetic Osteolysis: Natural History, Progression, Causes

PO is bone loss around prosthetic components and may be a significant complication of JR in the medium to long-term. It is implicated as a reason for revision in almost two-thirds of revision JR. If progressive and untreated, PO can lead to prosthetic loosening, migration of components into host bone and/or fracture of supporting bone. In contrast to osteoarthritic joints, in which the progression of the ostreoarthritis limits the use of the joint, a well-fixed and otherwise well functioning prosthetic joint may be asymptomatic. In most cases of osteolysis, even when it is progressive,

patients remain active and osteolysis may remain undiagnosed until catastrophic failure, such as fracture (Berry et al., 1999, Chatoo et al., 1998, Sanchez-Sotello et al., 2000, Berry et al., 2003). Failure of implants due to osteolysis usually requires revision of one or more of the prosthetic components. Revision THR is a complex surgical procedure, which is associated with significant morbidity and mortality. The loss of bone stock associated with, in particular, failed THR compromises the outcomes of revision THR and multiple revisions on the same joint are not uncommon, with a reduction in average survivorship of each revision procedure. Importantly, the risk of infection and joint instability is significantly increased with each revision. Often the bone loss is of a similar magnitude and complexity as that seen with osteolytic bone tumours, and requires bone grafting and expensive revision prostheses. If bone loss is too extensive, the joint may not be able to be reconstructed, leaving patients disabled and dependent on community support for the remainder of their lives.

Significant PO was thought to be associated with the use of cemented THR prostheses and more specifically the response of tissues to cement debris (Harris, 1995, Vernon-Roberts et al., 1977, Willert et al., 1989, Howie, 1990, Neale et al., 2000). However, since the introduction of cementless THR prostheses, subsequent findings confirm that similar problems can be associated with cementless prostheses as well, and some degree of osteolysis may be present in up to 30-40 percent of the cases within 10 years of the primary operation. Osteolysis may be present around either or both acetabular and femoral components. Components may remain well fixed in the presence of significant bone loss. The natural history of PO is not well understood but it has been commonly believed that once osteolysis appears, it tends to progress and may lead to implant failure (American National Institutes of Health Consensus Development Conference on Total Hip Replacement 1994).

There is now convincing evidence that osteolysis is associated with wear particles, generated from the bearing surfaces of the prosthesis (Harris et al., 1995; Vernon-Roberts et al., 1977; Willert et al., 1989; Howie et al., 1990; Neale et al., 2000). Goldring et al. (1983), Horowitz et al. (1991) and Howie et al. (1993) have described the concept that prosthesis-derived wear particles stimulate macrophages to produce inflammatory mediators, which stimulates bone resorption (Fig.1.2).

It is recognised that the predominant process is one of cytokine production in response to phagocytosis of implant wear particles, resulting in increased proliferation and differentiation of osteoclast precursors into mature osteoclasts. Several cell types observed in periprosthetic tissues, including macrophages, fibroblasts, and osteoblasts, are believed to play a role in the osteolytic process. Nevertheless, because osteolysis ultimately involves bone resorption, investigators have focused on understanding the role of the osteoclast. Recent breakthroughs in the understanding of osteoclast biology, namely the roles of the OPG/RANKL/RANK system in mediating osteoclast formation, are relevant to osteolysis. The OPG/RANKL/RANK cytokine system is the predominant, final mediator of osteoclast formation (Aubin et al., 2000). This system coordinates the interaction between osteoblasts and osteoclasts that is necessary for differentiation of preosteoclasts (monocytes and macrophages) into mature, bone resorbing osteoclasts (Fig.1.3). RANKL is a member of the TNF superfamily (Hofbauer et al., 2000) that is essential for osteoclast formation, function and survival. Osteoprotegerin (OPG), a secreted member of the TNF receptor family, is the natural antagonist of RANKL, inhibiting osteoclastogenesis by binding to RANKL and blocking its interaction with its receptor (RANK) (Hofbauer et al., 2000). Both the expression and activity of these mediators are regulated by a number of skeletally active cytokines. For example, PGE_2 and IL-1 can stimulate RANKL expression (Yasuda et al., 1998) and there is evidence (Lam et

The pathological cascade of the wear particle-mediated periprosthetic osteolysis

(Modified from D. Haynes, Discipline of Pathology, the University of Adelaide)

Fig.1.2 Diagram showing the pathological cascade of the wear particle-mediated periprosthetic osteolysis: 1. Prolonged use of the artificial joint results in wear of the bearing surfaces, especially the polyethylene liner. 2. Wear particles stimulate a chronic cellular response dominated by macrophages. 3. Macrophages produce pro-inflammatory bone-resorbing mediators that induce osteoclast formation. 4. The increased osteoclast formation stimulates resorption of bone, so called osteolysis.

(Cartoon by Susan Neale, Discipline of Orthopaedics and Trauma, the University of Adelaide)

Fig.1.3 Involvement of RANKL and RANK in wear-particle associated osteolysis.

al., 2000, Holding et al., 2006), that TNFα greatly enhances RANKL activity. It was shown that macrophages exposed to prosthetic particles secrete elevated levels of inflammatory mediators, including prostanoids, IL-1α, IL-6, TNFα, and M-CSF (Rogers et al., 1997). These mediators are present at high levels in tissues adjacent to PO obtained at revision surgery, where an accumulation of polyethylene (PE) particles was associated with a marked increase in RANK and RANKL expression (Holding et al., 2006).

Animal models of PO show efficacy of anti-resorptive agents in inhibiting progression of osteolysis. For example, bisphosphonates and anti-RANKL molecules, such as OPG or RANK-Fc are effective, the latter treatments supporting a central role for RANKL/RANK in the development of particle-mediated osteolysis. In vivo RANK signalling blockade, using the RANK-Fc, effectively prevents and ameliorates wear debris-induced osteolysis via osteoclast depletion without inhibiting osteogenesis. (Childs et al., 2002).

Howie et al. (1990) reported various tissue responses to different types of wear particles around uncemented THR. The tissue around ceramic-ceramic prostheses contained few or no particles. Tissue adjacent to metal-metal prostheses contained a large number of metal wear particles, macrophages and multinucleate giant cells. The tissues from around metal-polyethylene prostheses usually contained a great number of small and large polyethylene wear particles. It was concluded that the type of prosthesis determines the type of the particulate debris and the type of pathological responses. (Konttinen et al., 2005, Takagi et al., 2001, Kim et al., 2001).

The type, size and the number of wear particles also determine the type and severity of tissue response. Metal particles are in the range from 0.3 microns to 2 microns. PE wear particles released from hip articulations are from 2 to 14 microns (Lee et al., 1992). Wear of early design metal-on-metal implants was sometimes associated with PO, and it has been reported that metal particles stimulate pro-inflammatory responses in cells in culture (Rogers et al., 1997). However, it is generally acknowledged that wear of PE components of metal on PE articulations and the associated osteolysis is a major problem (Vernon-Roberts et al., 1977; Willert et al., 1989) and analyses of retrieved metal-on-polyethylene implants and surrounding periprosthetic tissues have shown a strong correlation between PE wear and PO (Kadoya et al., 1998; Wan et al., 1996; Oparaugo et al., 2001). Moreover, correlations were found between PO and the number of PE particles, but not other particles, in the surrounding tissues (Kadoya et al., 1998), consistent with more mild tissue responses that have been observed with metal particles in tissues retrieved from around metal-on-metal prostheses (McGee et al., 2000).

The loss of prosthetic implants can be attributed to biological, microbiological or biomechanical factors, but the causes and mechanisms involved in early aseptic loosening are still unclear. Cases, in which a single individual loses several implants, support the hypothesis that individual characteristics have an important role in the process of early aseptic loosening. However, there is little knowledge about genetic susceptibility in relation to failure of implants to integrate with the bone. Genetic polymorphisms are genetic variations that are considered biologically normal and can be found in at least 1% of the population. Polymorphism of the genes that express Matrix metalloproteases (MMPs) is associated with many diseases: development of ovarian cancer (Rasquinha et al., 2003), endometrial carcinoma (Hegemann et al., 2002), changes in tooth mineralization (De Souza et al., 2003), premature rupture of

the fetal membrane (Thompson et al., 1991) and severe periodontitis (Kanamori et al., 1999). In a clinical study of 58 patients older than 50 years, Godoy-Santos et al. (2009) found that polymorphism in the region that promotes the gene for (MMP-1) was fundamentally strong evidence for an association with failure of osseointegration of THA among nonsmokers. Homozygous 1G/1G patients are individuals who have received a genetic inheritance of 1G alleles both from their father and from their mother, and they consequently have lower expression of MMP-1. On the other hand, homozygous 2G/2G patients are individuals who only have the 2G allele in their genetic inheritance, with high synthesis of MMP-1. These two types are important for comparison with heterozygous individuals (1G/2G). The findings from this study show that 2G polymorphism in the region of the gene promoting MMP-1 is associated with early aseptic loosening of the prosthetic components. The 2G allele was observed in 20.97% of the patients without aseptic loosening but in 83.33% of the patients with a diagnosis of aseptic loosening. This finding has also been reported among patients with failure of osseointegration relating to dental implants (Santos et al., 2004). Although there are many studies correlating diseases and pathological conditions with genetic polymorphism, this is the first study to associate genetic polymorphism and THA.

1.2.1 Acetabular periprosthetic osteolysis

The presence and treatment of OL of the pelvis has been reported by various authors (Schmalzried et al., 1994, Maloney et al., 1997, Fowble et al., 1997, Maloney et al., 1993, Hozack et al., 1996). Acetabular OL may be present near the prosthesis-bone interface margin (peri-acetabular), or occur further away from the joint in the ilium and ischium (retro-acetabular). With cementless components, the incidence of pelvic osteolysis has been reported to range from 5% to 78%, (Xenos et al., 1999, Clohisy

et al., 1999, Bono et al., 1994). Xenos et al. (1995) reported 11% femoral osteolysis and 4% acetabular osteolysis during a minimum 7 year follow up after the primary operation of 100 uncemented PCA cobalt-chrome components.

Zicat et al. (1996) described patterns of osteolysis around all-polyethylene cemented acetabular components. Twelve of 63 patients required revision of the components within 7 years of implantation. Eight of these cases had circumferential linear osteolysis (parallel to the acetabular component) and three had local “ballooning” lesions.

Soto et al. (2000) investigated the clinical and radiographic results of the Harris-Galante acetabular cups, performed in 112 patients with 127 THR. A total of 82 patients with 93 hips were available for follow-up. The mean follow-up period was 87 months (range 48-113 months). Radiographic evaluation demonstrated peri-acetabular osteolysis in 22 (24%) hips and 16 of these 22 (73%) were associated with the fixation screws. Twenty-two hips (23%) demonstrated femoral osteolysis around the stem. The prevalence of the peri-acetabular lesions has been further investigated in this thesis, using the more sensitive approach of quantitative CT.

A multicenter retrospective review by Maloney et al. (1999) was performed to analyse 1081 primary THR in 944 patients with Harris-Galante-I cementless acetabular component with screw fixation. The follow-up period was a minimum of five years. Acetabular osteolysis was seen in 25 patients (2.3%). A subgroup of patients was reanalysed at a minimum period of 10 years. Twenty-two percent of patients younger than 50 years had development of pelvic osteolysis. Only 7.8% of patients older than 50 years of age had pelvic osteolysis. Patients older than 70 years of age had no pelvic osteolysis identified. Although the numbers were small, this study clearly

suggested that younger patients had higher wear rates of the PE cup and a higher incidence of osteolysis.

Zicat et al. (1996) reviewed plain radiographs of 137 THR patients (137 hips) with porous-coated uncemented femoral components. Cemented, porous-coated acetabular components had been inserted in 63 patients and uncemented in 74 patients. Acetabular osteolysis was observed in 37% of the cemented components. The rate of acetabular osteolysis for the uncemented components was 18%. The osteolysis associated with uncemented components was localised and expansile, but not associated with loosening of the stem.

1.2.2 Femoral periprosthetic osteolysis

Femoral PO following total hip arthroplasty can be a cause of component loosening and periprosthetic fracture (Harris et al., 1995, Berry et al., 1999, Dunkan et al., 1995, Heekin et al., 1996, Lewallen et al., 1997) (Fig.1.4). The incidence of femoral osteolysis has been reported to range from 11% to 71% (11% at 7 years, Engh et al., 2000), (11% at 10 years, Burt et al., 1998), (39% at 10 years, Xenos et al., 1999), (71% at 5 years, Bono et al., 1994).

Maloney et al. (1990) reported 25 cases of focal femoral osteolysis in radiographically stable, cemented femoral implants. The interval between the operation and appearance of focal osteolysis was 40 to 168 months. The most common site for osteolysis was “Gruen” zones 2 and 3 on the antero-posterior radiograph and zones 5 and 6 on the lateral radiograph. In 15 cases (60%), the area of osteolysis corresponded to a defect in the cement mantle or an area of very thin cement. In 8 cases, from which tissue was available, histology showed a histiolytic reaction with evidence of particulate polymethylmethacrylate (PMMA). The authors considered that

Osteolysis-Related Femoral Periprosthetic Fracture

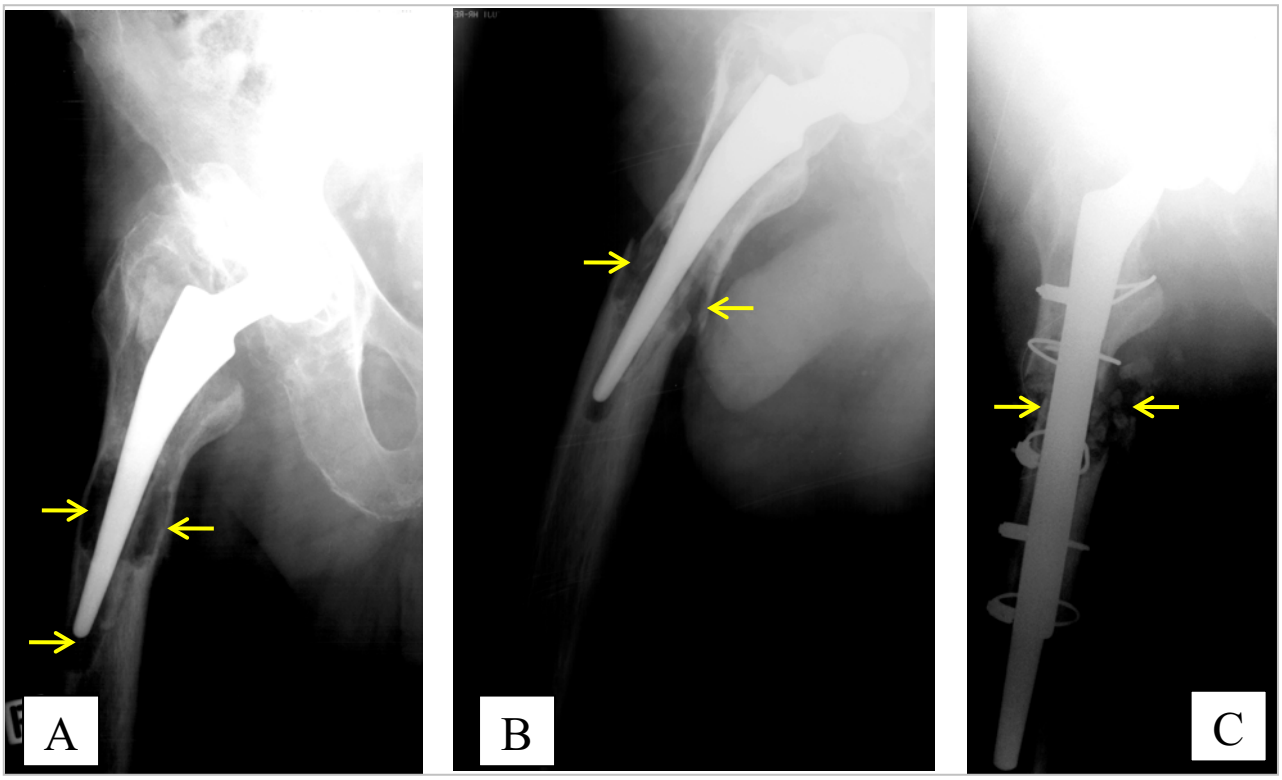

Fig.1.4 Plain radiography of right hip joint showing fracture associated with femoral periprosthetic osteolysis.

A. Extensive “scalloping” osteolysis at the bone-cement interface at Gruen zones 3, 4 and 5 (arrows).

B. Periprosthetic fracture through osteolytic lesions (arrows).

C. Complex revision surgery required long stem, plate, cables and bone grafting (arrows).

this fragmentation of the cement was the stimulus for local osteolysis in a stable cemented femoral component.

Learmonth et al. (1996) reported on 24 hips that developed femoral OL following cementless THR with Porous-Coated Anatomic (PCA) prosthesis, after a mean of 8 (6-10) years implantation. All of the hips were asymptomatic. Fifteen of the hips showed hardly any radiographic progression of the osteolysis, and in two hips the osteolysis worsened, with significant loss of bone stock. The remaining 7 hips showed mild-to-moderate enlargement of the lesions. The authors concluded that serial radiography remains the cornerstone of the monitoring of osteolysis following cementless THR, and also, that the extent of bone loss was usually far greater than indicated by radiographic examination.

Wan et al. (1996) reviewed 185 hips implanted with porous-coated titanium femoral stems. Seventy-two hips had osteolysis. Seventy-one percent of these lesions were evident on the AP radiographs. Proximal femoral osteolysis was reported to be most common and was seen in zones 2, 3, 5 and 6. Focal osteolysis was directly correlated with the amount of PE wear. The authors concluded that osteolysis is more likely when linear PE wear exceeds 150mm^3/year or when the patient is under 60 years of age.

1.3 Imaging of Osteolytic Lesions Adjacent to Metallic THR Prostheses

1.3.1 Use of plain radiography

The incidence, severity and progression of PO have been difficult to measure accurately because of the lack of adequate techniques for identifying and measuring the volume of OL. Much of the knowledge on the incidence of osteolysis and what

influences osteolysis development around THR has come from studies using plain radiographs. However, based on human cadaver studies, plain radiography is not sufficiently sensitive for the reliable detection and measurement of peri-acetabular osteolysis. The work of Jerosch et al. (1996) highlighted the fact that identification and quantification of PO using plain radiographs is often difficult, or inaccurate. These authors created experimentally different acetabular defects, according to Paprosky's classification (Paprosky et al., 1994) in 18 human cadaveric pelvis specimens. Standardised X-rays of these specimens were taken and analysed by six orthopaedic surgeons with different levels of surgical experience. The OL of the acetabular rim were correctly interpreted in only 66% of the cases. The interpretation of radiographs showing bone loss was even less accurate. A medial wall defect was correctly assessed in only 49% of cases, giving a correlation (r) of 0.60 between the real defect and the radiological estimation. While large defects were recognised in most of the cases, moderate sized defects were correctly estimated in about 50% of cases. Moderate defects included migration of the cup, which was overlooked in between 46% and 69% of the cases. Similar results were achieved in the judgement of bone loss. Only in 25% of cases was correct classification successful, according to Paprosky et al. (1994). In general, in most of the cases, the defects were underestimated. This study raises the question of whether classification systems can provide the information needed for clinical management, as the real bone loss is underestimated.

In other cadaveric studies by Claus et al. (2003), and Walde et al. (2005), plain radiography was also found not sufficiently sensitive for the reliable detection and measurement of periacetabular osteolysis, particularly in hips with large metal-backed cups.

Clinically, AP and lateral hip radiographs are the standard, by which orthopaedic surgeons preoperatively plan for THA. The use of optional radiographic views including obliques, or angled inlet and outlet views can vary between clinics. In revision THR, pain factors may preclude the use of these views. However, these additional views may add little to the evaluation of the medial acetabulum or the joint space. A high inter-observer variability for interpreting radiographic lucencies for periacetabular bone of total hip reconstructions has been reported when using plain radiographs (Carlsson et al., 1984, Brand et al., 1985).

Radiographic studies suggest that an AP view of the pelvis may grossly underestimate bone loss due to osteolysis, with a sensitivity of only 41.5% and specificity of 93% (Claus et al., 2003, Looney et al., 2002, Puri et al., 2002). Although multiple views may improve the sensitivity to approximately 74%, accurate characterisation still depends on the location of the lesion, with a very low sensitivity for lesions in the ischium and acetabular rim. There are clearly important limitations in the use of plain films for planning revision THR.

Measurement of acetabular periprosthetic osteolysis on plain radiographs

`Maloney et al. (1997) reported on 35 patients who had had a primary THR with a porous-coated uncemented acetabular component and who presented with radiological evidence of osteolysis. The acetabular component was left in situ and the lesions were debrided and bone grafted. Although the study focused on surgical techniques, Maloney et al. (1997) described their method for analysis of the lesions size. They used plain radiographs to determine the two dimensions of the lesion and calculated a two-dimensional area. The size of the lesion was determined by measuring its longest diameter and then measuring a second diameter perpendicular to the first diameter (Fig.1.5) However, because of the recognised limitation of plain

radiographs for identification and localisation of OL (Jerosch et al., 1996, Robertson et al., 1998), this technique is, at best, semi-quantitative.

Measurement of femoral periprosthetic osteolysis on plain radiographs

A similar two-dimensional method has been used to measure femoral osteolysis as well. In a clinical study by Wan et al. (1996) on femoral osteolysis in 185 hips implanted with a porous-coated titanium stem, the proximal femur on AP radiographs was divided into four zones and the lesions were analysed consecutively in each zone using planimetric measurement and mathematical formulas. The greatest width and length were measured and recorded (Fig.1.6). However, there was no ‘gold standard’ in this procedure to be used for validation.

In another clinical study, Garsia-Cimbrelo et al. (1997) analysed 63 cases of femoral OL in a series of 680 THR’s performed in 598 patients. Follow-up time averaged 16 years (range 2-22 years). Most of the cavities were seen in Gruen zones 3, 5 and 7, in decreasing order of frequency. The volume of the cavity was calculated by considering the endosteal cavity as an ellipsoid and measuring it on both the AP and true lateral views. The volume was calculated with the formula V=V1-V2 (Fig. 1.7). However, in both the acetabular and femoral regions, some parts of the periprosthetic osteolysis remains “hidden” behind the components. Furthermore, OL have a three-dimensional characteristic and their volume cannot be quantified by two-dimensional measurements. Using two-dimensional plain film radiographs, however, the amount of bone loss is often underestimated (Carlsson et al., 1984, Southwell et al., 1999, Sutherland et al., 1988, Zimlich et al., 2000).

Measurement of acetabular periprosthetic osteolysis on plain radiographs

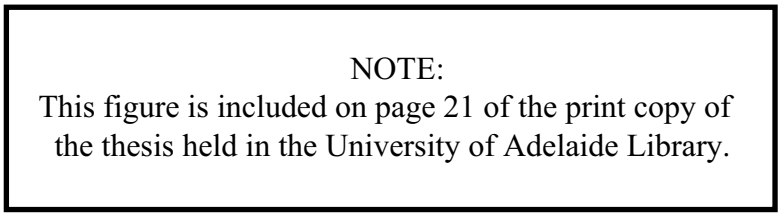

(Maloney et al., *J Bone Joint Surg* 79-A: 1628-1634, 1997)

Fig.1.5 Measurement of acetabular periprosthetic bone defect on plain radiograph. The size of the lesion is determined by measuring it's longest diameter and then measuring a second diameter perpendicular to the first diameter (Maloney et al., 1997).

Measurement of femoral periprosthetic osteolysis on plain radiography (Gruen zones)

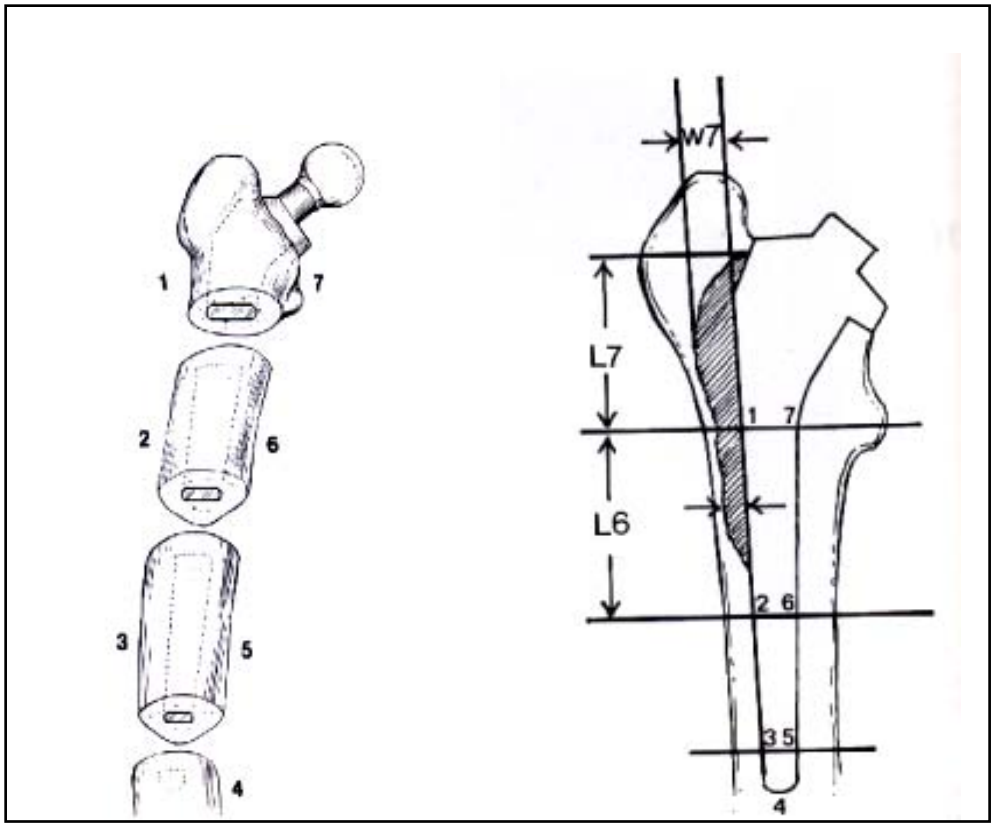

(Wan et al., *J Arthroplasty* 11: 718-725, 1996)

Fig. 1.6 Measurement of femoral periprosthetic bone defect on plain radiographs. The proximal femur is divided into four zones. The greatest width and length are measured and recorded. (Wan et al., 1996).

Measurement of femoral periprosthetic osteolysis on plain radiographs (ellipsoid)

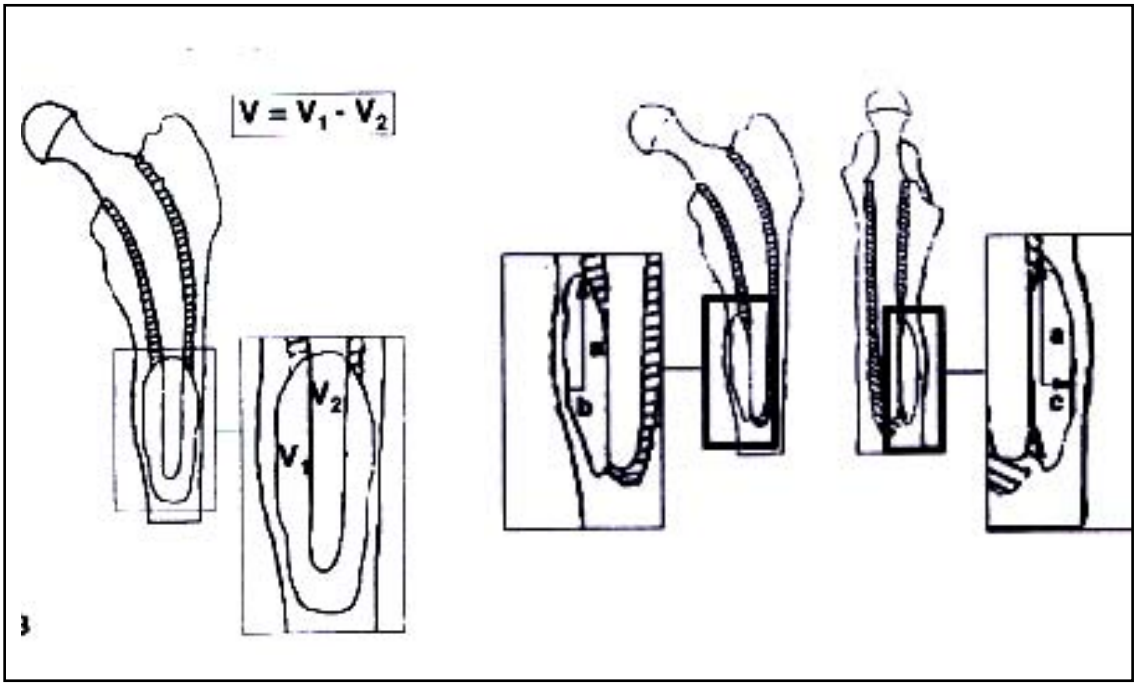

(Garcia-Cimberelo et al., *J Arthroplasty* 12: 624-634, 1997)

Fig.1.7 Measurement of femoral periprosthetic bone defect on plain radiographs. The volume is calculated by considering the endosteal cavity as an ellipsoid and measuring it on both the anteroposterior and true lateral views. The volume is calculated with the formula V=V1-V2 (Garcia-Cimberelo et al., 1997).

V_1 = Volume of endosteal cavity

V_2 = Volume of the part of the stem involved

Intra-operatively, bone loss is frequently found to exceed what was predicted by plain films, which limits the effectiveness of using radiographs in the evaluation of osteolysis for pre-operative planning. Therefore, these methods are semi-quantitative.

1.3.2 Use of magnetic resonance imaging

The application of Magnetic Resonance Imaging (MRI) to the evaluation of osteolysis following THR has not generally been considered useful due to presence of metal artifact. However, using a cadaveric model, it was demonstrated that with a modified protocol and using commercially-available soft-ware, MRI can be more accurate in the detection of pelvic osteolysis than plain film radiographs. Walde et al. (2005) compared CT, MRI, and plain radiographs in a cadaveric model of PO. MRI was 95% sensitive, 98% specific and 96% accurate. Lesion detection was not statistically dependent on lesion location (p=0,27). There was a correlation between increasing lesion size and lesion detection (p=0.02). The largest lesion that was missed by MRI analysis measured 2.8cm^3. Although MRI could detect OL, it was inferior to CT in estimating the lesion volume, which is critical in determining non-surgical type of treatment of PO. The advantage of MRI over other imaging modalities, such as CT with metal reduction protocols, is that there is no ionising radiation. However, compared to CT, it is almost twice as expensive, is available in fewer imaging facilities and the scan time required is twice as long.

1.3.3 Use of computed tomography

CT is a valuable tool for musculo-skeletal imaging. CT is a radiologic modality containing an X-ray source, detectors, and a computer-data processing system. The

essential components of a CT system include a circular scanning gantry, which houses the X-ray tube and image sensors, a table for the patient, an X-ray generator, and a computerized data-processing unit. The patient lies on the table and is placed inside the gantry. The X-ray tube is rotated 360° around the patient while the computer collects the data and formulates an axial image, or “slice”. Each cross-sectional slice represents a thickness between 0.3 and 1.5 cm of body tissue. CT provides contrast resolution that is far superior to conventional radiography. Three-dimensional reconstruction images and volumetric measurement algorithms support patient treatment management significantly.

CT is widely accepted as a sensitive imaging technique for pelvic bone. CT has been proven superior to plain radiographs for identification of acetabular anatomy (Dias et al., 1989, O’Sullivan et al., 1992), providing detail of fractures (Harley et al., 1987, Mack et al., 1982, Magid et al., 1986, Scott et al., 1987, Shirkhoda et al., 1980, Young et al., 1990), determining the extent of diastasis of the sacroiliac joints and pubic symphysis (Young et al., 1990), detecting small intra-articular bone fragments, measuring acetabular cup anteversion and retroversion (Young et al., 1990, Mian et al., 1992), and identifying musculoskeletal trauma (Hubbard et al., 1982). In cases with abnormal acetabular anatomy, it has been shown that CT can provide geometric information for preoperative evaluation for uncemented THR, which is not available from plain radiographs (Dias et al., 1989).

Orthopaedic hardware presents a challenge for sensitivity in the use of CT for detection of acetabular bone deficiencies. The CT study may be compromised to a certain degree by metal artifact.

1.3.3.1 Metal artifact reduction in CT

Mechanism of artifact generation

An x-ray beam is composed of individual photons with a range of energies. As the beam passes through an object, its mean energy increases because lower-energy photons are absorbed more rapidly than are higher-energy photons. The result is a beam-hardening artifact, which appears as dark bands or streaks near a dense object (Barret et al., 2004). Metallic hardware causes severe beam hardening and dramatically attenuates the x-ray beam. Thus, metallic hardware significantly degrades image quality to the extent that the resultant image is either incomplete or is a faulty projection of the data with reconstruction artifacts (Barret et al., 2004).

Factors that affect artifacts

The factors that may increase to or decrease the production of artifacts at multi-detector CT include:

- Metallic hardware composition and orientation,
- Image acquisition parameters (peak voltage, tube charge in milliampere-seconds, collimation, and section thickness),
- Image reconstruction parameters (reconstructed section thickness, reconstruction algorithm [kernel], and extended CT scale).

<u>Orthopedic hardware composition</u>

The specific metallic content of an implant may affect the severity of artifacts on CT images (Haramati et al, 1994). Metals have higher atomic number and density than soft tissues and bones. They attenuate X-rays in the diagnostic range much more than surrounding tissues. Titanium alloy hardware causes the least obtrusive artifact at CT imaging, whereas stainless steel implants cause significant beam attenuation and artifact (Barret et al., 2004, Haramati et al., 1994). Knowledge of the composition

of the implanted material at the time of the CT examination may be helpful, as technical parameters can then be adjusted to minimize artifacts and to spare the patient excess radiation (Barret et al., 2004).

Orientation and thickness of orthopedic hardware

In theory, the thickness of the hardware has a direct effect on the degree of x-ray beam attenuation. In other words, a smaller angle between the long axis of the gantry and the metallic implant can help reduce artifacts (Barret et al, 2004). The axis of a metallic implant in the human body cannot always be adjusted at imaging; however, to the extent that adjustment is possible, the axis of the metallic implant should be aligned so that the x-ray beam traverses the smallest possible cross-sectional area of the implant. With the optimization of imaging and reconstruction parameters, metal-related artifacts may be reduced.

Imaging parameters that affect artifacts

Peak voltage.

Technical scanning factors affect the ability of the x-ray beam to penetrate metal, and therefore they influence the production of image artifacts. Increasing the peak voltage increases the likelihood that x-rays will penetrate the metallic hardware (Barret et al., 2004,); thus, artifacts are expected to be decreased with higher peak voltage.

Tube charge.

A potential source of severe streak artifacts is photon starvation, which may occur in areas that cause high beam attenuation, such as the shoulders, or the pelvis. When the x-ray beam is travelling through a dense object, the attenuation is greatest, and an insufficient number of photons reach the detector. The resultant projections are very noisy at these tube angulations, and the reconstruction process greatly

magnifies the noise, which results in horizontal streaks on the image. If the tube charge (in milliampere-seconds) is increased for the duration of scanning, the problem of photon starvation is overcome and artifacts are reduced. However, the patient inevitably receives a higher radiation dose if the beam passes through a region with lower attenuation (Barret et al., 2004).

The automatic dose control option available on the current generation of CT scanners provides an efficient approach to tube current modulation along the z-axis and at various projection angles following the patient's anatomy. With the use of automatic exposure control, the image quality is at least as good as that with conventional scanning, and the dose is significantly reduced.

Collimation

The x-ray tube of most CT scanners may be adjusted to obtain narrow collimation (a small focal area) or wide collimation (a larger focal area). The size of the focal area, in conjunction with the image reconstruction algorithm, determines the image resolution (Barret et al., 2004). Artifacts may be reduced with the use of a narrow collimation setting. In general, thin-section acquisition is expected to help minimize artifacts by reducing the partial volume averaging effect (Wang et al., 2000). However, in some cases (e.g., a thick patient anatomy or significant bone and metal plus tissue), narrow collimation may have limited effectiveness in reducing artifacts.

Image reconstruction parameters

Section thickness.

Partial volume artifacts can best be avoided by acquiring thin sections (Barret et al., 2004, Link et al., 2000). However, during image reconstruction, thicker sections may be generated by combining several thin sections to reduce image noise. The

increased thickness of the reformatted sections dramatically affects image quality, decreasing the severity of metal-related artifacts and thereby allowing increased accuracy at image review and interpretation (Barret et al., 2004).

Reconstruction algorithm (Kernel)

Selection of an appropriate reconstruction filter may play a critical role in the appearance of a metal related artifact. The use of a standard or smooth reconstruction filter is preferred, particularly in the presence of dense metallic hardware and in patients with a large body habitus; however, the usefulness of smooth reconstruction filters is limited by a consequent reduction of spatial resolution (Barret et al., 2004).

1.3.3.2 Extended CT scale technique

The current CT scanners use a rotating fan of x-ray beams, a fixed ring of detectors, and a predetector collimator. A highly collimated x-ray beam is transmitted through the area being imaged. The tissues absorb the x-ray beam to various degrees depending on the atomic number and density of the specific tissue. The remaining, unabsorbed (unattenuated) beam passes through the tissues and is detected and processed by the computer. The CT computer software converts the x-ray beam attenuations of the tissue into a CT number (Hounsfield units) by comparing it with the attenuation of water.

Hounsfield arbitrarily assigned water the number 0, 1000 to bone and -1000 to air (Fig.1.8). Objects with beam attenuation less than that of water have an associated negative number. Conversely, substances with attenuation greater than that of water have a proportionally positive Hounsfield unit.

The extended CT scale, developed by Kalender et al. (1990), is an expansion of the Hounsfield scale from a standard maximum window of 4,000 HU to 40,000 HU (Fig.1.9). This technique makes use of the fact that metals have high linear attenuation coefficients that lie outside the normal range of reconstructed CT numbers. Most metallic implants are in the range of 8,000–20,000 HU, whereas the standard upper limit of CT scanners is 4,096 HU because of their 12-bit storage capacity. The cut off of very high CT values produces blurring and distortion of the contours of metallic implants on images (Link et al., 2000).

With a 5-mm acquired section thickness, differences in diagnostic performance with use of the standard window versus that of the extended CT scale are only moderately significant; however, differences are more significant with a 2-mm section thickness. Thus, use of the extended CT scale may be more effective with thin-section acquisitions (Link et al., 2000).

The extended CT scale is not available on every scanner, but its use when available helps reduce metal-related artifacts by allowing for a window width as large as 40,000 HU (Barret et al., 2004, Link et al., 2000).

Currently available picture archiving and communication systems offer radiologists the potential to improve the accuracy of CT image interpretation beyond the level achievable with traditional film-based display, and the unlimited CT scale available on standard monitors with these systems has reduced the usefulness of the extended CT scale (Reiner et al., 2002).

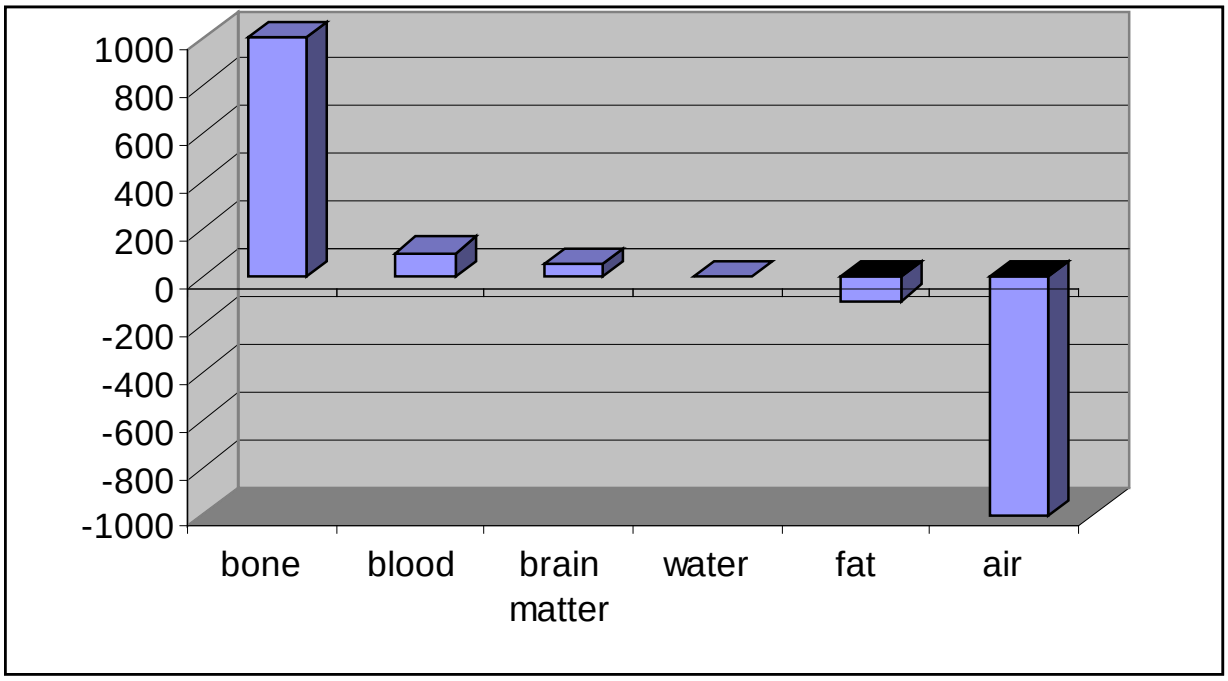

Fig.1.8 Diagram showing the attenuation of different materials in Hounsfield units (HU). Hounsfield arbitrarily assigned water the number 0. The number 1000 is assigned to bone and number -1000 to air. Objects with beam attenuation less than that of water have an associated negative number. Substances with attenuation greater than that of water have proportionally positive Hounsfield units.

Extended CT Scale Technique

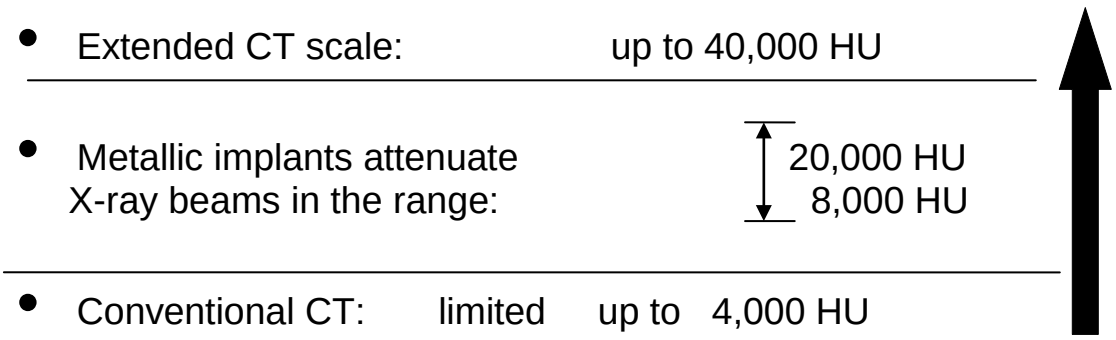

Fig.1.9 Limitations of the conventional CT in term of metal artifact suppression (Link et al., 2000).

In an experimental study Link et al., (2000) examined an extended CT scale technique as a new method to reduce artifacts due to metal implants to optimise CT imaging parameters. One hundred cobalt screws and 24 steel plates were used for osteosynthesis in 20 porcine femur specimens. All specimens were examined using 8 different CT protocols: 4 conventional and 4 spiral CT scans. Different milliamperes (mAs) and kilovolt (kV) potentials were examined. The images were analysed by three independent observers using standard window 4 000 HU and extended CT scale to 40 000 HU. Metal artifacts were significantly reduced using the extended CT scale. The highest diagnostic performance was obtained using extended CT scale and the thinnest CT slice thickness of 2mm. No significant effects of exposure dose and kilovolt potential were noted.

This technique is now available in the latest generation spiral CT scanners and was used, where indicated, in the present study of the thesis with the VOLUME ZOOM multislice SIEMENS CT scanner.

The orthopaedic implant should be positioned so that the x-ray beam traverses the metallic cross section with the smallest diameter. During image acquisition, the use of a high peak voltage (kilovolts peak), high tube charge (milliampere-seconds), narrow collimation, and thin sections helps reduce metal-related artifacts. During image reconstruction, the use of thick sections, lower kernel values (similar to the standard reconstruction algorithm), and the extended CT scale helps reduce these artifacts. With these methods, depiction of the region of interest near the metallic implant may be significantly improved.

1.3.3.3 Spiral (Helical) computed tomography

The introduction of spiral (helical) CT has revolutionized cross-sectional imaging. This technique, also called volume-acquisition CT, has made possible a data-gathering system using a continuous rotation of the X-ray source and the detectors (Fig.1.10). The advantages of this technology include shortened examination time, lower radiation dose and the ability to reconstruct overlapping cross-sectional images and greater lesion depiction. The data volume may be viewed either as conventional transaxial images or as multiplanar and three-dimensional reconstruction. Early CT was associated with high radiation doses to the patient. However, technical improvements in CT, in particular use of the spiral technique, have offered new possibilities in both diagnostics and dose reduction.

1.3.3.4 Radiation dose from computed tomography

The resulting amount of radiation from a CT procedure is very important issue for the patient's safety. (Hidajat et al., 1999). The main selectable parameters that contribute to radiation dose are tube current (mA), peak kilovoltage (kVp), pitch (table distance travelled in one 360^0 rotation) and gantry cycle time (in seconds) (Table 1.1). Most efforts at reducing radiation dose through selectable parameters are focused on tube current (mAs) and peak kilovoltage (kVp). Additional strategies include reduction of the coverage (field of view) and bismuth shielding. Bismuth breast shields have shown to reduce breast dose by 26.9% to 52.4% in the adult population depending on the thickness of the shield (Hopper et al., 1997).

The basics of CT

(*Appl Radiol*©Anderson Publishing, LTD, 2008)

Fig.1.10. The basics of CT. A motorized table moves the patient through the CT imaging system. At the same time, a source of x-ray rotates within the circular opening, and a set of x-ray detectors rotates in synchrony on the far side of the patient. The x-ray source provides a narrow, fan-shaped beam, with widths ranging from 1 to 20 mm. In conventional CT **(A)** the table is stationary during a rotation, after which it is moved along for the next slice. In spiral (helical) CT **(B)** the table moves continuously as the x-ray source and detectors rotate, producing a spiral or helical scan. The illustration shows a single row of detectors, but current machines typically have multiple rows of detectors operating side by side, so that many slices (currently up to 128) can be imaged simultaneously. The advantages of the spiral (helical) CT technology include shortened examination time, lower radiation dose and the ability to reconstruct overlapping cross-sectional images and greater lesion depiction.

Tube current (mA) must be customised for each patient, according to patient size and body weight. A protocol mA is generally defined for “standard” size patient and has to be adjusted for larger and for smaller patients to ensure consistent image quality.

Automatic Exposure Control (AEC) systems are now available from all major CT manufacturers. Each system operates on different basis, using a range of control methods (Table 1.2). Overall aim is to control the image quality and radiation dose in repeatable and predictable way, by changing the x-ray tube current (mA). AEC vary the intensity of the X-ray beam relative parameters. First, it is related to the attenuation due to the patient’s size, so that larger and thicker patient cross sections receive higher tube currents than smaller patients and thinner cross sections. This can avoid the tendency to have higher mA than needed for “average” sized patient and not to underexpose larger patients. Second, it is related to the Z-axis (along patient length) (Fig.1.11). Third, it is related to the tube rotation, which is to ensure adequate exposure to the different attenuation of the body cross sections (Fig.1.12). The tube current time product for spiral CT usually cannot be set as high as for conventional CT owing to the limited tube heat capacity; therefore, the radiation dose should be effectively lower for spiral than for conventional CT (Kalender et al., 1990). The results of older surveys that were based on investigations of dose for conventional CT therefore over represent the current situation.

Dose “savings” with AEC can be quite substantial. For the adult abdominal pelvis CT, z-axis AEC has been shown to reduce mean tube current-time product by 31.9% (range 18.8% to 87.5%) as compared with fixed tube current scanning (Kalra et al., 2004). Combined AEC (x-, y-, and z-axis modulation) in the setting of adult abdomen pelvis CT has been shown to decrease dose by 43% (Rizzo et al., 2006).

Table 1.1 CT parameters and effect on CT radiation dose

Variable	**Relationship Variable to dose***
Tube current	Direct, linear
Gantry cycle time	Direct, linear
Kilovoltage	Direct, nonlinear
Pitch	Indirect, linear

***Relationship to dose when other variables are held constant

Table 1.2. Automatic Exposure Control (AEC)

CT scanner	**Patient size** mA adjustment	**Z-axis** mA adjustment	**Rotational** mA adjustment
GE	Auto mA		Smart mA
Philips	Dose Right ACS		Dose Right DOM
Siemens	Care Dose 4D		Care Dose
Toshiba	Sure Exposure		

Tube currents (mA) are modulated on three levels:

- to the patient size,
- to the Z axis (along patient length)
- to the tube rotation.

Automatic exposure control:
Tube current (mA) adjustment in Z-axis

Appl Radiol©Anderson Publishing, LTD, 2008.

Fig.1.11.Automatic exposure control delivered by tube current adjustment along the z-axis (patient's length). Tube currents are relatively higher at the level of the shoulders and the pelvis, and lower at the level of midthorax and lower abdomen.

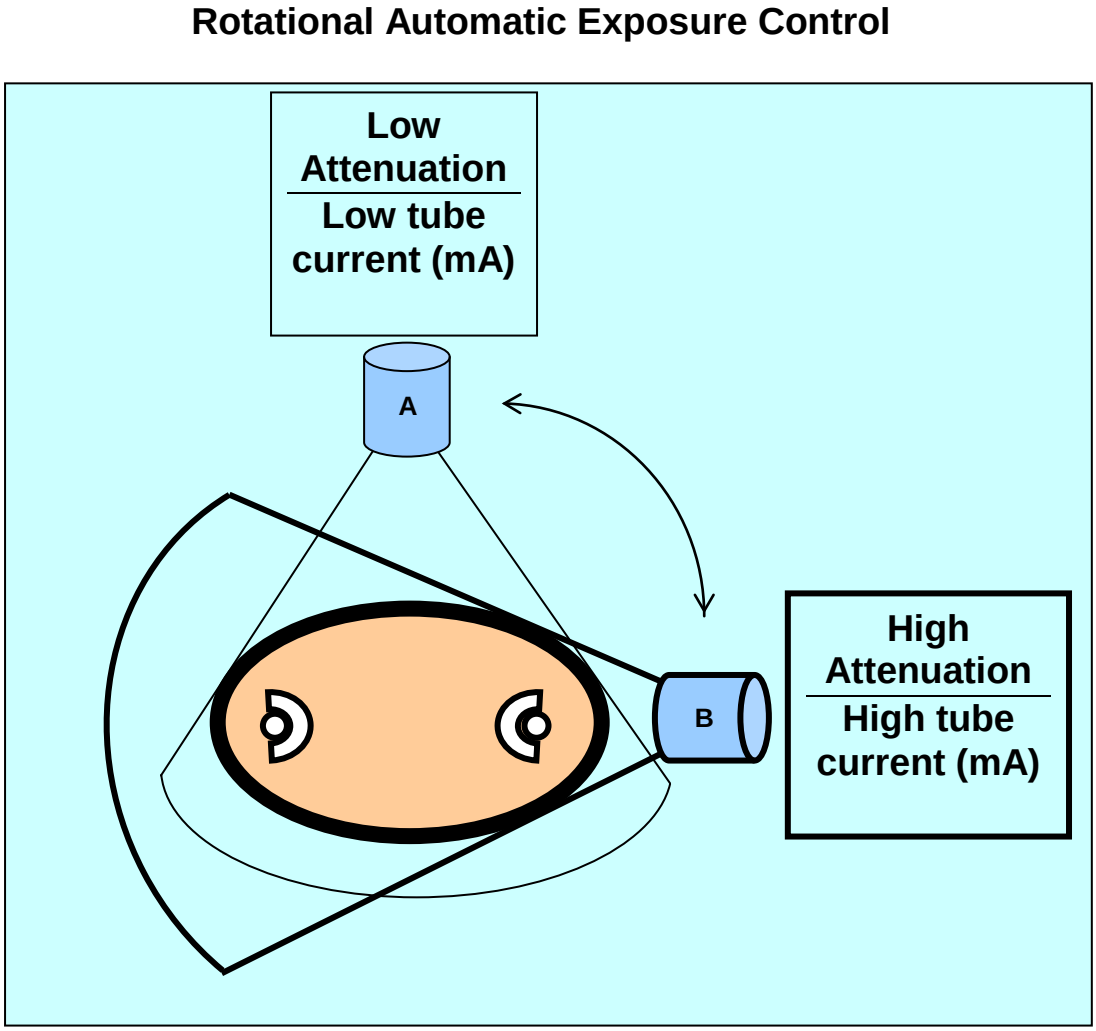

(Cartoon by Roumen Stamenkov, Discipline of Orthopaedics and Trauma, the University of Adelaide)

Fig.1.12 Diagram showing rotational Automatic Exposure Control (AEC) in Computed Tomography (CT) of the pelvis on the level of the hip joints. Tube current (mA) is adjusted relative to the patient's attenuation in different cross-sections of the body in axial plan. Lower tube current is produced in the direction of low attenuation (**A**); higher tube current is produced in the direction of high attenuation (**B**).

The AEC option available on the new generation of CT scanners provides an efficient approach to tube current modulation along the z-axis and at various projection angles following the patient's anatomy. With the use of AEC, the image quality is at least as good as that with conventional scanning, and the dose is significantly reduced.

1.5.3 Use of CT in experimental and clinical studies

With the advent of new CT techniques, using high-resolution multi-slice CT imaging and metal artifact reduction protocols, sensitive and accurate measures of complex three-dimensional OL can now be achieved. Recently, attention has turned to the detection of peri-acetabular osteolysis using CT. New generation high resolution multi-slice spiral or helical CT with metal artifact reduction techniques has recently been developed and found to provide a sensitive and accurate measure of the volume of osteolysis close to metal prostheses (Walde et al., 2005, Link et al., 2000, Puri et al., 2002, Looney et al., 2002, Kitamura et al., 2005, Schwarz et al., 2003).

Claus et al. (2004), using human cadavers, demonstrated the efficacy of using CT to localize OL surrounding noncemented acetabular components and to estimate their size. One hundred percent of lesions created in the pelvis were localized on CT; however, it was less accurate in the ischium (78%) and pubis (50%). Leung et al. (2005), in another cadaveric model, showed the increased sensitivity of CT scans over plain radiography. In addition, they found that the volume of the OL measured with CT was highly accurate.

Puri et al. (2002) reported on a similar study of forty patients (50 hips), assessed for acetabular bone loss by plain radiographs and spiral CT. Using a metal artifact

suppression protocol, CT scanning was performed from 6cm proximal to the acetabular component to a point distal to the end of the implant. Evidence of OL on these scans was compared with that on the radiographs. Two-dimensional wear analysis was performed with use of digitized radiographs, and the results were compared with loss of bone volume, as calculated from the CT scans. Acetabular osteolysis was identified on the radiographs of 16 hips and on the CT scans of 26 hips. The results showed that the minimum diameter of lesions seen on radiographs was 1.7 cm (standard deviation, 1.1). Furthermore, of hips with radiographic evidence of osteolysis, the amount of osteolysis was underestimated, as confirmed by CT scans. However, the volumetric measurement in this study was not validated and the use of a reference point 6cm superior to the acetabular component was not appropriate, as the implant could migrate. All CT scans were reviewed by surgeons and radiologists, but no inter-observer and intra-observer errors were reported.

1.4 Summary

PO around THR is a major clinical problem in the mid-to long term post-operative period. Some implants remain well fixed in the presence of significant bone loss, and the hips may also be asymptomatic. If underestimated, the PO could lead to dramatic implant failure, or periprosthetic fracture (Berry et al., 2003, Chatoo et al., 1998, Sanchez-Sotello et al., 2000), requiring expensive revision surgery with associated morbidity. Early identification, localization and measurement of these lesions using plain radiographs are not sensitive enough. The two-dimensional methods are not able to give adequate information. Without a three-dimensional understanding of the lesion, an appropriate treatment protocol for these lesions cannot be developed.

Osteolysis incidence, severity and progression have been difficult to measure accurately because of the lack, until recently, of adequate techniques for identifying

and measuring the volume of PO. Based on limited intraoperative data, it is generally accepted that plain radiography is not sufficiently sensitive for the reliable detection of and measurement of PO. Therefore, much of the knowledge on the incidence of PO and what influences PO development, gathered in studies using plain radiography, could be put into question Furthermore, clinical management decisions regarding the need to revise prostheses for PO have been based on this unreliable diagnostic tool.

Accurate diagnosis of the severity of peri-acetabular osteolysis is essential for evaluating the load-carrying capacity of the deficient acetabulum. Accurate description of the extent and location of acetabular bone stock loss is becoming increasingly important in judging the dimensions and character of bone graft, or producing custom acetabular prostheses needed to provide stability for the revised acetabulum. Segmental deficiencies may affect the prosthetic shape, size, and placement for restoration of normal joint mechanics. Severity of the cavitary deficiencies can determine adjunctive fixation technique and screw or pin placement. Inadequate or non-precise description of the acetabular deficiency can have an impact on the efficacy of surgical planning and the accuracy of retrospective studies, in which classifications of defects are made based on plain radiography. If total hip reconstructive surgery is to be performed, plain radiographs may prove inadequate for optimal pre-surgical planning.

Accurate data on the natural history of osteolysis, in terms of its location, incidence and progression over time, in concert with an understanding of the cellular mechanisms of PO, are crucial to advances in the effective clinical management of this complication and potentially its prevention. The latest achievements in the understanding of the biological mechanisms of particle-induced osteolysis could lead

to drug treatments that prevent periprosthetic bone loss. The long-term goal is to identify novel targets for therapeutic intervention and inhibition of particle-induced osteolysis. The ability to reverse or to slow the process of PO by pharmacological therapy would represent a major milestone in THR.

The CT volumetric measurement methods reported to date (Claus et al., 2003, Looney et al., 2002, Puri et al., 2002) were not validated and the accuracy of the use of CT for detection of acetabular deficiencies had not been quantified at the beginning of this thesis. There were no reports on the CT radiation dose, when new CT scanning protocols were presented in practice. The radiation dose (Faulkiner et al., 1987) is a very sensitive issue and every CT scanning protocol should follow the recommended reference levels by the International Commission on Radiological Protection (ICRP 1991) and meet the references of the Australian National Standards (ARPANSA, 2008).

At the time of performing the work described in this thesis, no reliable and validated methods for volumetric measurement of PO were available.

Therefore, the aim of this thesis was to develop a valid, accurate and reliable CT technique for the measurement and monitoring of bone defects adjacent to uncemented acetabular components of THR prosthesis that meets the references of the Australian National standards for radiological protection.

Chapter 2

Hypotheses and Study Design

2.1 Introduction

Osteolysis is a recognised consequence of uncemented THR (Nayak, 1996). The traditional clinical assessment of the THR patients for PO relies on plain radiographs. Various studies have identified the presence of osteolytic lesions to be 7% to 37% (7.4% at 9 years, Berger et al., 1997), (17% at 5 years, Schmalzried et al., 1994), (37% at 9 years, Zikat et al., 1996), based on a single anteroposterior (AP) X-ray view.

However, radiographic studies suggest that an AP view of the pelvis may grossly underestimate bone loss due to osteolysis, with a sensitivity of only 40% and specificity of around 90% (Claus et al., 2003, Looney et al., 2002, Puri et al., 2002). Although multiple views may improve the sensitivity to approximately 70%, accurate characterisation still depends on the location of the lesion, with a very low sensitivity for lesions in the ischium and acetabular rim.

Until recently, the use of CT in this area was not effective because of the resulting artifact from the metallic components of THR prostheses. Recently developed new generation high resolution multi-slice spiral CT with metal artifact reduction techniques is reported to provide more sensitive and accurate quantification of PO (Link et al., 2000, Looney et al., 2002, Puri et al., 2002, Schwarz et al., 2003, Claus et al., 2003, Walde et al., 2005, Kitamura et al., 2005).

However, at the outset of the work described herein, no experimental or clinical study had provided detailed validation of the CT volume measurement of PO in all acetabular areas. Attempts to obtain better image quality of the bone surrounding the THR prosthesis by increasing the scanning parameters may result in a high radiation dose. None of the above studies reported on the resulting radiation dose, which is a very important issue for patient safety.

2.2 Hypotheses

This thesis examined the reliability of CT scanners of two different generations for the detection and measurement of the acetabular PO following THR in two experimental *in-vitro* studies.

In the first *in-vitro* study, when a conventional CT scanner (CT scale limited to 4,000 HU) was used to measure the volume of simulated bone defects of known volume in the ilium alone in both bovine and human cadaver specimens, the hypotheses tested were:

- The accuracy, precision, intra-observer and inter-observer errors of the CT measurements is not different when a CT slice thickness of 3mm or 4mm, and a beam angle of -25^0, 0^0 or 25^0 were examined.`

In the second *in-vitro* study, when a multi-slice spiral CT scanner (extended CT scale up to 40,000 HU) was used to measure the volume of simulated bone defects in all acetabular areas in bovine specimens, the hypotheses tested were:

- The sensitivity and specificity of the detection, and the accuracy and reproducibility of the CT measurement of simulated single bone defects in all areas of the acetabulum *in-vitro* is not different.

- The accuracy and reproducibility of the CT measurement *in-vitro* of simulated bone defects in all areas of the acetabulum will be not affected by the presence of a contralateral THR prosthesis.
- The intra-observer and inter-observer errors of the CT measurement *in-vitro* of simulated bone defects in all areas of the acetabulum will not be dependent on the CT slice thickness, the size and the location of the defect.

The in-vitro validated CT technique was applied in two clinical studies.

In the first clinical study the hypothesis tested was:

- The volume, location and number of acetabular PO lesions in patients with long-term uncemented THR of two different acetabular component designs will depend on the component design.

In the second clinical study the hypothesis tested was:

- There is a linear relationship between the size and the progression in size of the osteolytic lesions adjacent to uncemented acetabular components of THR prostheses.

2.3 Aims

To test the above hypotheses, the study was designed with the following main aims:

- To develop bovine and human cadaver pelvis models of acetabular PO following THR, that could be used to examine the sensitivity and specificity of detection, and the accuracy and precision of measuring PO using CT scanners of two different generations.
- To optimize CT scanning conditions in the presence of metallic THR components.
- To develop a CT scanning protocol in accordance with the recommended reference levels by the Australian National Standards for radiation.

The specific aims were:

In the first *in-vitro* study, when a conventional CT scanner (CT scale limited to 4000 HU) was used to measure the volume of simulated bone defects of known volume in the ilium alone in both bovine and human cadaver THR models:

- To examine the effect of different CT slice thickness (3mm and 4mm) and different CT beam angle (-25^0, 0^0 or 25^0) on the accuracy, precision, intra-observer and inter-observer errors of the CT volume measurement.
- To examine the effect of the presence of a contralateral THR prosthesis on the accuracy, precision, intra-observer and inter-observer errors of the CT volume measurement.

In the second *in-vitro* study, when a multi-slice spiral CT scanner (extended CT scale up to 40,000 HU) was used to measure the volume of simulated bone defects in all acetabular areas in bovine THR models:

- To determine the volume of the smallest created and detected simulated bone defect in different pelvic areas that was detectable when titanium or cobalt-chrome THR prostheses are present, using different CT slice thicknesses.
- To examine the sensitivity and specificity of the detection, and the accuracy and reproducibility of the CT measurement of simulated single bone defects of similar size in different pelvic areas when titanium or cobalt-chrome, or both THR prostheses are present, using different CT slice thicknesses.
- To examine the sensitivity and specificity of the detection, and the accuracy and reproducibility of the CT measurement of simulated single bone defects of different size in different pelvic areas when titanium or cobalt-chrome, or both THR prostheses are present, using different CT slice thicknesses.

- To examine the sensitivity and specificity of the detection, and the accuracy and reproducibility of the CT measurement of simulated combined bone defects that involve different neighboring areas of the acetabulum, when titanium or cobalt-chrome, or both THR prostheses are present, using different CT slice thicknesses.

2.4 Study Design

The development and the validation of the CT technique were performed in two separate studies. At the time the thesis was commenced, the extended CT scale as a method for metal artifact reduction was not available in conventional CT scanners.

2.4.1 In-vitro validation using a conventional CT scanner (CT scale limited to 4,000 HU)

Therefore, the first study was to examine the accuracy and reproducibility of quantitative CT on simulated bone defects of known volume in the ilium superior (cranial) to the acetabular roof in a bovine and human cadaver models of THR. The image of the rest of the acetabular areas was still severely affected by metal artifact. This study is described in Chapter 3 of the thesis.

2.4.2 In-vitro validation using multi-slice spiral CT scanner (extended CT scale up to 40,000 HU).

The second study was to examine the accuracy and reproducibility of quantitative CT with extended CT scale technique on simulated bone defects in all acetabular and periacetabular areas in a bovine model of THR. This study is described in Chapter 4 of the thesis.

In the first study, simulated acetabular bone defects were created only in the ilium. These were measured using CT with and without the presence of THR components and the fixation screws. In the second study simulated bone defects were examined in the ilium, anterior wall, medial wall, posterior wall, pubis and ischium. Different parameters of the CT such as slice thickness, kV and mAs were examined and 3 independent observers reported on the accuracy, reliability, specificity and sensitivity of the measured volumes.

2.4.3 Clinical application.

This new, validated and quantified CT technique was used in two different clinical studies. The specific aims were as follows:

First clinical study: To examine the volume, location and number of periacetabular osteolytic lesions in patients with long-term uncemented THR of two acetabular components design: multi-hole shell with additional screw fixation and solid shell with single central hole.

Second clinical study: To determine the size and progression in size of osteolytic lesions adjacent to uncemented acetabular components of THR prostheses, to investigate their relationship with wear of the polyethylene liner, and then to examine the association between these findings and component migration and several clinical and implant-related variables.

2.5 Statistical analysis

In-vitro validation studies

CT scans were analysed three times in each instance by three different observers. Intra- and inter-observer errors were determined by calculating the correlation between observations. Intra-observer errors were calculated by a test-retest measure

(Cronbach's correlation coefficient alpha). Inter-observer errors were calculated using an intra-class correlation coefficient. SAS statistical software package (SAS System for Windows TM Release 6.12. 1989-1996, SAS Institute Inc., Cary, NC, USA).

First clinical study. Differences between the two patient cohorts, with respect to patient and implant-related variables and the distribution and size of the osteolytic lesions, were examined using Fisher Exact, Chi-square and Mann-Whitney U tests. Statistical analysis was performed using Graph Pad Prism software (V4.00 for Windows, Graph Pad Software, San Diego, California USA). Probability values less than 0.05 indicated a significant difference.

Second clinical study. Statistical analysis was performed with use of Graph Pad Prism software (version 4.00 for Windows; Graph Pad Software, San Diego, California), with the level of alpha set at 0.05. Correlation analysis was undertaken with use of the Spearman rank correlation coefficient. Associations between the size of the osteolytic lesions at the time of the initial CT scan and the rate of osteolysis progression as well as patient-related, clinical, and implant-related variables were examined with use of the Mann-Whitney U, Kruskal-Wallis, Fisher exact, or chi-square tests.

2.6 Ethical considerations

In-vitro validation studies.

Ethical approval was given by the Royal Adelaide Hospital Human Ethics Committee for the use of human cadavers, donated for medical research.

Clinical studies. All patients gave informed consent and the clinical studies were approved by the Royal Adelaide Hospital Human Ethics Review Committee.

Chapter 3

Use of Conventional CT scanner with Limited CT Scale

3.1 Introduction

CT scanning is used for preoperative planning for primary THR (Barmeir et al., 1982, Berman et al., 1987, Clark et al., 1992) and is used as a diagnostic tool to measure volumetric changes of musculoskeletal and other tumours (Wellings et al., 1994). However, attempts to extend this application of CT scanning to the measurement of osteolytic lesions around THR prostheses had, at the commencement of the work described in this thesis, been limited because of the artifact produced by the metallic components of THR or the screws used to fix the acetabular components (Link et al., 2000, Robertson et al., 1997).

As mentioned in Chapter 1, metal implants are in the range 8,000 up to 20,000 Hounsfield units (HU). To overcome the resulting metal artifact, the scanning machine needs the capability for CT scale extension to more than 20,000 HU. However, at the time when the present in-vitro validation study began (1999), the extended CT scale as a method for metal artifact reduction was not available on most of the CT scanning machines. Conventional CT scanners have had a limit of up to 4,000 HU.

It has been reported that osteolytic lesions adjacent to metal-backed acetabular components of THR most commonly occur in the ilium in association with fixation screws (Soto et al., 2000).

Therefore, the aim of the study described in this chapter was to examine the accuracy and the precision of a conventional CT scanner (Picker PQ 6000) for the

measurement of simulated bone defects of known volume in the ilium adjacent to the superior (cranial) aspect the acetabular component in the presence of fixation screws.

3.2 Methods and Materials

The availability of human pelves from cadavers was very limited and the initial experience demonstrated that the cancellous bone of the formalin-treated bones was soft and demineralised by formalin, making it impossible to create simulated bone defects with a volume smaller than 1 cm^3. Also, formalin-treated bones had far inferior radiodensity to fresh-frozen bones. Therefore, the initial development and validation of the CT scanning technique was performed using a fresh-frozen bovine hemi-pelvis containing unilateral THR prosthesis. Additional validation of the technique was done in a pelvis from a human cadaver, into which unilateral and bilateral acetabular components were inserted consecutively.

3.2.1 Bovine hemi-pelvis specimen

A fresh-frozen bovine hemi-pelvis, comparable in size to an acetabulum in a human, was defrosted from -20° C to room temperature. The bovine acetabulum was orientated in the same anatomic orientation as in the human, and the specimen was mounted in a table vice and the acetabulum was prepared. The acetabulum was reamed initially using a 44-mm outer diameter reamer, followed by 54-, 55-, 56- and 57-mm outer diameter reamers (Zimmer Inc., Warsaw, IN) to accept a 58-mm outer diameter TiAlV Trilogy fibre metal coated shell with three screw holes (Zimmer Inc.). The acetabular component was inserted into the acetabulum of the specimen in 40^o of operative Inclination and 25^o of operative anteversion (Murray et al., 1993) and

rotated so that one screw hole was superior, one screw hole was postero-superior, and one screw hole was antero-superior. A Kirshner (K) wire was placed through the superior screw hole into the ilium and orientated with its axis parallel to the longitudinal axis of the specimen. After marking the position of the cup on the reamed surface of the acetabulum, the cup was removed. A large, 40-mm deep cylindrical defect was created by drilling over the K wire with a 12-mm canulated drill. The axis of the large simulated defect was parallel to the longitudinal axis. The procedure was repeated in the postero-superior screw hole to create a small 25-mm deep cylindrical defect, orientated postero-superiorly, using a 9-mm canulated drill (Fig. 3.1). The volumes of the simulated defects were determined by filling with water and measuring three times using a 0.01-mm graduated 1-mL syringe. The acetabular component was reinserted using an impactor-positioner (Zimmer Inc.). A 30-mm long, 6.5-mm diameter TiAlVself-tapping bone screw (Zimmer Inc.) was inserted into the supero-lateral screw hole so that it engaged in 5 mm of bone distal to the created defect. A 25-mm long similar screw was inserted through a supero-medial screw hole with no created defect. A Trilogy PE liner (Zimmer Inc.) was inserted into the component. The specimen was placed into a plastic container and orientated so that its longitudinal axis was parallel to the midline of the container and its sagittal plane was perpendicular to the base of the container. The proximal aspect of the specimen was fixed to the vertical wall of the container with three screws. The ischium was rested on the base of the container and was fixed with one screw. A cementless PCA CoCr alloy femoral stem (Howmedica International, Ltd, Rutherford, NJ) and a 28-mm diameter CoCr alloy head (Howmedica International) were positioned into the liner.

Bovine hemi-pelvis THR model of periprosthetic osteolysis

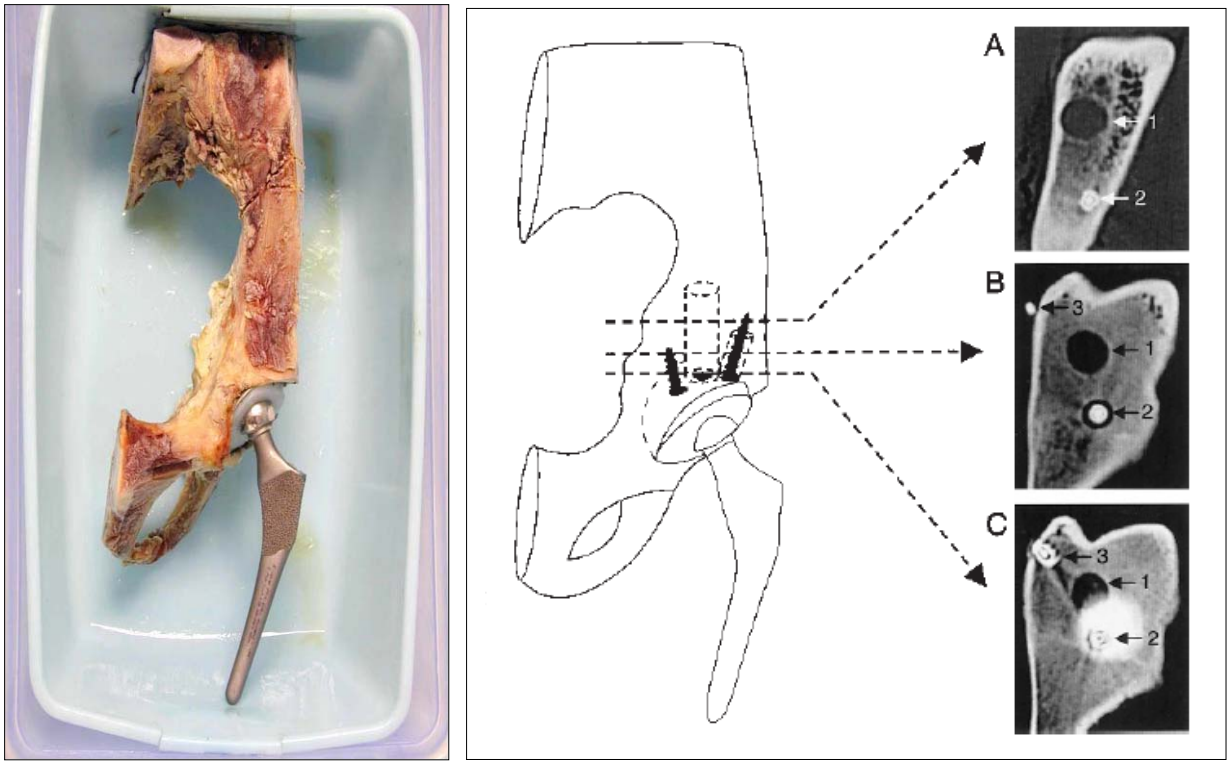

Fig. 3.1 A bovine hemipelvis total hip replacement model is shown. The diagram shows the large bone defect adjacent to the acetabular component and the small defect around a lateral fixation screw. Computed tomography scans at several levels show the following defects: **(A)** 1, large bone defect; 2, lateral screw; **(B)** 1, large bone defect; 2, bone defect around lateral screw; 3, tip of medial screw that penetrated medial cortex; and **(C)** 1, large bone defect; 2, lateral screw with artifact interference from top of acetabular component; and 3, medial screw.

3.2.2 Human cadaver pelvis specimen

An intact pelvis with L4, L5 vertebra and femoral bones was retrieved from the cadaver of a 70-year-old man. The specimen was defrosted from –20^{o} C to room temperature and the muscles and the hip capsules were removed. The right acetabulum was prepared in the same manner as that for the bovine acetabulum, except that 46-mm, 48-mm, 50-mm, and 51-mm outer diameter reamers were used consecutively.

For the human pelvis, one acetabular defect in the ilium was created (Fig. 3.2). A 52-mm outer diameter Harris-Galante-II (Zimmer Inc.) uncemented, metal–backed acetabular component was inserted in 40^{o} of operative Inclination and 25^{o} of operative anteversion (Murray et al., 1993). The component was fixed with two self-tapping TiAlV screws 6.5-mm diameter and 30-mm long (Zimmer Inc.). A polyethylene liner (Zimmer Inc.) was inserted into the component. An uncemented Versys fiber metal mid-coat femoral stem (Zimmer Inc.) was inserted into the right femur, using a standard uncemented technique. A 28-mm CoCr femoral head (Zimmer Inc.) was inserted. The pelvis was placed in a supine position so that the spinous tubercules of the sacrum and posterior superior spines of the ilium rested on the base of a container. The line joining the midpoints of the symphysis pubis and the L5 vertebra was represented as a longitudinal axis of the specimen and was orientated parallel to the midline of the container in coronal plane. The pelvis was fixed to the container using plastic ties. Both specimens were covered with tap water, which was used to simulate soft tissues during scanning.

Human cadaver pelvis THR model of periprosthetic osteolysis

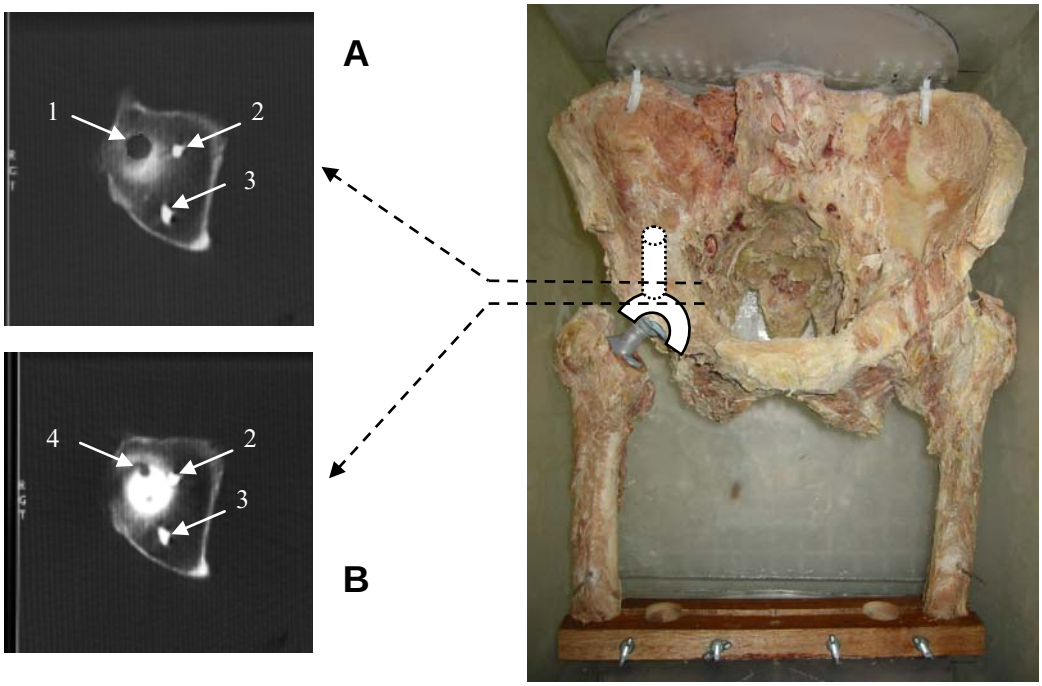

Fig.3.2 A human cadaver pelvis total hip replacement model is shown.
Computed tomography scans at two levels show:
(A) 1, large bone defect in the iliac bone;
2, medial fixation screw;
3, posterior fixation screws;
(B) 4, empty screw-hole of the acetabular component;
2, fixation screw with artefact interference from top of the acetabular component;
3, fixation screw.

To investigate the effects on CT scanning caused by a contralateral THR prosthesis, an uncemented metal-backed Trilogy acetabular component (Zimmer Inc.) and an uncemented PCA CoCr alloy femoral stem (Howmedica International, Inc., London, United Kingdom) and 28-mm CoCr head (Howmedica, International, Inc.) were inserted into the contralateral hip and the CT scans of the original study hip were repeated.

3.2.3 PICKER PQ 6000 CT scanner

CT scanning was performed using a Picker PQ6000 spiral CT (Picker International Inc., Cleveland, OH) scanner with Voxel Q FALCON metal artifact reduction software (Picker International Inc.). CT scans were taken at 120 kV and 200 mAs to maximize the resolution and contrast of the trabecular and cortical bone. To allow standardization of measurements, the top end of the sacroiliac joint was used as the anatomic reference point and scans were taken to the end of the ischium. A metal pin was inserted into the ilium of the bovine hemi-pelvis to mark the reference point.
The simulated bone defects were measured in consecutive CT slices displayed on the computer screen by tracing the inner border of the defect using a computer mouse. Volume measurement was done using algorithms coded into the commercial image-analysis software (PQ6000 Voxel Q FALCON, Picker International Inc.).

To determine the optimal CT scanning operating conditions for measuring the volume of bone defects adjacent to metal-backed acetabular components, two parameters were investigated in the bovine hemi-pelvis model. These were the angle of the CT beam, +25° (cephalad) (cranial), 0° and –25° (caudad), and the two thicknesses of CT slice routinely used in clinical practice, 3 mm and 4 mm.

Once the protocol and operating conditions were determined, the impact of metal artifact using this protocol was then examined by comparing volumetric measurements of the large defect from CT scans taken with and without the prosthesis *in situ*. The radiodensity of the bovine bone was markedly higher than that of the bone from an elderly man. The operating conditions and protocol tested in the bovine hemi-pelvis model were, therefore, investigated again using the human pelvis model implanted with unilateral THR prosthesis and containing a large superior defect adjacent to the acetabular component. To examine the interference effect of the contralateral THR prosthesis on the volumetric measurements, scans were repeated on the human pelvis after insertion of THR prosthesis on the contralateral side.

3.2.4 Statistical analysis

The accuracy of the volumetric measurements from the CT scans was determined by calculation of the percent error between the physical measurement of the simulated defects, undertaken using water and syringe and the measurements from the CT scans. Volumetric measurements from the CT scans were repeated five times in each instance by two different observers, an orthopaedic research registrar and a research officer. The reliability of the quantitative measurements was determined by calculation of the intra-observer and inter-observer errors. The intra-observer error was reported as the percent coefficient of variation and the inter-observer error was measured by the percent variance. Interferential analysis was done using analysis of variance (ANOVA) and the Fisher's least-significant-difference test. Data summary statistics were calculated using Microsoft Excel and interferential analyses were done using the SAS statistical software package (SAS® System for Windows™ Release

6.12 1989-1996, SAS Institute Inc., Cary, NC). A probability value of less than 0.05 was considered to indicate statistical significance.

3.3 Results

Bovine acetabulum study

The actual volume of the large simulated acetabular defect adjacent to the component, measured using a syringe and water, was 5.03 mL (standard deviation, 0.04 mL). The actual volume of the small defect adjacent to the lateral screw was 1.24 mL (standard deviation, 0.02 mL).

The estimated volumes of the large simulated defect measured from each of the CT scans taken using the different operating conditions are shown in Fig. 3.3. There was a significant effect of beam angle and slice thickness on the volumetric measurement of the large defect ($p < 0.0001$). The most accurate measurement of defect volume was obtained using a beam angle of 0° and a slice thickness of 3 mm (error, -1.7%). The volume was significantly greater than the volumes measured from scans taken with a beam angle of +25° and -25° ($p < 0.0001$) and significantly greater, and closer to the true volume, than that determined from scans taken using a slice thickness of 4 mm and a beam angle of 0° ($p < 0.0001$). The intra-observer error and inter-observer error of the volume measurements of the large defect were 2.27% and -2.73%, respectively, using the operating parameters of 3-mm slice thickness and a beam angle of 0°. Using a scan thickness of 3mm and a beam angle of 0 degrees, there was no significant difference between the volumes measured from the scans taken with and without the prosthesis *in situ* ($p = 0.944$).

The effect of the CT beam angle and slice thickness on the CT volume of a large bone defect in a bovine THR model.

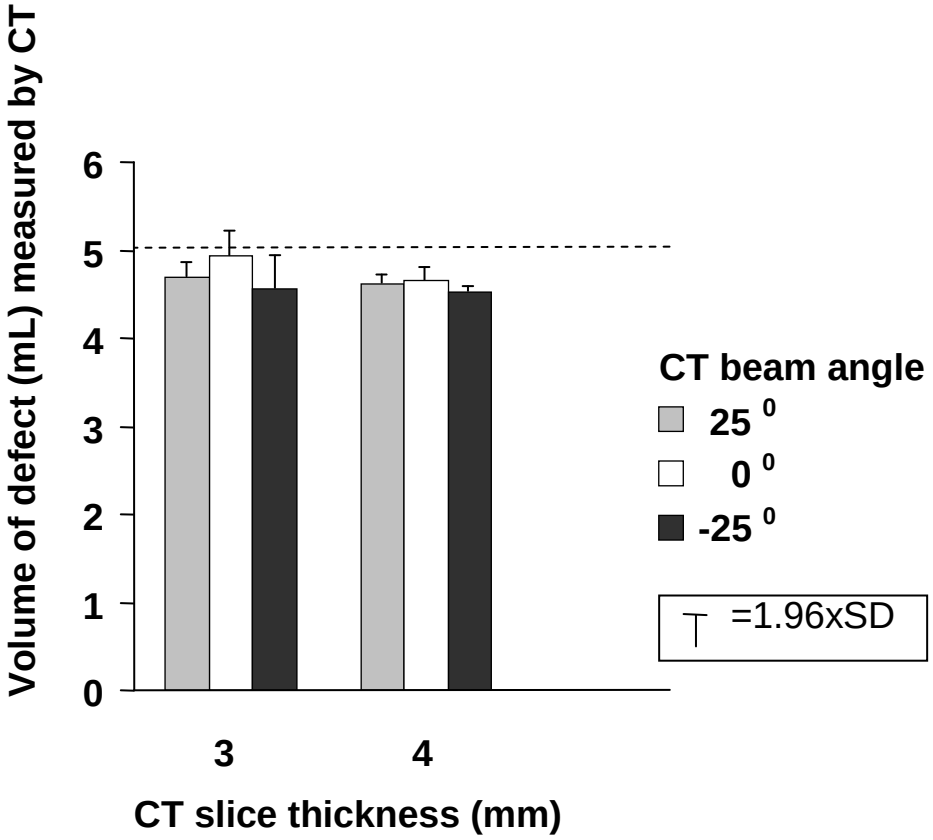

Fig. 3.3 The effect of the CT beam angle and CT slice thickness on the volume of a large acetabular bone defect measured from CT scans in a bovine hemi pelvis model. The dashed line indicates the volume of the bone defect measured using water and syringe. SD=standard deviation.

For the small simulated defect adjacent to the lateral screw, measurement of the CT scans taken using a beam angle of +25° gave significantly more accurate measures of volume than when using scans taken at 0° ($p < 0.0001$) (Fig. 3.4). The CT scan taken using a beam angle of -25° resulted in the least accurate measurement of volume. There was also a significant difference in the volumes measured from the CT scans taken at 3-mm and 4-mm slice thickness ($p = 0.0072$). The mean intra-observer and inter-observer error of the volume measurements of the small defect were 0.62% and 0.9%, respectively, using the operating parameters of 3-mm slice thickness and a beam angle of 0°.

Human Cadaver study

The actual volume of the simulated acetabular defect adjacent to the component, measured using a syringe and water, was 3.42 mL (standard deviation, 0.03 mL). There was a significant effect of beam angle ($p < 0.0001$) but no effect of slice thickness ($p = 0.647$) on the volume of the defect measured when a unilateral THR prosthesis was inserted (Fig. 3.5). With a 3-mm slice thickness, the most accurate measurements of the defect volume were obtained with scans taken using a beam angle of 0° (error, -1.9%) and +25° (error, -2.5%), which were both significantly more accurate than measurements taken using a beam angle of -25° ($p = 0.0005$). The intra-observer and inter-observer errors for the scans taken at 0° were 2.8% and 2.15%, respectively.

With bilateral THR prostheses inserted, the volumetric measurements taken using a slice thickness of 3-mm and a beam angle of 0° were less accurate (error, -4.2%) than when a unilateral THR prosthesis alone was implanted (error, -1.9%) (Fig.3.6).

The effect of the CT beam angle and slice thickness on the CT volume of a small bone defect in a bovine THR model.

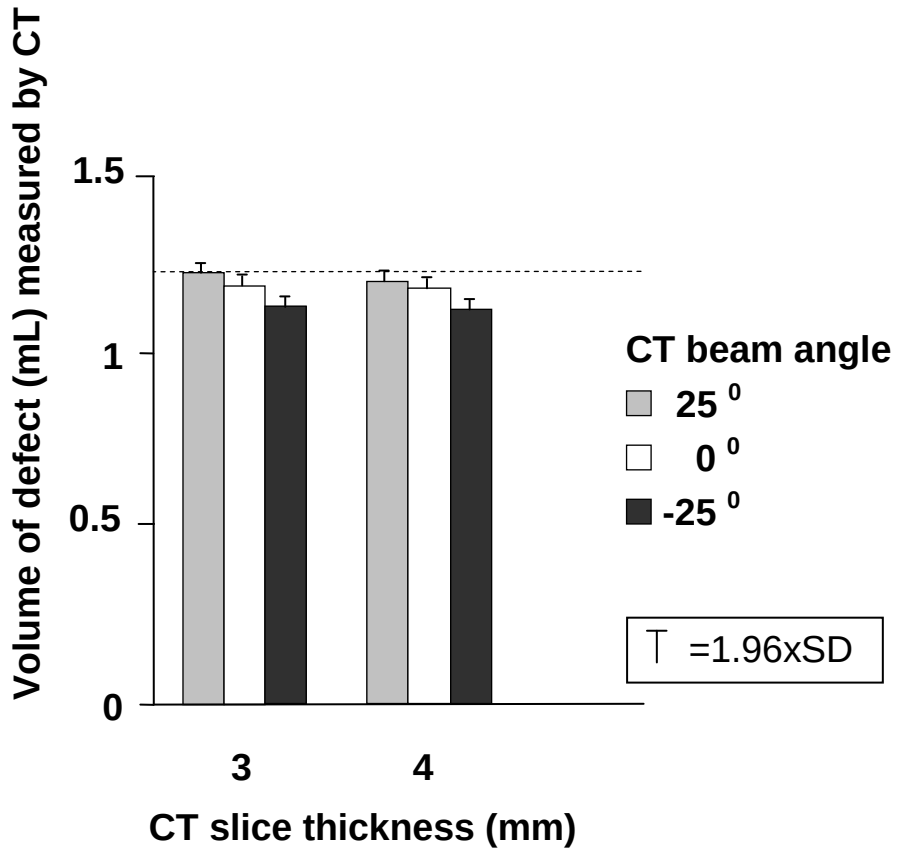

Fig. 3.4 The effect of CT beam angle and CT slice thickness on the volume of a small bone defect around a fixation screw measured from CT scans in a bovine hemi pelvis model. The dashed line indicates the defect volume measured using water and syringe.

SD= standard deviation.

The effect of the CT slice thickness on the CT volume of a large bone defect in a human cadaver THR model.

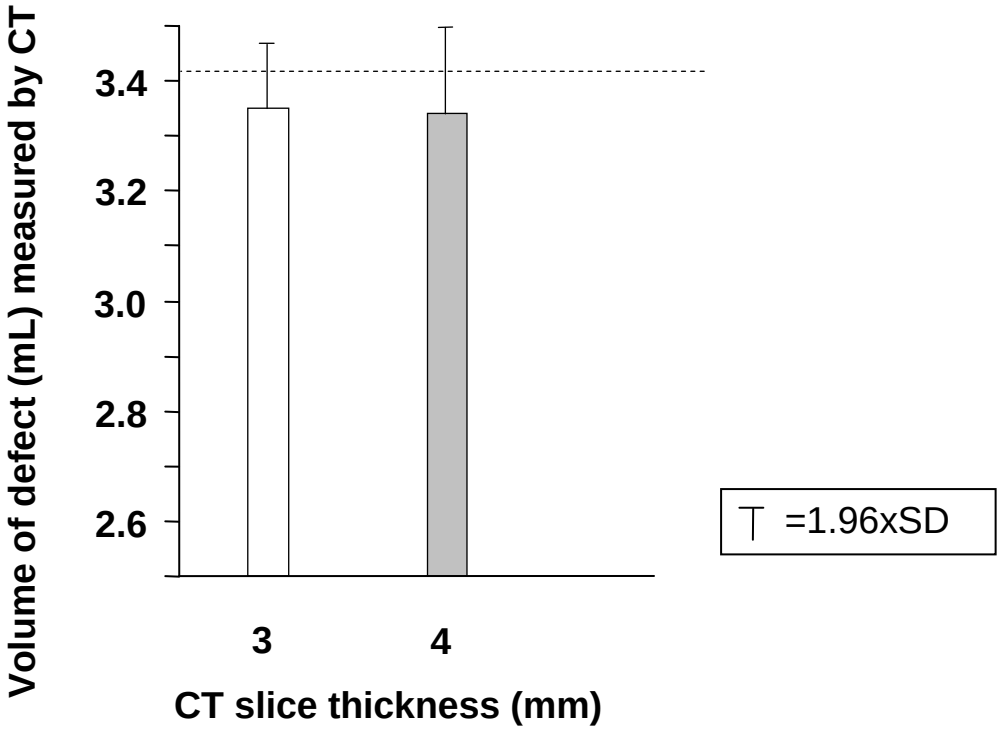

Fig.3.5 The effect of CT slice thickness on the volume of bone defect adjacent to the acetabular component measured from CT scans in a pelvis from a cadaver. The CT beam angle was 0^0. The dashed line indicates the bone defect volume measured using water and a syringe. SD=standard deviation.

The effect of bilateral THR on the CT volume of bone defects in a cadaver THR model.

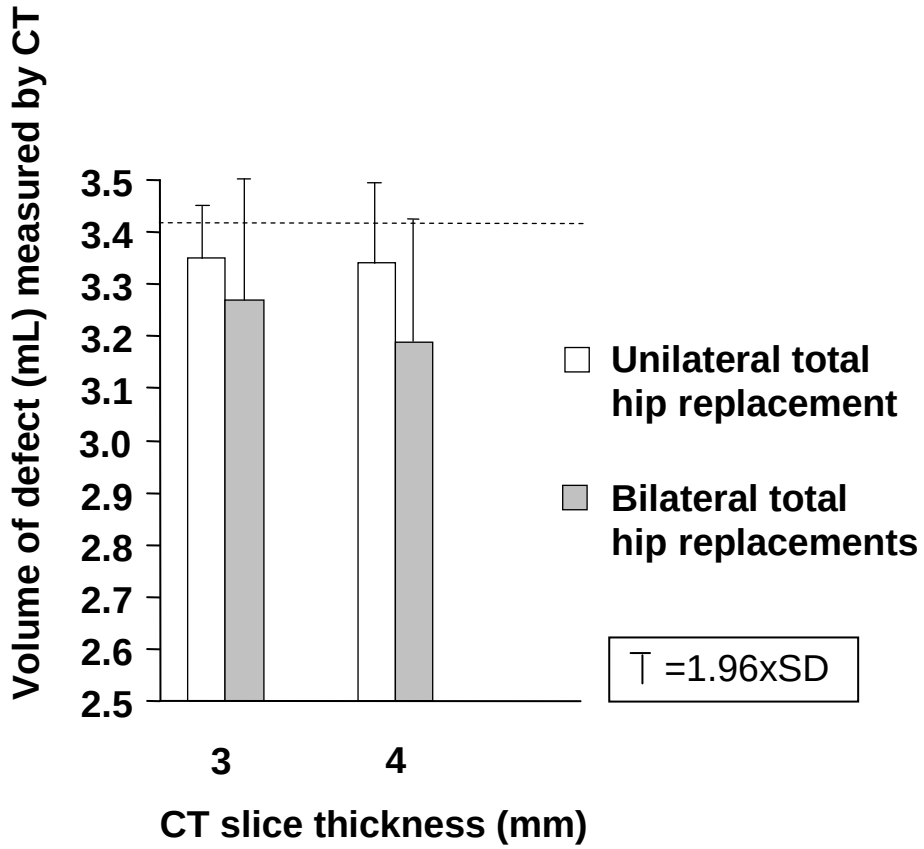

Fig. 3.6 The effect of bilateral total hip replacement on the volume of the bone defects adjacent to the acetabular component measured from CT scans of a pelvis from a cadaver. The CT beam angle was 0^0. The dashed line indicates the bone defect volume measured using water and a syringe, SD=standard deviation.

THR CT Protocol

(Conventional CT scanner with CT scale limited up to 4,000 HU)

Application:	CT assessment of THR patients for Periprosthetic osteolysis
Pre-programmed Protocol:	Hip Spiral
Patient Position:	Supine, Feet first
Scan Area / Direction:	Top of SI joint down to the end of ischium
Scanner Used:	Picker 6000
kV:	120kV
mAs:	200mAs
Time per Rotation (sec):	0.55s rotation
Detector Collimation (mm):	1X0
CT Slice Thickness (mm):	3mm
Data Reconstruction Interval (mm):	3X3
Table Speed (mm per rotation) / Pitch:	1.5mm
Filter:	Bone filter
FOV:	120mm/ 180mm/ Colimated to the hip
Matrix:	520X520
Reconstructions:	3X3 axial coronal sagittal

The difference in the measured volume of the defect in the acetabulum when bilateral THR prostheses were inserted was not statistically significant ($p = 0.164$) to that measured when only a unilateral THR prosthesis was implanted. The intra-observer (4.2%) and inter-observer (-2.3%) errors were similar to those obtained for the unilateral THR model.

3.4 Discussion

In this study, a conventional spiral CT scanner with limited CT scale (up to 4,000 HU) was able to accurately and reliably measure small and large bone defects in the ilium adjacent to titanium metal-backed acetabular components inserted in a bovine hemi-pelvis and a pelvis from a cadaver. Volumetric measurements of simulated defects were accurate to within 96% for small and large defects and precise to 99% and 98% for small and large defects, respectively. There was a small loss of accuracy in the estimate of the volume of the acetabular defect when a contralateral THR prosthesis was present, but this was unlikely to be clinically significant.

The findings described here show that, in experimental models of THR-associated bone loss, it is feasible to use CT scanning to measure the volume of defects in the cancellous bone superior (cranial) to metal-backed acetabular implants. Using the scanning parameters that were determined, including CT slice thickness and beam angle, together with metal artifact reduction software, accurate and reliable volumetric measurements can be obtained.

There were differences in the accuracy of volumetric estimation between CT scans taken with different angles of the gantry. The likely explanation of this is the angle of the gantry. The CT volume measurement of the large defect using 0° angle of beam

had better accuracy than that using +25° or -25°. This was probably because the longitudinal axis of the large defect was parallel to the longitudinal axis of the specimen resulting in more of the large defect being visualised by axial view at 0°.

The CT volume measurement of the small defect using +25° angle of beam had better accuracy than that using 0° or -25°. That was probably because the longitudinal axis of the small defect was orientated posteriorly from the tip of the acetabular component. In this position, most of the small defect could be detected only by a posteriorly tilted CT beam, which was at +25° cephalad.

This CT technique is likely to be superior to AP radiographs of the pelvis in measuring osteolysis around THR acetabular components. Studies using plain radiographs have been restricted to using two-dimensional measurements of osteolysis (Maloney et al., 1997, Wan et al., 1996) or volumetric measurements using planimetric measurements and mathematical formulas assuming ellipsoidal cavities (Garcia-Cimberelo et al., 1997). Because of the recognized limitations of plain radiographs for identification and localization of osteolytic lesions (Berry et al., 1999, Learmonth et al., 1997, Robertson et al., 1998, Zimlich et al., 2000), these techniques are, at best, semi-quantitative. CT scanning, using the techniques described, offers significant advantages and will allow definitive studies of the cause and outcomes of treatment of osteolysis.

A limitation of this study is that simulated defects were used to investigate the usefulness of CT scanning in this application. Osteolytic defects may be filled with granulomatous tissue and fluid, and therefore the fluid-filled defects, may not truly represent the clinical situation. Subsequent studies in patients, however, resulted in similar CT images as seen in the current model (Fig.3.7). In addition, osteolysis may

Use of Conventional CT with limited CT scale in clinical practice

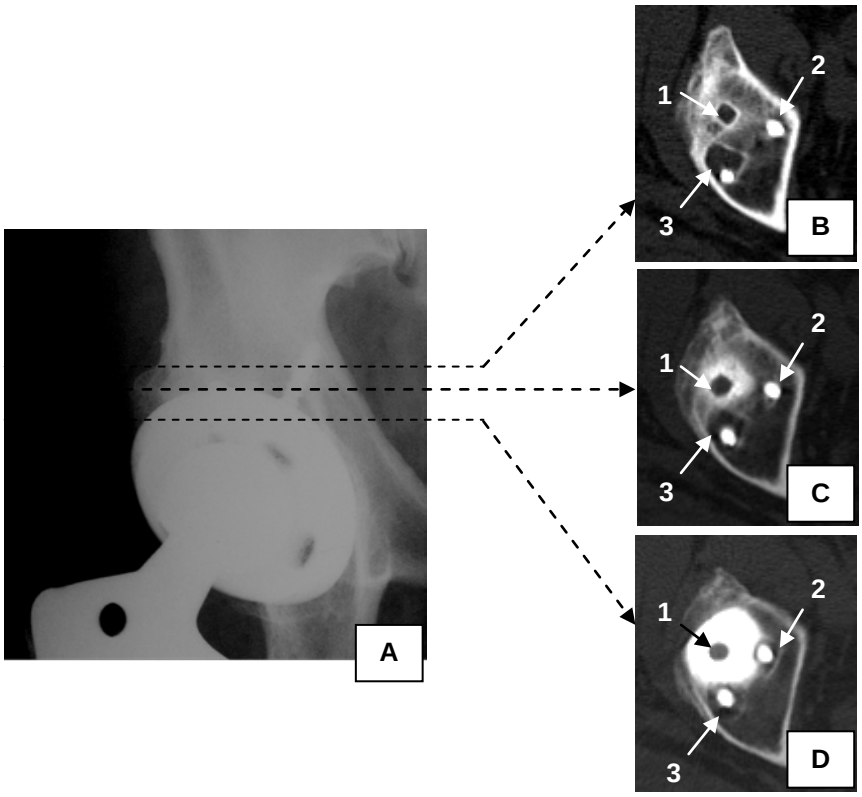

Fig.3.7 A plain film radiograph (A) of right hip (clinical case) showing uncemented THR acetabular component with fixation screws. Computed tomography scans (B, C and D) at several levels show: **(B)** 1, isolated osteolysis; 2, medial fixation screw; 3, osteolysis adjacent to the lateral fixation screw; **(C)** 1, osteolysis adjacent to empty screw-hole; 2, medial fixation screw; 3, osteolysis adjacent to lateral fixation screw; **(D)** 1, empty screw-hole; 2, osteolysis adjacent to medial fixation screw; 3, osteolysis adjacent to lateral fixation screw.

produce changes in the density of the surrounding bone, making the perimeter of the osteolytic defect difficult to discern compared with the easily visible margins of the created defects.

The CT assessment of THR patients for PO has a big potential for the clinical practice and when necessary, could be combined with some other diagnostic tools. For example, it would be of interest to apply dual energy x-ray absorptiometry (DEXA) in parallel with CT scanning to investigate associations between CT measurements and overall bone density measurements. This would be of particular interest in exploring the potential benefit of pharmacological treatment of osteolysis, including the use of bisphosphonates, in which treatment would be expected to influence bone generally, as well as inhibiting bone resorption at the specific site of bone loss.

3.5 Conclusions

An accurate and reliable CT quantitative technique for the measuring the volume of PO lesions by conventional CT scanners in the ilium area alone has been described.

This study has been published, as listed on page vii, and was performed in collaboration with the authors listed under the study.

When a new generation multi-slice CT scanner with extended CT scale (up to 40,000 HU) became available, this technique was further developed to allow assessment of osteolysis in all other areas of the acetabulum. This further development and research uses of this technique are described in the following chapters.

Chapter 4

Use of Multi-slice Spiral CT scanner with Extended CT scale

4.1 Introduction

As discussed in Chapter 1, recent generations of multi-slice CT scanners with extended CT scale have increasingly greater ability to reduce metal artifact. This has been demonstrated in several *in-vitro* (Claus et al., 2004, Leung et al., 2005) and *in-vivo* studies (Link et al., 2000, Looney et al., 2002, Puri et al., 2002, Schwarz et al., 2003, Kitamura et al., 2005, Walde et al., 2005) and discussed in section 1.5.3. When such a CT scanner became available in our institution, further development of the CT technique around metal hip prostheses was undertaken.

The main aim of the study described in this chapter was to develop a validated CT protocol that provides (a) good sensitivity and specificity of the detection, and accurate and reproducible quantification of periprosthetic bone defects in all acetabular and periacetabular areas and (b) meets the International (ICRP, 1996) and Australian (ARPANSA, 2008) safety guidelines for radiation protection in diagnostic and interventional radiology.

The specific aims of this study were:

1. To examine the effect of different CT tube currents (100 mAs, 200 mAs and 300 mAs) in 3 separate protocols with constant CT slice thickness (1.25mm), peak voltage (140kV) and field of view (FOV) (region of interest) on the resulting radiation dose
2. For the CT images reconstructed with 1.25mm and 3mm CT slice thickness:

- To examine the sensitivity and specificity of the CT detection of simulated bone defects of different sizes adjacent to either HG or PCA acetabular components of THR.

- To determine the volume of the smallest measurable CT-detectable bone defect in different acetabular and periacetabular areas.
- To determine the volume of the largest bone defect not detected by CT in different acetabular and periacetabular areas.
- To examine the accuracy and the precision of the CT measurement of simulated bone defects of similar volume in different acetabular and periacetabular areas, in the presence of acetabular components made of different alloys (Titanium or Cobalt-Chrome).
- To examine the interference effect of a contralateral prosthesis on the accuracy and the precision of the CT measurements of simulated bone defects of similar volume in different acetabular and periacetabular areas.
- To compare bias (difference between the true and observed values) according to prosthesis type, site of lesions, CT slice thickness and bone lesion size, using a linear mixed effects model for single bone defects.
- To compare bias according to prosthesis type, site of bone lesions, CT slice thickness and bone lesion size, using a linear mixed effects model for combined bone defects that involve any two neighbouring areas.

4.2 Methods and Materials

The limitations mentioned in the previous chapter that related to the availability, poor quality and low radiodensity of the formalin-treated pelvis from human cadavers were taken into account. There was a need for a bone specimen (or a phantom) with good radiodensity to represent the surrounding bone stock cranial (ilium), on the level (anterior wall, medial wall and posterior wall) and caudal (pubis and ischium) to the acetabular component. Fresh-frozen bovine hemi-pelvis was chosen for the following reasons. First, the bovine acetabulum was a similar in size to the human acetabulum. Second, the spatial orientation of the ilium, pubis and ischium to each other was

close to the human anatomy. Third, the fresh frozen bovine cancellous bone had better radiodensity compared to the formalin-treated cadaver bone. This would allow creation of simulated bone defects as small as 3-5mm in diameter, to examine the sensitivity end specificity of the CT in the 3-5mm wide area surrounding (parallel to) the acetabular component.

4.2.1 Bovine acetabulum specimens

Three fresh-frozen bovine left hemi-pelves, comparable in size to a human acetabulum, were prepared following the same routine technique used in section 3.2.1 of the previous chapter to accept a 58-mm outer diameter TiAlV Harris-Galante fibre metal coated shell with three screw holes (Zimmer Inc., Warsaw, IN), or 58-mm outer diameter PCA (Howmedica International, Ltd, Rutherford, NJ) shell. The acetabular component was inserted into the acetabulum of the specimen in 40^{o} of operative inclination and 25^{o} of operative anteversion (Murray et al., 1993). A Trilogy (Zimmer Inc., Warsaw, IN) or PCA (Howmedica International, Ltd, Rutherford, NJ) PE liner was inserted into the component. The specimen was placed into a plastic container and orientated so that its longitudinal axis was parallel to the midline of the container and the ischial tubercule was rested on the base of the container. The proximal aspect of the specimen was fixed with two Steinman pins to a wooden plate, which was then clamped to the plastic container. A cementless Harris-Galante (Zimmer inc.) or PCA (Howmedica International, Ltd, Rutherford, NJ) femoral stem with a 28-mm diameter CoCr alloy head (Howmedica International) was inserted into a plastic femur, which was then distally fixed with two Steinman pins to a wooden plate and clamped to the plastic container (Fig 4.1). During CT scanning, every specimen was covered with tap water, which was to simulate the additional beam attenuation from the surrounding soft tissues.

Bovine acetabulum specimen model of total hip replacement

Fig.4.1 Photograph showing bovine acetabulum specimen model of total hip replacement positioned in a plastic container. The femoral component is inserted in to a plastic tube for additional stability. The specimen is fixed proximally and distally by Steinman pins to wooden plates and then clamped to the container.

Three different CT scan protocols were undertaken to examine the effect of different CT tube currents (100 mAs, 200 mAs and 300 mAs) with constant CT slice thickness (1.25mm), peak voltage (140kV) and field of view (FOV) on the resulting radiation dose. The protocol with tube currents of 200mAs provided the best metal artifact reduction with effective radiation dose in agreement with the International and Australian safety guidelines for Radiation Protection in Diagnostic and Interventional Radiology. These CT settings were added to the preliminary CT protocol to be tested in the following steps.

After a baseline set of CT images was obtained, the acetabular component was removed and simulated bone defects of different sizes representing areas of osteolysis were created in six possible anatomic locations: ilium, anterior wall, medial wall, posterior wall, pubis and ischium. The bone defects were created using Ø3mm, Ø5mm and Ø10mm burrs (Linvatec Corp., Largo, FL 33773, USA) as non-linear, not parallel to the surface of the acetabular component, in communication with the joint space and more than 3mm in diameter (Maloney et al., 1999). After each defect was created, it was moulded with Blu-Tack plasticine (Blu-Tack®, Bostik Findley Pty. Ltd., Thomastown, Victoria, Australia) and the volume was calculated from the weight of the mould and the density of the material. Each of these steps was followed by a routine CT scan. This procedure was performed a total of seven times with all of the three specimens, creating 126 possible locations (6 possible locations in 3 specimens examined on 7 consecutive experimental steps). A total of 65 simulated bone defects were created (59 single and 6 combined). The simulated bone defects were presented randomly (new bone defects were created in any one of the six anatomic locations, and existing bone defects were either enlarged, or left the same, or combined).

In the first three steps, all of the simulated bone defects were isolated, but in the last three steps some of them were connected, to represent a “combined” bone defect that involves two neighbouring areas: ilum + medial wall (Fig. 4.2), anterior wall + pubis (Fig. 4.3) and posterior wall + ischium (Fig. 4.4).

Physical measurement of the simulated bone defects volume

The simulated bone defects were moulded with plasticine Blu-Tack (Blu-Tack®, Bostik Findley Pty. Ltd., Thomastown, Victoria, Australia). The weight of the mould in grams (g) was measured by 0.01g sensitive scale (Electronic Balance ER-182A, A&D Company Ltd, Tokyo, Japan) and the density/specific gravity data of 1.8g/ml was given from the material specification (Technology Supplies Ltd, Shropshire, UK). The volume of the simulated bone defects was calculated using the formula:

Volume = **M**ass / **D**ensity

4.2.2 Siemens Volume Zoom CT Scanner

A high resolution spiral multi-slice CT scanner (Siemens Volume Zoom; Siemens, Munich, Germany) was used. This scanner has ultra-fast gantry design (500 milliseconds for a full rotation, and flexible selection of slice thickness (0.5-10mm), prospectively and retrospectively. For this instrument, an extended Hounsfield scale is available in the range from –10 240 to + 30 710 HU.

Different tube currents (100 mAs, 200 mAs and 300 mAs) were tested in 3 protocols with constant CT slice thickness (1.25mm), peak voltage (140kV) and field of view (FOV) to calculate the resulting CT radiation dose.

Special software filter program B50s (Kernel) with extended CT scale was used to reduce metallic artifacts.

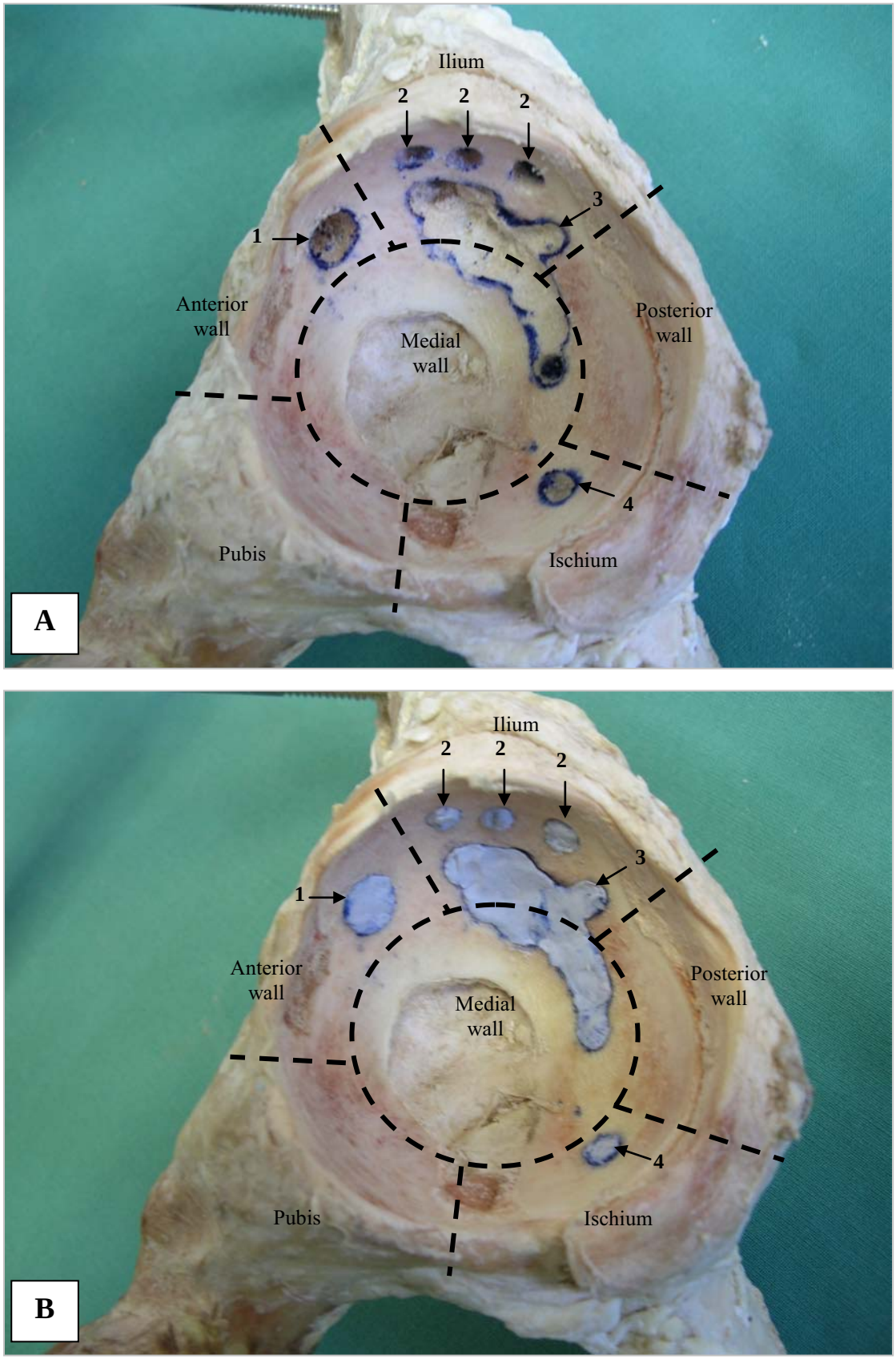

Fig.4.2 Photographs showing first bovine acetabulum specimen. (A) Simulated single bone defects of different size in: 1, anterior wall; 2, ilium; 4, ischium; combined bone defect 3, involving ilium and medial wall. (B) The same bone defects moulded with plasticine (Blutack).

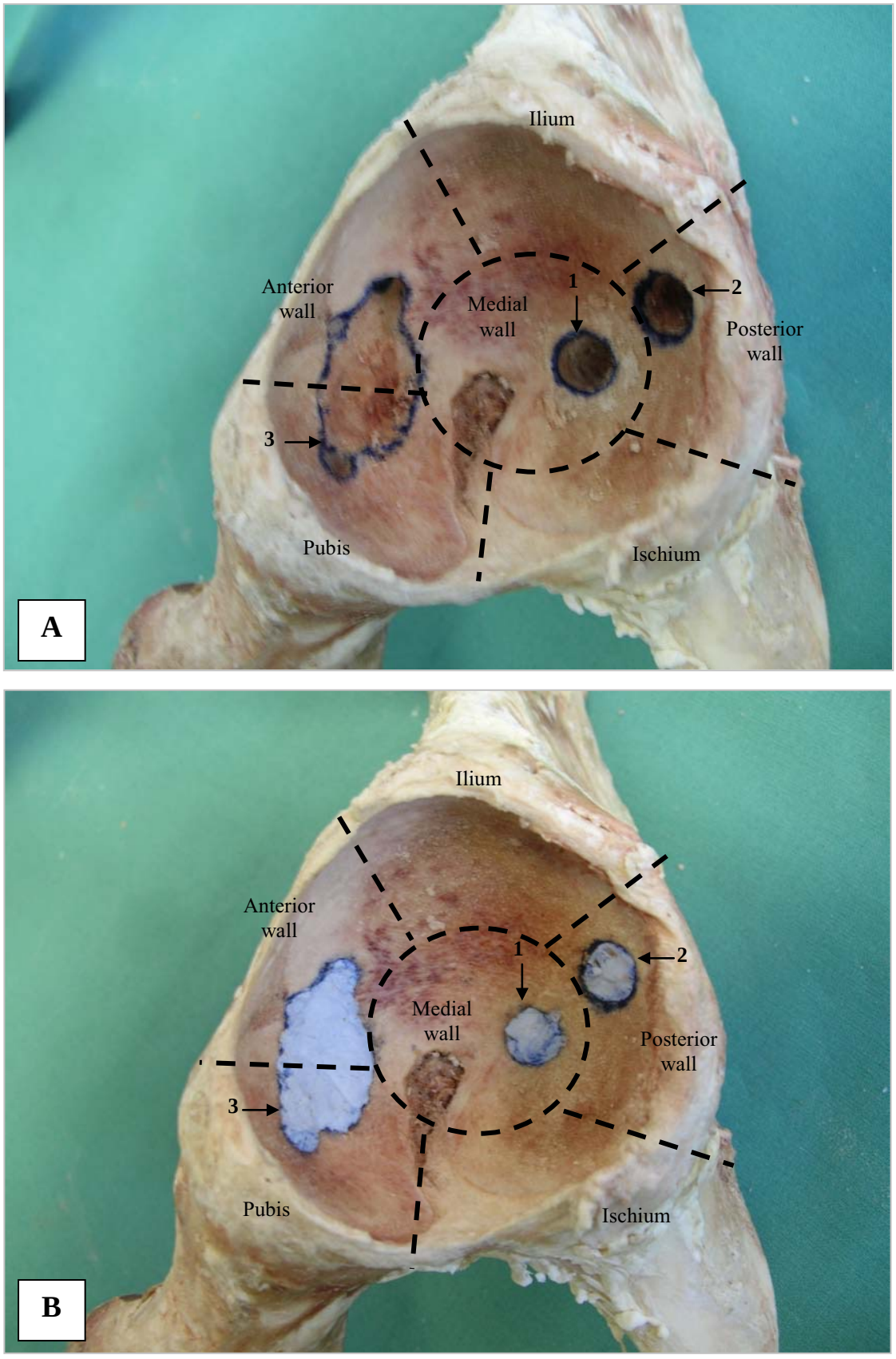

Fig.4.3 Photographs showing second bovine acetabulum specimen. (A) Simulated single bone defects in: 1, medial wall; 2, posterior wall; combined bone defect 3, involving anterior wall and pubis. (B) The same bone defects moulded with plasticine (Blutack).

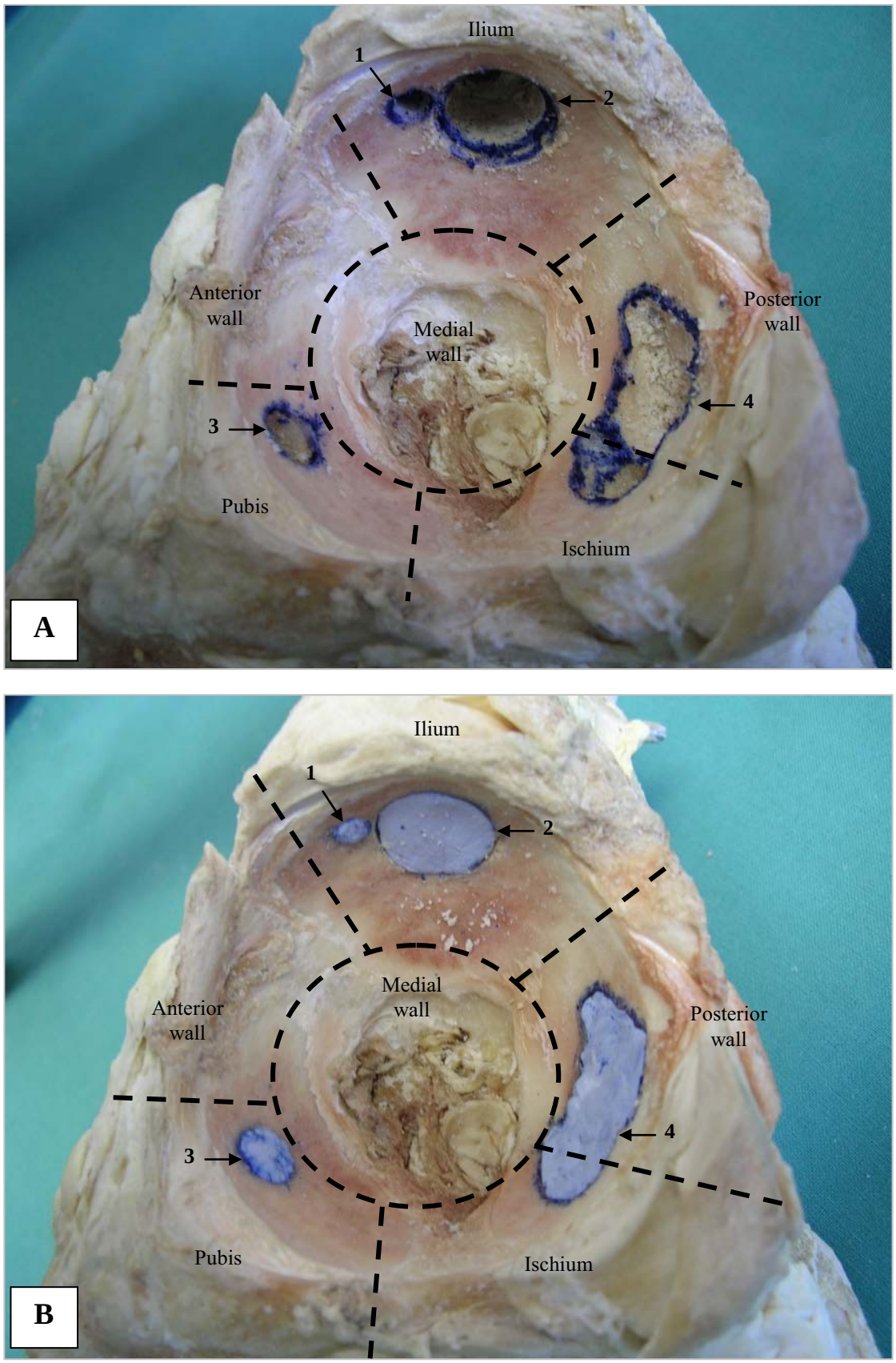

Fig.4.4 Photographs showing third bovine acetabulum specimen. (A) Simulated single bone defects of different size in: 1 and 2, ilium; 3, pubis; combined bone defect 4, involving posterior wall and ischium. (B) The same bone defects moulded with plasticine (Blutack).

Initial CT scans of the three intact specimens (without bone defects) were taken as “base line” images for comparison. The acetabular component was then removed and simulated bone defects of different size were created and physically measured on every following step. Each of these steps was followed by a routine CT scan. From the raw CT data multi-planar images were reconstructed with 1.25mm and 3mm slice thickness for analysis. The CT data was formatted in DICOM (Digital Imaging and Communications in Medicine) and saved to compact disk via a picture archiving and communication system and then downloaded into a Picker PQ6000 workstation (Picker International, Cleveland, Ohio) for analysis. The quality of the CT images was significantly improved in post-processing manipulation by additional adjustment of the Window and Level settings. The simulated bone defects were measured in consecutive CT slices displayed on the computer screen by tracing the inner border of the defect using a computer mouse. Volume measurement was done using algorithms coded into the commercial image-analysis software (PQ6000 Voxel Q FALCON, Picker International Inc.).

4.2.3 Statistical Analysis

The accuracy of the volumetric measurements from the CT scans was determined by calculation of the percent error between the physical measurement of the simulated defects, undertaken by moulding with plasticine (Blu-Tack®, Bostik Findley Pty. Ltd., Thomastown, Victoria, Australia) and the measurements from the CT scans. Volumetric measurements from the CT scans were repeated three times in each instance by three independent observers, an orthopaedic research registrar, a research officer and a research assistant. The reliability of the quantitative measurements was determined by calculating the intra-observer and inter-observer errors. The intra-observer error was assessed by calculating the standard deviation (SD) because the standard deviation between observations is independent of the

true size of the volume, whereas the coefficient of variation (CV) is not. The inter-observer error was assessed by calculating intra-class correlation coefficient (ICC), with values above 0.90 were considered excellent, between 0.75 and 0.90 good, and bellow 0.75 poor (Portney et al., 2000). Interferential analysis was performed using analysis of variance (ANOVA) and the Fisher's least-significant-difference test. Data summary statistics were calculated using Microsoft Excel and interferential analyses were performed using the SAS statistical software package (SAS® System for Windows™ Version 9.1 (SAS Institute Inc., Cary, NC, USA). A probability value of less than 0.05 was considered to indicate statistical significance.

Bias (difference between the true and observed values) was examined for single and combined bone defects in the presence of unilateral or bilateral THR prostheses.

1. Single bone defects (HG or PCA)

A linear mixed effects model was used to compare bias according to the following factors:

- Prosthesis type (HG or PCA)
- Site of bone defects (ilium [I], anterior wall [aw], medial wall [mw], posterior wall [pw], pubis [p] and ischium [isch])
- CT slice thickness (1.25mm or 3mm)
- Size of bone defects (>0.05 &≤0.4; >0.4&≤2; >2&≤9; >9cm³)

2. Combined bone defects (HG or PCA)

A linear mixed effects model was used to compare bias according to the following factors:

- Prosthesis type (HG or PCA)
- Sites involved (i+mw, aw+p, pw+isch)
- CT slice thickness (1.25mm or 3mm)
- Size of bone defects (>2&≤9, >9cm³)

3. Single bone defects (Bilateral THR prosthesis)

A linear mixed effects model was used to compare bias according to the following factors:

- Site of bone defects (ilium [I], anterior wall [aw], medial wall [mw], posterior wall [pw], pubis [p] and ischium [isch])
- CT slice thickness (1.25mm or 3mm)
- Size of bone defects (>0.4&≤2; >2&≤9; >9cm³)

4. Combined bone defects (Bilateral THR prosthesis)

A linear mixed effects model was used to compare bias according to the following factors:

- Sites involved (i+mw, aw+p, pw+isch)
- CT slice thickness (1.25mm or 3mm)
- Size of bone defects (>2&≤9, >9cm³)

All calculations were performed using SAS Version 9.1 (SAS Institute Inc., Cary, NC, USA).

4.3 Results

The effect of different CT scanning parameters on the resulting radiation dose is presented in Table 4.1. The protocol with CT settings of 1.25mm slice thickness, 140 kV and 200mAs provided the best image quality with the least radiation dose. The radiation doses resulting from this protocol are in agreement with the guidelines from the ICRP (International Commission on Radiological Protection, 1996), the European guidelines on quality criteria for computed tomography (Report EUR 16262, Luxembourg, 1999) and ARPANSA (Australian Radiation Protection and Nuclear Safety Agency, RPS 14.1, 2008).

This study examined 65 simulated bone defects of different sizes (0.013cm³-10.81cm³) and characteristics (59 single and 6 combined).

Table 4.1 The effect of different CT tube currents on the resulting radiation dose

CT slice thickness (mm)	1.25	**1.25**	1.25
kV	140	**140**	140
mAs	100	**200**	300
CTDIw (mGyair)	13.6	**26.6**	39.8
DLP (mGyaircm)	266	**521**	780
Effective dose (mSv)	5.05	**9.89**	14.82

Reference levels and effective dose for CT pelvic examination proposed by:
International Commission on Radiological Protection, 1996.
Australian Radiological Protection and Nuclear Safety Agency, RPS 14.1, 2008.

CTDIw (mGyair)	**35**
DLP (mGyaircm)	**570**
Effective dose (mSv)	**10.83**

Single bone defects

For the group of 59 single bone defects, the volumes ranged from 0.013cm^3-10.81 cm^3, with a mean of 1.14 ± 2.6cm^3.

Thirty-eight of the defects were in the range 0.013cm^3-0.087cm^3. The size of these defects was not clinically relevant, but they were created to examine the sensitivity and the specificity of the CT in the 3-5mm wide area parallel to the acetabular component.

The remaining 21 single bone defects, with volumes ranging from 0.4cm^3-10.81cm^3 had a mean of 3.12±3.7cm^3 and were of more clinically-relevant size.

This study included three additional size ranges:

- >0.4 & ≤2cm^3 (n=10) 0.4-0.8cm^3, mean volume 0.54 cm^3
- >2 & ≤9cm^3 (n=7) 2.014-4.16cm^3, mean volume 2.73 cm^3
- >9cm^3 (n=4) 9.65-10.81cm^3, mean volume 10.23cm^3

Combined bone defects

There were 6 combined bone defects (that involve two neighbouring areas) with a mean volume of 4.56cm^3 ± 3.7cm^3 (range 1.27-9.21cm^3). They were as follow: ilium+medial wall (Fig.4.5), anterior wall+pubis (Fig.4.6), posterior wall+ischium (Fig.4.7).

The three reviewers assessed 126 possible locations (6 possible locations in 3 specimens examined on 7 consecutive experimental steps) for the presence or absence of simulated bone defects. The same 126 locations were assessed under different conditions:

1. HG THR prostheses inserted, CT slice thickness of 1.25mm.
2. HG THR prostheses inserted, CT slice thickness of 3mm.
3. PCA THR prostheses inserted, CT slice thickness of 1.25mm.

PCA THR prostheses inserted, CT slice thickness of 3mm.

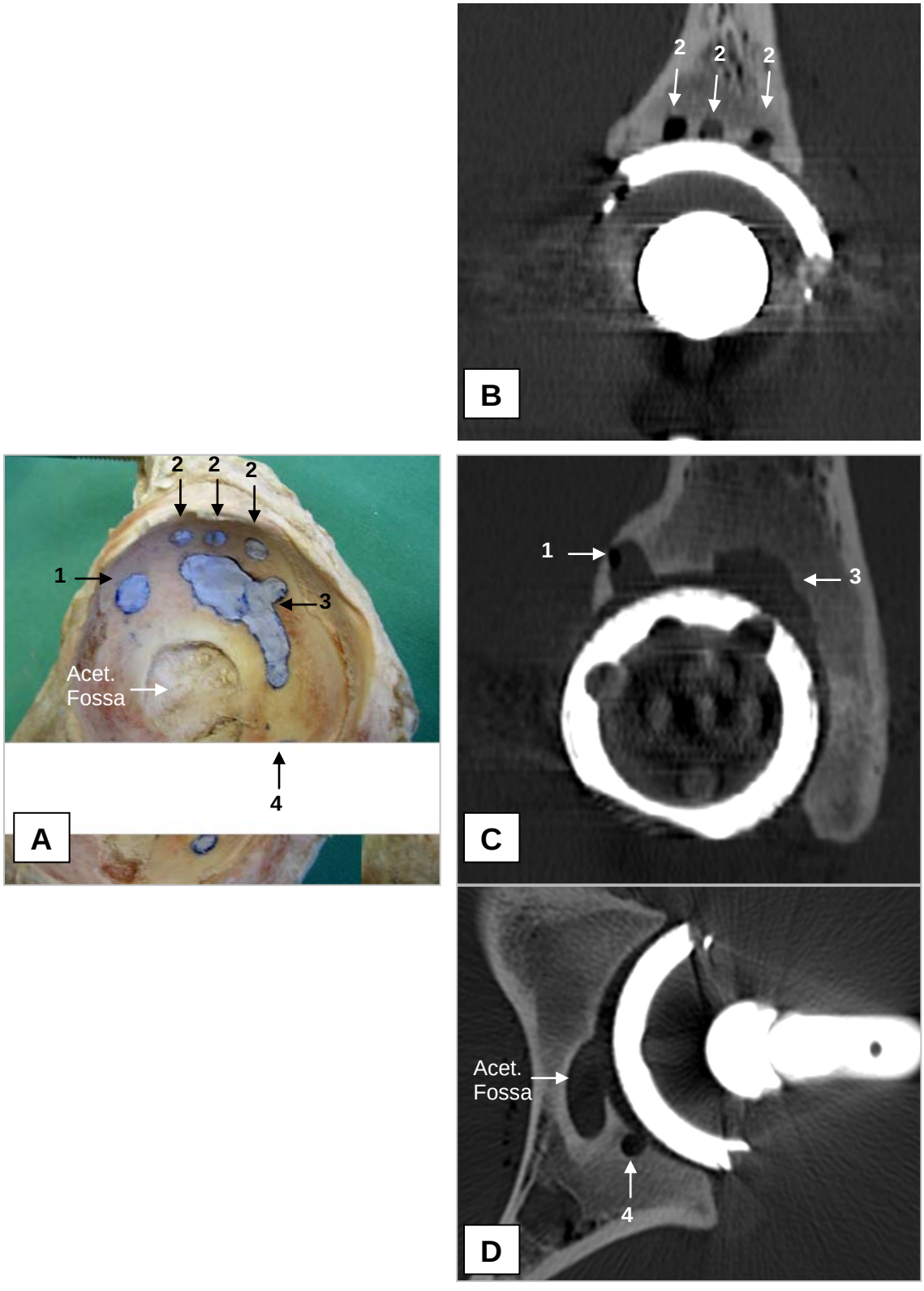

Fig.4.5 First bovine acetabulum specimen. A – Photograph showing simulated bone defects moulded with plasticine (Blutack). 1-Single bone defect in anterior wall; 2-Single bone defects in ilium; 3-Combined bone defect involving ilium and medial wall; 4- Single bone defect in ischium. B, C, D – CT scans from axial and sagittal planes showing the same simulated bone defects (arrows).

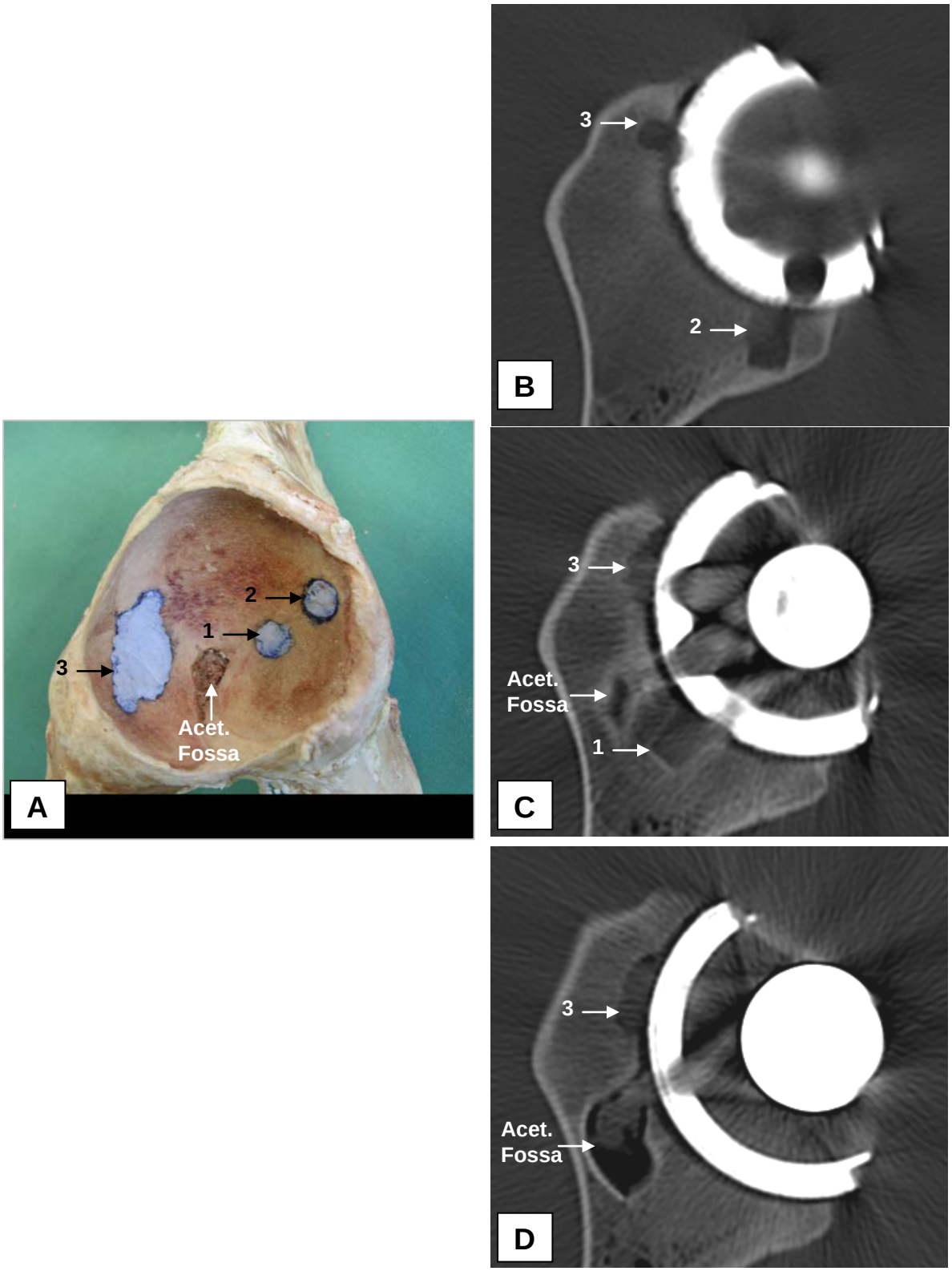

Fig.4.6 Second bovine acetabulum specimen.

A – Photograph showing simulated bone defects moulded with plasticine (Blutack). 1-Single bone defect in medial wall; 2-Single bone defects in posterior wall; 3-Combined bone defect involving anterior wall and pubis. B, C, D – CT scans from axial plane showing the same simulated bone defects (arrows).

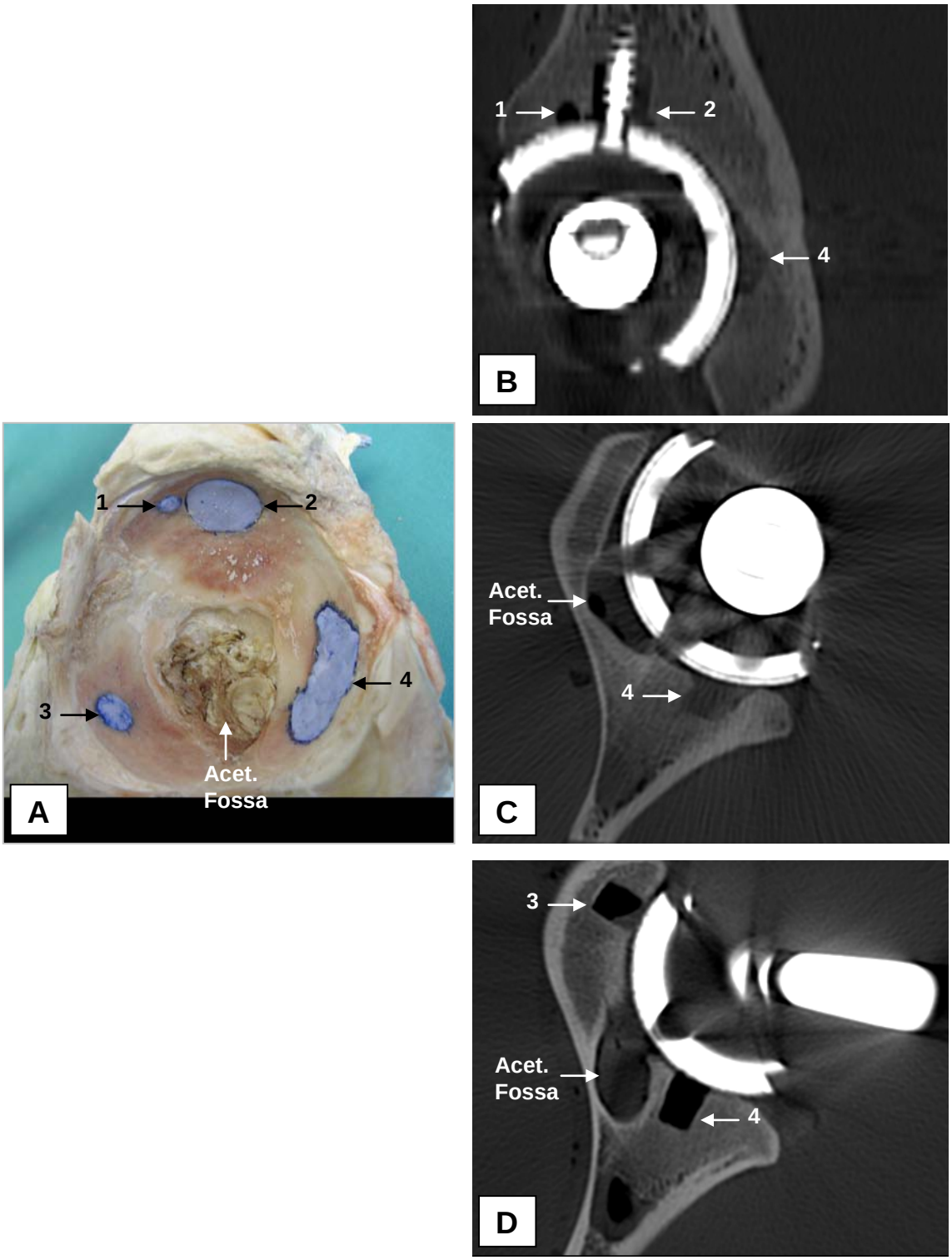

Fig.4.7 Third bovine acetabulum specimen.

A – Photograph showing simulated bone defects moulded with plasticine (Blutack). 1-Single bone defect in ilium; 2-Single bone defect in ilium adjacent to the fixation screw; 3-Single bone defect in pubis; 4-Combined bone defect involving posterior wall and ishium. B, C, D – CT scans from axial plane showing the same simulated bone defects (arrows).

CT detection and quantification of bone defects adjacent to HG acetabular component:

Single bone defects:

- The overall sensitivity of CT detection of periprosthetic bone defects was 97% (57 out of 59 possible) using 1.25mm CT slice thickness and 93% (55 out of 59 possible) for 3mm CT slice thickness (Table 4.2).
- For 1.25mm CT slice thickness, sensitivity ranged from 100% for bone defects in ilium, anterior wall, pubis and ischium, to 86% for bone defects in medial wall and posterior wall (Table 4.3).
- For 3mm CT slice thickness, sensitivity ranged from 100% for bone defects in ilium, pubis and ischium, to 71% for bone defects in posterior wall (Table 4.3). That was probably because the area on the level of the acetabular component was affected by an additional amount of metallic artifact from the femoral head and neck (Fig.4.8).
- The overall specificity was 100% for both 1.25mm and 3mm CT slices (67 out of 67 anatomic locations with no lesions correctly identified as having no lesions).
- Despite the low sensitivity in medial wall and posterior wall, specificity remained high, indicating that once the bone defect is evident on the CT, the likelihood that a bone defect truly exists is high.
- The volume of the smallest measurable CT-detectable bone defect was 0.014 cm^3 (Ø3mm diameter) in the medial and posterior wall of the acetabulum for both 1.25mm and 3mm CT slice thickness.
- The volume of the largest bone defect that was miss-detected by CT measured 0.017cm^3 (Ø 3mm diameter) in posterior wall (1.25mm CT slice thickness) and 0.019 cm^3 in anterior wall (3mm CT slice thickness).

Table 4.2 Bone defect detection according to prosthesis type, CT slice thickness and bone defect size

Prosthesis Type	CT slice thickness (mm)	Size Group (cm3)	Mean Size (cm3)	№ of detected bone defects (№ of detectable bone defects)	Percentage of bone defects identified correctly
HG	1.25	<0.05	0.017	16 (out of 18)	89
		>0.05 & ≤0.4	0.077	20 (out of 20)	100
		>0.4 & ≤2	0.539	10 (out of 10)	100
		>2 & ≤9	2.73	07 (out of 07)	100
		>9	10.23	04 (out of 04)	100
				57 (out of 59)	97
	3	<0.05	0.017	14 (out of 18)	78
		>0.05 & ≤0.4	0.077	20 (out of 20)	100
		>0.4 & ≤2	0.539	10 (out of 10)	100
		>2 & ≤9	2.73	07 (out of 07)	100
		>9	10.23	04 (out of 04)	100
				55 (out of 59)	93
PCA	1.25	<0.05	0.017	10 (out of 18)	56
		>0.05 & ≤0.4	0.077	17 (out of 20)	85
		>0.4 & ≤2	0.539	10 (out of 10)	100
		>2 & ≤9	2.73	07 (out of 07)	100
		>9	10.23	04 (out of 04)	100
				48 (out of 59)	81
	3	<0.05	0.017	09 (out of 18)	50
		>0.05 & ≤0.4	0.077	17 (out of 20)	85
		>0.4 & ≤2	0.539	10 (out of 10)	100
		>2 & ≤9	2.73	07 (out of 07)	100
		>9	10.23	04 (out of 04)	100
				47 (out of 59)	80

Table 4.3 Sensitivity according to bone defect location

Bone defect location (n=number of bone defects)	Mean bone defect size (cm^3)	Sensitivity (%)							
		HG				PCA			
		1.25mm	p Value	3mm	p Value	1.25mm	p Value	3mm	p Value
Ilium (n=19)	2.45±4.2	100	<0.0001	100	<0.0001	100	<0.0001	100	<0.0001
Anterior wall (n=7)	0.18±0.2	100	<0.0001	86	<0.0001	57	<0.0001	57	<0.0001
Medial wall (n=7)	0.15±0.2	86	<0.0001	86	<0.0001	71	<0.0001	57	<0.0001
Posterior wall (n=7)	0.17±0.2	86	<0.0001	71	<0.0001	43	0.0001	43	0.0001
Pubis (n=10)	1.04±1.5	100	<0.0001	100	<0.0001	90	<0.0001	90	<0.0001
Ischium (n=9)	0.77±1.3	100	<0.0001	100	<0.0001	89	<0.0001	89	<0.0001

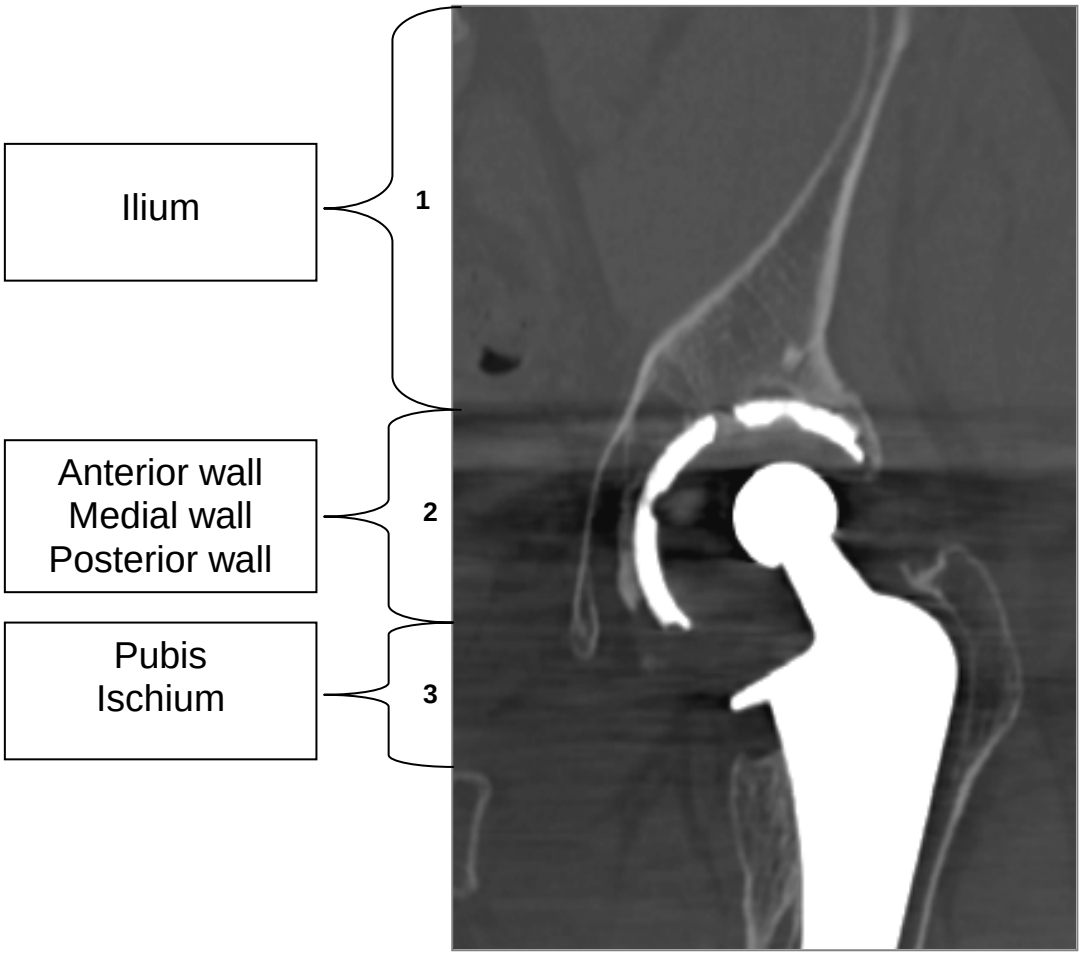

Fig.4.8 CT coronal reconstruction image of left hip joint in a patient with an uncemented total hip replacement prosthesis. Shown are 3 zones with different amount of metal artefact: Zone 1-involves the area cranial to the acetabular roof (ilium); Zone 2-involves the area on the level of the acetabular component (anterior wall, medial wall and posterior wall); Zone 3- involves the area caudal to the acetabular component (pubis and ischium).

- All 21 single bone defects with a mean volume 3.12 cm^3 (range 0.4-10.81cm^3) were correctly identified and measured with an accuracy error of -0.23cm^3±0.47cm^3 (1.25mm CT slice thickness) and -0.4±0.81 cm^3 (3mm CT slice thickness).
- Bone defects >0.4 &≤2cm^3 (Table 4.4) with a mean volume 0.54±0.11 cm^3 were measured with a mean accuracy error of 0.11±0.08cm^3 (1.25mm CT slice thickness) and 0.15±0.07cm^3 (3mm CT slice thickness).
- Bone defects >2≤9&cm^3 (Table 4.5) with a mean volume 2.73±0.75cm^3 were measured with a mean accuracy error of 0.30±0.33cm^3 (1.25mm CT slice thickness) and 0.39±0.46cm^3 (3mm CT slice thickness).
- Bone defects >9cm^3 (Table 4.6) with a mean volume 10.23±0.67cm^3 were measured with a mean accuracy error of -0.6±0.36cm^3 (1.25mm CT slice thickness) and -0.9±0.39cm^3 (3mm CT slice thickness).
- Overall, bone defects with most clinically relevant volumes in the range 2.01cm^3-10.81cm^3, (mean 5.46±3.8cm^3), were measured with a mean accuracy error of -0.55±0.45 (1.25mm CT slice thickness) and 0.9±0.86cm^3 (3mm CT slice thickness).

Combined bone defects

- All 6 combined bone defects with mean volume 4.56±3.7cm^3 were correctly identified and measured with a mean accuracy error of -0.18±0.6cm^3 (1.25mm CT slice thickness) and -0.68±1.09cm^3 (3mm CT slice thickness).

Table 4.4 Mean volumetric errors for detected bone defects ≥0.4 & <2cm³ adjacent to HG acetabular component according to anatomical location and CT slice thickness.

Bone defect location (n=number of bone defects)	Mean bone defect size (cm^3)	CT slice thickness (mm)	Accuracy Error (cm^3)	Intra-observer error (cm^3)	Inter-observer error
Ilium (n=1)	0.799	1.25	0.12	0	0.996
		3	0.2	0.006	0.84
Anterior wall (n=2)	0.531	1.25	-0.03	0.02	0.613
		3	0.08	0.03	0.471
Medial wall (n=2)	0.43	1.25	0.06	0.03	0.222
		3	0.12	0.04	0.095
Posterior wall (n=2)	0.514	1.25	0.15	0.03	0.687
		3	0.18	0.04	0.681
Pubis (n=2)	0.482	1.25	0.2	0.03	1
		3	0.23	0.05	0.21
Ischium (n=1)	0.672	1.25	0.15	0.04	0.947
		3	0.12	0.03	0.862

Table 4.5 Mean volumetric errors for detected bone defects >2 & ≤9cm³ adjacent to HG acetabular component according to anatomical location and CT slice thickness.

Bone defect location (n=number of bone defects)	Mean bone defect size (cm³)	CT slice thickness (mm)	Accuracy Error (cm³)	Intra-observer error (cm³)	Inter-observer error
Ilium (n=2)	2.01	1.25	-0.03	0.09	0.996
		3	0.003	0.08	0.84
Pubis (n=3)	3.06	1.25	-0.34	0.07	0.933
		3	-0.53	0.07	0.827
Ischium (n=2)	2.96	1.25	-0.51	0.06	0.947
		3	-0.56	0.134	0.862

Table 4.6 Mean volumetric errors for detected bone defects >9cm³ in ilium according to prosthesis type and CT slice thickness.

Bone defect location (n=number of bone defects)	Mean bone defect size (cm³)	Prosthesis Type	CT slice thickness (mm)	Accuracy Error (cm³)	Intra-observer error (cm³)	Inter-observer error
Ilium (n=4)	10.23	HG	1.25	-0.6	0.127	0.901
			3	-0.92	0.163	0.407
		PCA	1.25	-1.16	0.12	0,958
			3	-1.7	0.22	0.763

CT detection and quantification of bone defects adjacent to PCA acetabular component

Single bone defects:

- The overall sensitivity of CT for the detection of periprosthetic bone defects was 81% (48 out of 59 possible) for 1.25mm CT slice thickness and 80% (47out of 59 possible) for 3mm CT slice thickness (Table 4.2).
- For both 1.25mm and 3mm CT slice thickness, sensitivity ranged from 100% for bone defects in ilium, to 43% for bone defects in posterior wall (Table 4.3).

  That was probably because the area on the level of the acetabular component was affected by an additional amount of metallic artifact from the femoral head and neck, while the area of the ilium was almost artifact-free (Fig.4.8).
- The overall specificity was 100% for both 1.25mm and 3mm slice thickness (67 out of 67 anatomic locations with no lesions correctly identified as having no lesions). Despite the low sensitivity in anterior wall, medial wall and posterior wall, specificity remained high, indicating that once the bone defect is evident on the CT, the likelihood that a bone defect truly exists is high.
- The volume of the smallest measurable CT-detectable bone defect was 0.014cm^3 (Ø 3mm diameter) in the medial wall of the acetabulum for both 1.25mm and 3mm CT slice thickness.
- The volume of the largest bone defect that was not detected by CT, measured 0.074cm^3 (Ø 5mm diameter) in anterior and medial walls for both 1.25mm and 3mm CT slice thickness.
- In the presence of PCA acetabular component, all 21 single bone defects with mean volume 3.12cm^3 (range 0.4-10.81cm^3) were correctly

identified and measured with an accuracy error of -0.69cm³±0.78cm³ (1.25mm CT slice thickness) and -0.57±1.22cm³ (3mm CT slice thickness).

- Bone defects >0.4 ≤2cm³ (Table 4.7) with a mean volume of 0.54±0.11cm³ were measured with an overall accuracy error of 0.06±0.11cm³ (1.25mm CT slice thickness) and -0.003 ± 0.14 cm³ (3mm CT slice thickness).
- Bone defects >2 ≤ 9cm³ (Table 4.8) with a me an volume of 2.73±0.75cm³ were measured with an overall accuracy error of -1.1±0.78cm³ (1.25mm CT slice thickness) and -0.95 ± 0.85cm³ (3mm CT slice thickness).
- Bone defects >9cm³ (Table 4.6) with a mean volume of 10.23±0.67cm³ were measured with an overall accuracy error of -1.16±0.5cm³ (1.25mm CT slice thickness) and -1.7±0.5 cm³ (3mm CT slice thickness).
- Overall, bone defects with most clinically relevant volumes in the range 2.01cm³-10.81cm³, (mean 5.46±3.8cm³), were measured with a mean accuracy error of -0.72±0.64 (1.25mm CT slice thickness) and -0.74±0.9cm³ (3mm CT slice thickness).

Combined bone defects:

- All 6 combined bone defects with mean volume 4.56±3.7cm³ were correctly identified and measured with a mean accuracy of -0.92±0.4cm³ (1.25mm CT slice thickness) and -1.28±1.18cm³ (3mm CT slice thickness).

Table 4.7 Mean volumetric errors for detected bone defects ≥0.4 & <2cm³ adjacent to PCA acetabular component according to anatomical location and CT slice thickness.

Bone defect location (n=number of bone defects)	Mean bone defect size(cm³)	CT slice thickness (mm)	Accuracy Error (cm³)	Intra-observer error (cm³)	Inter-observer error
Ilium (n=1)	0.799	1.25	-0.17	0.01	0.99
		3	-0.12	0.02	0.991
Anterior wall (n=2)	0.531	1.25	-0.05	0.02	0.196
		3	-0.01	0.03	0.462
Medial wall (n=2)	0.43	1.25	-0.09	0.05	0.138
		3	-0.03	0.06	0.01
Posterior wall (n=2)	0.514	1.25	-0.16	0.04	0.324
		3	-0.19	0.05	0.807
Pubis (n=2)	0.482	1.25	0.12	0.03	0.633
		3	0.19	0.03	0.949
Ischium (n=1)	0.672	1.25	-0.1	0.02	0.646
		3	0.09	0.01	0.655

Table 4.8 Mean volumetric errors for detected bone defects >2 &≤9cm³ adjacent to PCA acetabular component according to anatomical location and CT slice thickness.

Bone defect location (n=number of bone defects)	Mean bone defect size (cm³)	CT slice thickness (mm)	Accuracy Error (cm³)	Intra-observer error (cm³)	Inter-observer error
Ilium (n=2)	2.01	1.25	-0.35	0.03	0.99
		3	-0.25	0.06	0.991
Pubis (n=3)	3.06	1.25	-1.37	0.09	0.452
		3	-1.17	0.08	0.368
Ischium (n=2)	2.96	1.25	-1.5	0.1	0.646
		3	-1.327	0.153	0.655

Bilateral THR prostheses

Single bone defects

- In the presence of a contralateral prosthesis, single bone defects with mean volume 4.7±3.49cm³ (range 2.01-10.81cm³) were measured with a mean accuracy error of -0.53±0.78 cm³ (1.25mm CT slice thickness) and -0.62 ± 0.84cm³ (3mm CT slice thickness).

Combined bone defects:

- In the presence of a contralateral prosthesis, combined bone defects with mean volume 3.63±3.3cm³ were measured with a mean accuracy error of 0.03 ± 0.37 cm³ (1.25mm CT slice thickness) and -0.28±0.54cm³ (3mm CT slice thickness).

Bias (difference between the true and observed values) according to prosthesis type, site, thickness and size using a linear mixed effects model.

Single bone defects (HG or PCA prosthesis)

Bias was assessed according to the following factors:

1. Prosthesis type (HG or PCA)
2. Site of bone defects (ilium, ant.wall, med.wall, post.wall.pubis, ischium)
3. CT slice thickness (1.25mm or 3mm)
4. Size of bone defects (>0.05&≤0.4cm³; >0.4&≤2cm³; >2&≤9cm³; >9cm³)

Table 4.9 Type 3 Tests of Fixed Effects for single bone defects

Effect	P Value
Prosthesis Type	**<0.0001**
CT slice thickness	0.1917
Site of bone defects	**<0.0001**
Size of bone defects	**<0.0001**

Table 4.9 shows the significance of predictor variables in the model. The table shows that:

1. Independently of CT slice thickness (1.25mm or 3mm), site of bone defects (Ilium, ant.wall, med.wall, post.wall, pubis, ischium) and defects size (>0.05&≤0.4cm³; >0.4&≤2cm³; >2&≤9cm³; >9cm³), there was a significant difference in bias between Hg and PCA prostheses ($p < 0.0001$).
2. Independently of prosthesis, site and size, there was no evidence for a difference in bias between 1.25 and 3mm CT slice thicknesses ($p = 0.1917$).
3. Independently of prosthesis, CT slice thickness and size, there was a significant difference in bias between the six sites ($p < 0.0001$).
4. Independently of prosthesis, CT slice thickness and site, there was a significant difference in bias between the four sizes ($p < 0.0001$).

Table 4.10 Adjusted Means (Single bone defects, HG or PCA prosthesis)

Effect	Prosthesis type	CT slice thickness	Site of bone defects	Size of bone defects	estimate	Standard error
Prosthesis	Hg				-0.09418	0.08312
Prosthesis	PCA				-0.2174	0.08364
Thickness		1.25mm			-0.1375	0.08331
Thickness		3mm			-0.1741	0.08340
Site			ant.wall		-0.2055	0.09305
Site			ilium		-0.3225	0.08500
Site			ischium		-0.1285	0.08829
Site			med.wall		-0.1658	0.09237
Site			post.wall		-0.08735	0.09476
Site			pubis		0.09698	0.08744
Size				>0.4&≤2cm³	-0.02459	0.08503
Size				>0.05&≤0.4cm³	-0.04988	0.08569
Size				>9cm³	-0.8313	0.08853
Size				>2cm³&≤9cm³	-0.00495	0.08607

Table 4.10 shows the mean bias according to each predictor variable in the model, adjusted for dependence in the data. Bias was larger (in terms of the absolute distance from 0) in the PCA compared to the HG prosthesis (mean bias -0.2174 vs. -0.0942, p<0.0001). There was little difference in bias between the two CT slice thicknesses (mean bias -0.1375 vs. -0.1741, p=0.1917).

Overall conclusions: There was no difference in bias between 1.25mm and 3mm CT slice thicknesses (p = 0.1917). Bias was larger in the PCA prosthesis compared to the Hg prosthesis (p < 0.0001) and varied across the six sites of measurement (p < 0.0001) and four sizes (p <0.0001).

Combined Defects (HG or PCA prosthesis)

Bias was assessed according to the following factors:

1. Prosthesis type (HG or PCA)
2. Sites involved (i+mw, aw+p, pw+isch)
3. CT slice thickness (1.25mm or 3mm)
4. Size of bone defects (>2cm³&≤9cm³, >9cm³)

Again a linear mixed effects model was used to compare bias according to prosthesis type, site of bone defects, CT slice thickness and size of bone defects (Table 4.11).

Table 4.11 Type 3 Tests of Fixed Effects for combined bone defects

Effect	P Value
Prosthesis Type	**0.0005**
CT slice Thickness	**0.0019**
Site of bone defects	**0.0004**
Size of bone defects	**<.0001**

Table 4.12 Adjusted Means (Combined bone defects, HG or PCA prosthesis)

Effect	Prosthesis type	CT slice thickness	Site of bone defects	Size of bone defects	Estimate	Standard Error
Prosthesis	Hg				-0.3798	0.4964
Prosthesis	PCA				-0.8544	0.4959
CT slice thickness		1.25mm			-0.4089	0.4959
CT slice thickness		3mm			-0.8253	0.4964
Site			I+mw		-0.5910	0.7822
Site			aw+p		-1.4531	0.6084
Site			pw+isch		-0.2383	0.5692
Size				>9cm³	-1.1409	0.4999
Size				>2cm³&≤9cm³	-0.09333	0.4980

Table 4.12 shows the mean bias according to each predictor variable in the model, adjusted for dependence in the data.

Overall conclusions: Bias was larger in the PCA prosthesis compared to the Hg prosthesis (-0.8544 vs. -0.3798, p = 0.0005), larger for the 3mm thickness compared to the 1.25mm thickness (-0.8253 vs. -0.4089, p = 0.0019) and larger in the >9cm³ size compared to the >2cm³ & ≤9cm³ size (-1.1409 vs. -0.0933, p <0.0001). Bias was also found to vary across the three sites of measurement (p = 0.0004).

Single Defects (Bilateral THR prosthesis)

Bias was assessed according to the following factors:

1. Site of bone defect (ilium, ant wall, med wall, post wall, pubis, ischium)
2. CT slice thickness (1.25mm or 3mm)
3. Size of bone defects (>0.4&≤2cm³, >2&≤9cm³, >9cm³)

A linear mixed effects model was used to compare bias according to site, thickness and size (Table 4.13).

Table 4.13 Type 3 Tests of Fixed Effects for single bone defects (Bilateral THR prostesis).

Effect	P Value
CT slice Thickness	0.5677
Site of bone defects	**<0.0001**
Size of bone defects	**<0.0001**

Table 4.14 Adjusted Means (Single bone defects, Bilateral prosthesis)

Effect	CT slice thickness	Site of bone defects	Size of bone defects	Estimate	Standard Error
Thickness	1.25mm			-0.2176	0.1562
Thickness	3mm			-0.2747	0.1565
Site		ant.wall		-0.5899	0.2936
Site		ilium		-0.5269	0.1664
Site		ischium		-0.02320	0.1879
Site		med.wall		-0.5638	0.3268
Site		post.wall		-0.5502	0.2959
Site		pubis		0.2491	0.1768
Size			>0.4&≤2cm³	0.04313	0.2116
Size			>9cm³	-0.7814	0.1668
Size			>2&≤9cm³	0.2717	0.1943

Table 4.14 shows the mean bias according to each predictor variable in the model, adjusted for dependence in the data.

Overall conclusions: There was no difference in bias between the 1.25mm and 3mm CT slice thicknesses ($p = 0.5677$). Bias varied across the six sites of measurement ($p < 0.0001$) and across the three sizes ($p < 0.0001$).

Combined Defects (Bilateral THR prosthesis)

Bias was assessed according to the following factors:

1. Sites involved (i + mw, aw + p, pw + isch)
2. CT slice thickness (1.25mm or 3mm)
3. Size of bone defects (>2&≤9cm³, >9cm³)

A linear mixed effects model was used to compare bias according to site, thickness and size (Table 4.15).

Table 4.15 Type 3 Tests of Fixed Effects for combined bone defects (Bilateral THR prostesis).

Effect	P Value
CT slice Thickness	0.1368
Site of bone defects	**0.0015**
Size of bone defects	**0.0005**

Table 4.16 Adjusted Means (Combined bone defects, Bilateral prosthesis)

Effect	CT slice Thickness	Site of bone defects	Size of bone defects	Estimate	Standard Error
CT slice Thickness	1.25mm			-0.1046	0.1109
CT slice Thickness	3mm			-0.3009	0.1109
Site		I+mw		0.05361	0.1205
Site		aw+p		-0.7308	0.1664
Site		pw+isch		-0.1951	0.1205
Size			>9cm³	-0.5514	0.1246
Size			>2&≤9cm³	0.02967	0.1072

Overall conclusions: Bias appeared unrelated to thickness (p = 0.1361). Bias was larger in the size >9cm³ than the size >2&≤9cm³ (-0.5514 vs. 0.02967, p = 0.0005) and varied across the three sites of measurement.

The findings of this study resulted in the development of the following CT scan protocol for assessment of THR patients for PO.

THR CT Protocol (Extended CT scale)

Application: CT assessment of THR patients for Periprosthetic Osteolysis

Pre-programmed Protocol: Hip Spiral

Patient Position: Supine, Feet first

Scan Area / Direction: Top of SI joint to 2cm bellow the fem.stem

Mode: Spiral

Scanner Used: Siemens Volume Zoom

kV: 140kV

mAs: 200mAs

Time per Rotation (sec): 1second rotation (or 0.75)

Detector Collimation (mm): 4X1mm 0º Gantry Angle

Data Reconstruction Interval (mm): 1.25mm thick/0.8mm apart

Algorhitm / Kernel: B 50s Extended CT scale

FOV: 165

Multi-Planar Image Reconstruction: 1.5mm/1.5mm apart

axial

coronal

sagittal

Filming: 3mm/3mm apart + extended scale B 50s

4.4 Discussion

In this *in-vitro* validation study, a spiral multi-slice CT scanner with extended CT scale (up to 30,700 HU) was able to accurately and reliably measure single and combined bone defects in all acetabular and periacetabular areas adjacent to both titanium (HG) and cobalt-chrome (PCA) acetabular components inserted in a bovine hemi-pelvis. The CT technique described in this chapter was able to detect simulated bone defects in the range 0.013-10.81cm³ in all acetabular and periacetabular areas with overall sensitivity of 97% and 93% (1.25mm and 3mm CT slice thickness) for HG prosthesis and 81% and 80% (1.25mm and 3mm CT slice thickness) for PCA prosthesis and 100 % specificity for both of them. The accurate identification of bone defects as small as 0.013-0.087cm³ means that the 3-5mm wide area directly adjacent to the acetabular component could be adequately monitored to identify early pelvic osteolysis. This is essential to prevent the progression of these bone defects into uncontained segmental deficiencies. The correct detection of simulated bone defects adjacent to the fixation screws as demonstrated here and in section 3.3, would improve the monitoring of potential access channels for the join fluid to the surrounding bone.

Single bone defects of more clinically relevant volumes (range 2.01cm³-10.81cm³) adjacent to both HG and PCA prosthesis were correctly identified (100% sensitivity and 100% specificity). However, bias varied across the different sites ($p<0.0001$) and related to the prosthesis type ($p<0.0001$) and bone defects size ($p<0.0001$), but not to the CT slice thickness ($p=0.1917$).

Combined bone defects (involving two neighbouring areas) with mean volume of 4.56cm³ (range 1.27cm³-9.21cm³) were correctly detected. The accuracy and

precision of the CT volume measurement depended on the prosthesis type, the CT slice thickness and the bone defect size.

In the presence of bilateral THR prostheses (HG+PCA) all bone defects in the range 2.01cm³-10.81cm³ were correctly detected. There were no differences in the accuracy of volume measurements of bone defects adjacent to bilateral THR (HG+PCA) or unilateral prostheses. The mean accuracy error was -0.02±0.4cm³, compared with 0.03±0.4cm³ for HG and -0.3±0.2cm³ for PCA unilateral THR prosthesis.

A limitation of this study is that the *in-vitro* validation was performed on bovine acetabular bone. An *in-vivo* validation study would be of greater value, however, intra-operative validation of the CT-derived measurement would be very difficult and impossible in some cases for the following reasons. First, lesions hidden behind stable acetabular components could not be accessed and measured properly. Second, in revision surgery there is unavoidable bone stock loss during the removal of the acetabular component that could compromise measurements. Third, another potential bone loss from the surrounding bone is during the surgical debridement of fibrous tissues from the osteolytic cavity, which could change the original volume. An *in-vitro* validation of the CT-derived measurement on fresh-frozen cadaver bones was not possible for some legal and ethical issues. Preliminary work showed that use of a human cadaver acetabulum specimen was made impossible by the very poor cancellous bone quality of the formalin-treated cadaver bones, as was the creation of simulated bone defects of volume smaller than $1cm^3$. In addition, the air that tracked into the porotic cadaver bone and the freezing/defrosting procedures (from -20°C to room temperature) provided additional challenges for the lesion detection. For the fresh-frozen bovine acetabulum specimens single and combined simulated bone

defects of different volume were reproduced in all 6 possible locations, which is unlikely to be observed in a single patient, but represented different clinical scenarios.

The use of a THR model in this in-vitro validation study created some challenges that probably have reflected on the detection and the accuracy of the volume measurements. First, the typical characteristic of an osteolytic lesion – the sclerotic border, was not simulated, which made the detection more difficult, especially in the presence of cobalt-chrome acetabular components (PCA) with higher attenuation coefficient. Second, the acetabular component was not in-grown by the surrounding bone, which created a “gap” (radiolucent line) and the mapping of the simulated bone defects by free-hand followed an imaginary line parallel to the surface of the component.

Another limitation is the absence of soft tissues in the specimens, which could have influenced the image quality of the canselous bone. Water was used to simulate soft tissues, following the experience of other authors (Claus et al., 2003).

The radiation dose from CT examinations is a very sensitive and important issue for the safety of the patient. The resulting radiation dose from the CT protocol developed in this study is in agreement with the guidelines proposed by the National and International standards. When adapted for use with different CT scanners, further reduction could be achieved with automatic exposure control technique.

4.5 Conclusions

The findings described in this chapter show that, in experimental models of THR-associated bone loss, it is feasible to use CT scanning to measure the volume of

defects in the cancellous bone in all acetabular and periacetabular areas adjacent to noncemented acetabular components of THR. Using the scanning parameters that were determined and presented in the CT protocol, together with metal artifact reduction software and extended CT scale technique, accurate and reliable volumetric measurements can be obtained.

Despite some limitations, this study is the first to date to provide detailed validation of the CT quantification of bone defects adjacent to THR acetabular components.

Chapter 5

Clinical Application

5.1 Introduction

This chapter describes two clinical applications of the CT technique developed for use around metal THR prostheses. These clinical studies were designed to investigate, first, the distribution of osteolysis around acetabular cups of two designs and, second, the factors that may influence the progression of osteolysis. The studies have been published as listed on page vii, and were performed in collaboration with the authors listed under each study.

5.2 Study 1

DISTRIBUTION OF PERIACETABULAR OSTEOLYTIC LESIONS VARIES ACCORDING TO COMPONENT DESIGN

Aims: To examine the volume, location and number of PO lesions in patients with long-term uncemented THR of two acetabular components design: multi-hole shell with additional screw fixation and solid shell with single central hole.

5.2.1 MATERIALS AND METHODS

At the Royal Adelaide Hospital (RAH) patients presenting to clinic for review of their long-term cementless THR are routinely sent for a CT scan if there is osteopenia suggesting osteolysis or an osteolytic lesion on plain radiographs. Patients are referred to this institution from multiple sources for either review of their THR or for symptoms suggesting that revision surgery is required. For this study, the CT scans of these patients were retrospectively analysed. The following inclusion criteria were applied: patients who had undergone a CT scan for suspected steolysis; a minimum of 10 years after primary THR; and the use of either a cementless commercially pure titanium fiber mesh-coated hemispheric HG-1 (Zimmer Ltd, Warsaw, Ind) acetabular component or a cementless cobalt-chrome PCA acetabular component (Howmedica, Rutherford, NJ). Only HG-1 acetabular components fixed with 2 screws and PCA

acetabular components with a single central dome hole, lateral peg, and no screw fixation were included. Forty-nine patients (57 hips) met the inclusion criteria. All patients gave informed consent, and this study was approved by the RAH Human Ethics Review Committee. Of the 57 hips, 38 hips in 31 patients had a primary cementless HG-1 acetabular component. All were implanted after line-to-line reaming and fixation with 2 screws. The HG-1 metal shell had 11 holes and a modular polyethylene liner inserted. The femoral component was an HG-1 stem in all hips. In 18 patients, 19 hips had a primary cementless PCA acetabular component. All were press-fitted into the acetabulum. A snaplock modular polyethylene liner was then inserted in all 19 hips. The femoral component was a PCA stem in 18 hips and an Exeter stem in 1 hip. Two patients with an HG-1 acetabular component and 6 patients with a PCA acetabular component had CT scans before revision surgery rather than as part of their routine clinical management. The median time since THR was 16 years (range, 10-19 years) for the HG-1 cohort and 15 years (range, 11-18 years) for the PCA cohort. The patient and prosthesis-related parameters of the 2 cohorts are summarized in Table 5.1. There was no difference between the 2 cohorts for any of the parameters listed apart from femoral head size ($P < .0001$).

Revision of hips during study period

Eleven of the thirty-eight hips (29%) with HG-1 acetabular components and 7 of the 19 hips (37%) with PCA acetabular components underwent reoperation during the study period. Three of the eleven hips with HG-1 acetabular components and 6 of the 7 hips with PCA acetabular components were from patients referred from other hospitals for reoperation at the RAH. In all cases, the revision surgery was performed by the same surgeon (DWH). Loosening of the acetabular component was graded intraoperatively using an established grading system (Howie et al., 1990). For cementless implants, the prosthesis-cement interface grading is not applicable, and the cement-bone interface becomes the prosthesis-bone interface.

TABLE 5.1 Patient and prosthesis-related parameters

	HG-1	PCA	p value from tests of association
Number of hips	45	22	-
Number of patients	35	20	-
Primary THR: revision resurfacing THR: revision THR	38:5:2	19:1:2	0.535[#]
Gender (male: female)	27:18	8:14	0.117[#]
Age at THR* - median (range)	59 (38 - 70)	55 (31 - 70)	0.114[†]
Years of implantation - median (range)	16 (10 - 19)	15 (11 - 20)	0.195[†]
Femoral head diameter ** (22:26:28:32mm)	19:23:3:0	0:11:1:10	<0.0001[#]
Harris Hip Score at latest follow-up - median (range)	78 (34 – 100)	83 (51 – 98)	0.399[†]

* Total hip replacement when HG-1 or PCA acetabular component implanted

** Difference between the two cohorts p<0.0001

[#]Chi square or Fisher exact test

[†]Mann Whitney U test

Computed Tomography

High-resolution spiral multislice CT scans (Somatom Volume Zoom, Siemens, Munich, Germany), using an extended CT scale technique (window level up to 30710 Hounsfield units) to suppress the resulting metal artefact (Link et al., 2000), were used to identify and measure the volume of acetabular OL. Scans of the hip were made according to specific parameters (140 kV, 200 mA, 0.75-second rotation speed, 1.25-mm slices, 1-mm feed) from the top of the sacroiliac joint to 2 cm distal to the end of the femoral prosthesis. The reconstruction interval was 0.8 mm, with a slice thickness of 1.25 mm. The CT data were formatted in DICOM, saved to CD, and then downloaded onto a Picker PQ6000 workstation (Picker International Inc, Cleveland, Ohio) for analysis. The quality of the CT images was improved by adjustment of the Window and Level settings. Osteolysis was defined as a demarcated nonlinear lesion more than 3 mm in diameter (Maloney et al., 1999). Cross sections of the defects were identified on consecutive axial slices, and the inner border of each defect was traced using a computer mouse (Fig.5.1). Osteolytic volume was calculated using algorithms coded into the commercial image analysis CT software (PQ 6000 Voxel Q FALCON, Picker International Inc). Lesion volumes were combined to give total OL volume for each hip. All measurements were made by a single observer (RS) trained in quantitative CT analysis. The *in-vitro* measurement error (mean ± SD) of this CT technique is 0.55 ± 0.45 cm^3 and 0.72 ± 0.64 cm^3 for a mean lesion size of 5.5 cm^3 adjacent to HG-1 and PCA components, respectively. Rim-related lesions were defined as those with at least part of the lesion being in contact with the rim of the acetabulum in one or more coronal or sagittal views and therefore communicating with the joint space. Screw or empty hole–related lesions were defined as those lesions adjacent to prosthesis fixation screws or empty shell holes. Combined lesions were defined as lesions that were both rim related and also adjacent to shell holes or fixation screws. The location of screw

holes were described as those in the central dome of the acetabular component or in the mid-dome of the acetabular component. The lesion classification was undertaken using coronal and sagittal images. The proportions of each lesion type were described according to the total number of OL lesions in each group. The bone sites used to describe the location of OL lesions were the ilium, medial wall, anterior wall, posterior wall, ischium, and pubis. The presence of OL lesions in these bone sites was identified on axial slices. Differences between the 2 patient cohorts, with respect to patient and implant-related variables and the distribution and size of the OL lesions, were examined using Fisher exact, χ^2, and Mann-Whitney U tests (Table 5.1). Statistical analysis was performed using GraphPad Prism software (V4.00 for Windows, GraphPad Software, San Diego, Calif). Probability values less than .05 indicated a significant difference.

5.2.2 RESULTS

Using CT, periacetabular OL was detected in 35 (92%) of the 38 hips with HG-1 components and in all hips with PCA acetabular components (100%).

Number and Volume of Osteolytic Lesions

One hundred eighteen OL lesions were detected adjacent to the 35 HG-1 components with detectable OL, giving a mean number of lesions per hip of 3.4. Thirty-five OL lesions were detected adjacent to the 19 PCA components with detectable OL, giving a mean number of lesions per hip of 1.8. However, despite the difference in the number of OL lesions per hip, the total volume of OL lesions was not significantly different between the 2 acetabular component designs (P = .32). The mean volume of OL lesions was 11.1 cm3 (range, 0.7-49 cm3; median, 6.6cm3) in hips implanted with HG-1 components and 9.8 cm3 (0.4-52 cm3; median, 4.4 cm3) in hips implanted with PCA components. Dividing the total lesion volume by the total number of lesions, the average lesion volume was 3.3 cm^3 in hips with HG-1 components and 5.0 cm^3 in hips with PCA components.

Mapping of osteolytic lesion on consecutive CT slices

Fig.5.1 Diagram showing mapping (yellow line) of a rim-related osteolytic lesion (arrows) in the ilium on consecutive CT slices. Presented are the classical characteristics of the acetabular periprosthetic osteolysis: a “ballooning” cavity with missing trabeculi, surrounded by a sclerotic border and communicates with the joint.

Location of Osteolytic Lesions According to Acetabular Component Design

The proportion of rim-related, screw or empty hole–related, and combined osteolytic lesions associated with HG-1 and PCA acetabular components is shown in Table 5.2. Eighteen percent of osteolytic lesions detected adjacent to HG-1 components were rim-related, 53% were screw or empty hole-related, and 29% were combined (Fig. 5.2). Of the 63 screw or empty hole–related lesions, 24 lesions were associated with holes containing screws, 30 lesions were associated with empty screw holes, and 9 lesions were larger and associated with 2 holes, one containing a screw and one empty. Of the 34 combined lesions, 79% were rim-related lesions combined with hole-related lesions located in the central dome, and 21% were rim-related lesions combined with hole-related lesions in the mid-dome of the component. In hips with PCA components, 51% of the osteolytic lesions detected were rim related, 9% were hole- related, and 40% were combined (Fig. 5.3). Because only a central hole is present in the PCA component, the latter group combined rim-related lesions with the central hole–associated lesions. A significant difference in the proportion of rim-related, hole-related, and combined lesions was found between the 2 acetabular component designs ($P < .0001$). This was primarily because of the large numbers of hole-related lesions detected adjacent to HG-1 components. These hole-related lesions made up 53% of the total number of lesions detected around HG-1 components and largely also explain the increase in the average number of lesions detected adjacent to the HG-1 components compared to PCA components. In contrast, only 3 (9%) of 35 osteolytic lesions detected adjacent to PCA components were only hole-related lesions.

Location of Osteolytic Lesions According to Bone Sites

The location of the periacetabular osteolytic lesions according to bone sites is presented in Fig. 5.4. All 35 hips with HG-1 acetabular components and detectable osteolysis had lesions in the ilium. The next most common site of osteolytic lesions

was the medial wall (63% of hips). In 71% of hips that had osteolysis around HG-1 components, osteolytic lesions were present in more than one bone site. Similarly, in hips with PCA acetabular components, osteolysis was most commonly detected in the ilium (89% of hips). The next most common site of osteolytic lesions was the medial wall (68% of hips). In 63% of hips THRt had osteolysis around PCA components, osteolytic lesions were present in more than one bone site. No osteolytic lesions were detected in the pubis in either group.

Revision of Hips during Study Period

At reoperation, 7 of the 11 HG-1 acetabular components were found to be well fixed at the prosthesis-bone interface, and only liner exchange was undertaken. In the other 4 hips, 2 HG-1 acetabular components were loose at the prosthesis-to-bone interface and were replaced, and 2 acetabular components were replaced due to severe liner wear and fracture of the metal shell. At reoperation of the hips with PCA acetabular components, 3 of the 7 PCA components were well fixed at the prosthesis-to-bone interface. Liner exchange was performed for one of these components. The other 2 acetabular components were replaced due to extensive osteolysis. Of the 7 PCA acetabular components, 4 were loose at the prosthesis-to-bone interface and were replaced. For the 2 HG-1 and 4 PCA acetabular components revised due to loosening, the mean volume of osteolysis was 23.2 cm^3 (range, 3.7-42.7 cm^3) and 3.8 cm^3 (range, 0.5-8.3 cm^3), respectively. This is in comparison to mean volumes of osteolysis of 12.7 cm^3 (range, 3.0-47.1 cm^3) and 14.7 cm^3 (range, 4.0-28.3 cm^3) for HG-1 and PCA acetabular components that remained well-fixed at revision. Although the number of acetabular components revised were small, there were no indications of an increase in volume of osteolysis around loose acetabular components.

TABLE 5.2 Proportion of rim-related, hole-related, combined and isolated osteolytic lesions associated with long-term implanted HG-1 and PCA acetabular components

Type of lesion	HG-1 n=42 hips	PCA n=21 hips
Rim-related	27 (19)	20 (51)
Hole-related	79 (54)	3 (8)
Combined	40 (27)	16 (41)
Isolated	0	0
Total	146	39

Results are expressed as the number of osteolytic lesions detected (% total number of lesions).

CT images of osteolytic lesions adjacent to H-G acetabular components

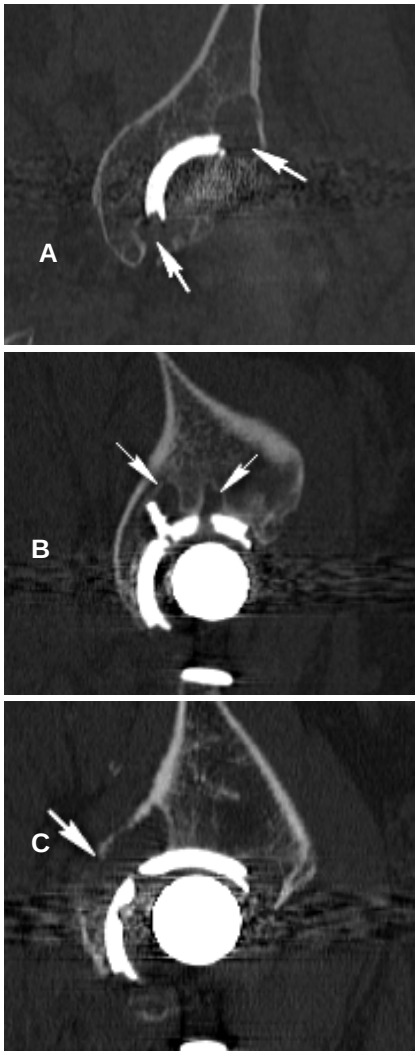

Fig.5.2 Coronal and sagittal CT images showing (A) rim-related, (B) hole-related and (C) combined osteolytic lesions (indicated by arrows) adjacent to H-G acetabular components.

CT images of osteolytic lesions adjacent to PCA acetabular components

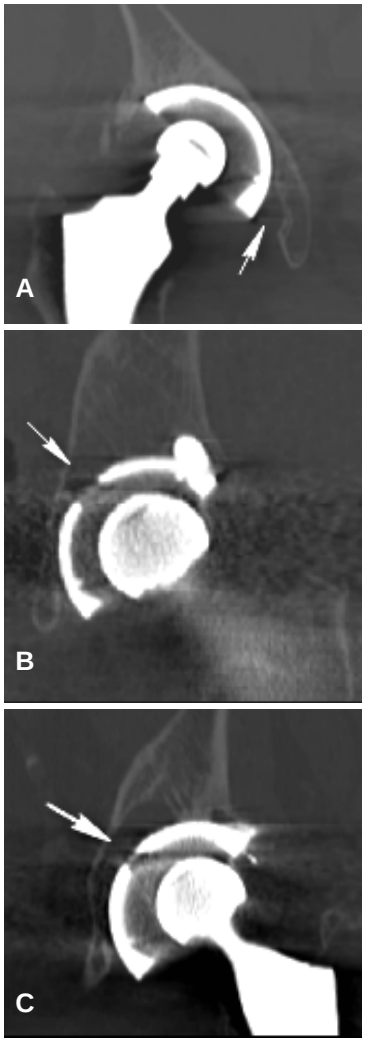

Fig.5.3 Sagittal and coronal CT images showing (A) rim-related, (B) hole-related and (C) combined osteolytic lesions (indicated by arrows) adjacent to PCA acetabular components.

5.2.3 DISCUSSION

The important finding in this study was that in the presence of a similar total volume of osteolytic lesions, there were significant differences in the distribution of osteolytic lesions around cementless acetabular components of different designs and methods of fixation. Acetabular components with multiple holes and screw fixation had more osteolytic lesions around screws or empty screw holes. In contrast, components with only one hole and press fit fixation had more rim-related lesions. A large number of the osteolytic lesions were detected in the ilium and medial, anterior, and posterior walls around both the HG-1 and PCA acetabular components. Most of these lesions would not easily be detectable on plain anteroposterior or oblique lateral radiographs. These findings emphasize the importance of CT as a radiographic tool for osteolysis detection and monitoring. Computed tomography has also been reported to aid in the planning of acetabular component revision surgery (Garcia-Cimbrelo et al., 2007). The most frequent locations of osteolytic lesions adjacent to a range of failed cemented and uncemented cups of different designs were reported to be the posterior wall, ischium, and medial wall (Garcia-Cimbrelo et al., 2007).

These results are consistent with the concept that the distribution of osteolytic lesions is dependent on the access of wear particles and joint fluid to the prosthesis-bone interface and reinforces the importance of potential channels of communication between the prosthesis-bone interface and the joint space in the development of the lesions (Schmalzried et al., 1997, Manley et al., 2002, Kitamura et al., 2005). Longitudinal studies using CT are required to investigate the origin of combined rim and central hole lesions and the role of screws and screw holes in the progression of periprosthetic OL. However, these results support the findings of others that the pattern of osteolysis is affected by acetabular component design (Schmalzried et al., 1999, Claus et al., 2001, Kitamura et al., 2005). Previous studies have found larger OL lesions around acetabular components with multiple holes compared with

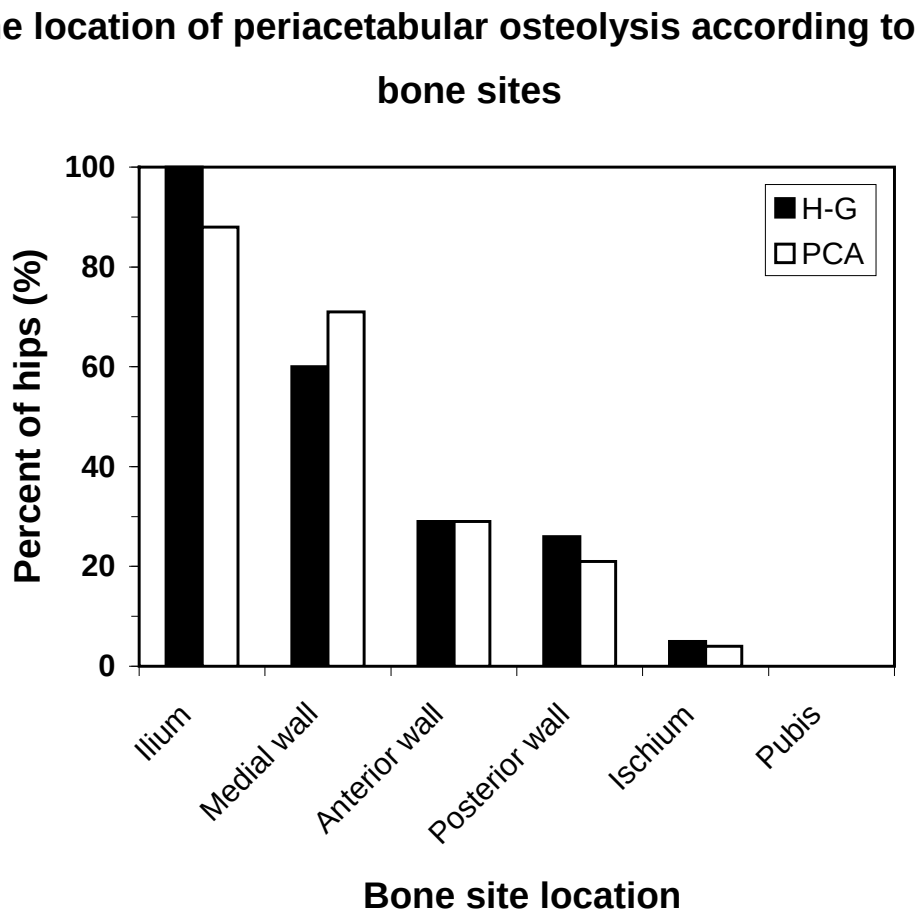

Fig.5.4 The location of periacetabular osteolysis according to the bone sites. The results are expressed as the percent of hips with osteolytic lesions detected in each of the bone sites adjacent to the 42 H-G and 21 PCA acetabular components with detectable osteolytic lesions.

acetabular components without holes (Claus et al., 2001, Kitamura et al., 2005), and these results do not support the use of screws. This needs to be balanced by the current findings, that demonstrate the greater propensity for peripheral OL of press-fit components, which likely makes these components more susceptible to loosening in the long term. Limitations of this study are that the PCA acetabular component is known to have worse long-term outcomes in terms of component loosening, and therefore, the results may not be able to be transposed to all press-fit designs. Further limitations include the differences in the metal combinations of the HG-1 and PCA shell and femoral head, being titanium/cobalt-chrome for the HG-1 and cobalt-chrome/cobalt-chrome for the PCA, which may have influenced the detection of OL lesions, particularly small lesions in bone immediately adjacent to the metallic implant (Rinkel et al., 2008). There are other limitations. The patients included in this study were those presenting either for long-term follow-up or for revision surgery and who had radiographic suggestion of osteolysis. The 2 patient groups were therefore not matched for the many patient and prosthesis-related factors that may affect wear of the prosthesis and, ultimately, development of osteolysis. These include patient activity and other clinically relevant variables and prosthesis design factors, including liner fixation, material differences, relative stiffness of the metal shell, and articulation differences, as well as differences in fixation technique. It was impossible to compare the volume of polyethylene wear between the 2 acetabular components in this study because the femoral head could not be visualized on the most recent radiographs for most PCA acetabular components due to the cobalt-chrome acetabular shell. However, it has been shown previously that PE wear is moderately associated with OL around HG-1 acetabular components but that the presence of outliers, in which hips with large volumes of PE wear were not associated with large OL lesions, suggests that factors other than wear may determine the extent of OL (Howie et al., 2007). The results of the current study suggest that access of wear particles and joint

fluid to periprosthetic bone is required, and this access is partially determined by acetabular component design. It has been suggested that both screw-in and bone ingrowth press-fit acetabular component designs lack long-term stability, whereas bone ingrowth with screw fixation results in a low rate of radiographic loosening (Illgen 2nd et al., 2002). The findings of the current study add to these observations. In a randomized study of 177 THR with a mean follow-up of 9 years (Xenos et al., 1999), the PCA acetabular component was found to have a lower survival to the end point revision for any reason compared to the HG screw-fixed acetabular component, and this has been attributed to poor fixation. The results of this study suggest, however, that the propensity to peripheral OL may be a further contributing factor to loosening in the long term and may have some influence on mid-term results. This supports the contention that poor initial fixation contributes to osteolysis-induced loosening.

5.2.4 Conclusion

This cross-sectional study demonstrates that despite a similar total volume of osteolytic lesions adjacent to cementless acetabular components of long-term duration, there were differences in the distribution of lesions between 2 different component designs.

Components with multiple holes had more hole-related osteolytic lesions, and components with only one hole had predominately peripheral rim-related lesions. Although there are concerns regarding screw or screw hole–associated osteolysis, these findings suggest that peripheral fixation may be well maintained in the long term with the use of a multiple-hole acetabular component with screw fixation.

This study has been accepted for publication as listed on page vii, and was performed in collaboration with the authors listed under the study.

5.3 Study 2

PROGRESSION OF ACETABULAR PERI-PROSTHETIC OSTEOLYTIC LESIONS MEASURED BY COMPUTED TOMOGRAPHY

Aims: To determine the size and progression in size of osteolytic lesions adjacent to uncemented acetabular components of THR prostheses, to quantify their relationship with the polyethylene wear, and then to examine the association between these findings and component migration and some clinical and implant-related variables.

5.3.1 Methods and Materials

The present study was approved by the institutional human ethics review committee, and all patients gave informed consent. At our institution, patients with THR, who are suspected of having PO around a cementless acetabular component on plain radiographs, are referred for a CT scan as part of their clinical management. In order to examine as homogenous a group of patients as possible, we established specific inclusion criteria for this retrospective study, including (1) a minimum duration of follow-up of 10 years after primary THR, (2) the use of a cementless Harris-Galante-1 acetabular and femoral component (Zimmer, Warsaw, Indiana), and (3) performance of the surgical procedure by the same surgeon. Twenty-eight patients (35 hips) met the inclusion criteria.

All acetabular components were implanted after line-to line reaming. Fixation of the metal shell was augmented with at least two screws. The median size of the metal shell was 52 mm (range, 48 to 62 mm), and all of the ultra-high molecular weight PE liners were sterilized by means of gamma irradiation in air. The femoral heads were constructed of modular cobalt-chromium and had a diameter of 22 mm (13 hips), 26

mm (18 hips), or 28 mm (4 hips). The median age of the patients at the time of the primary THR was 60 years (range, 35 to 70 years), and the mean time since the THR was 15 years (range, 10 to 19 years). Two patients (two hips) underwent revision surgery during the study period, and one patient (one hip) died 15 months after the initial CT scan. Of the remaining 25 patients (32 hips), 30 of the hips had a repeat CT scan at a median of 15 months (range, 12 to 27 months) after the initial CT scan.

High-resolution spiral multi-slice CT scans (SOMATOM Volume Zoom; Siemens, Munich, Germany), as described in Chapter 4, were used to identify and measure the volume of acetabular osteolytic lesions with use of a technique, whose validation is described in Chapters 3 and 4 (Stamenkov et al., 2003, Stamenkov et al., 2004). An extended CT scale technique with the window level up to 30710 Hounsfield units was used to suppress the resulting metallic artifact (Link et al., 2000). Scans of the hip were made according to specific parameters (140 kV, 200 mA, 0.75-second rotation speed, 3-mm slices, 1-mm feed) from the top of the sacroiliac joint to 2 cm distal to the end of the femoral prosthesis. The reconstruction interval on coronal and sagittal images was 0.8 mm, with a slice thickness of 1.25 mm. Osteolysis was defined as a demarcated nonlinear lytic lesion measuring >3 mm in diameter (Maloney et al., 1999). Cross sections of the defects were identified on consecutive slices, and the perimeter of each defect was determined by tracing the inner border of the defect with use of the computer mouse on a Picker PQ 6000 workstation (Picker International, Cleveland, Ohio). The volumes of isolated osteolytic lesions were calculated using algorithms coded into the commercial image-analysis software (Picker International) and were combined to give the total volume of osteolytic lesions (Fig.5.5). All measurements were made by a single blinded observer. To check reproducibility, a second blinded observer also measured the volume of the osteolytic lesions in five hips. The intra-observer and inter-observer measurement errors of

osteolysis volume were 2% and 3%, respectively. The change in the volume of osteolytic lesions between scans was expressed as the progression of osteolysis per year, with the assumption that osteolysis progression was linear over that time. Progressive osteolysis was defined as an increase in volume of >1 cm^3/yr. In all hips with progressive osteolytic lesions, and in particular those with large osteolytic lesions on the initial CT scan, the increase in the size of the osteolytic lesions was substantially greater than the error associated with the CT measurements (Walde, 2005).

For 31 of the 35 hips that underwent subsequent CT scans, immediate postoperative AP pelvic radiographs (made 8 to 10 days after surgery) and serial follow-up AP and lateral radiographs of the affected hip were available for review. As migration of the acetabular component into the osteolytic lesion might cause underestimation of the true size of the osteolytic lesion, the position of the acetabular component from the time of component implantation was measured on these serial digitized plain radiographs with use of Ein Bild Roentgen Analyse software (Krismer et al., 1995, Wilkinson et al., 2002, Phillips et al., 2002). The error of this technique has been reported to be ±1 mm (Krismer et al., 1995). A migrating component was defined as one with >3 mm of total migration since implantation (Shyterz et al., 1996).

The PolyWare software program (Draftware Developers, Vevay, Indiana), (Devane et al., 1999) was used to determine linear and volumetric polyethylene wear by comparing the immediate postoperative plain radiograph with radiographs made at the time of the CT scan. The mean of triplicate wear measurements made on each hip was used. The Poly Ware program has a reported accuracy of 0.38 mm for linear wear and 123 mm^3 for volumetric wear (Collier et al., 2003). To improve the accuracy

Three-dimensional images of acetabular periprosthetic osteolysis

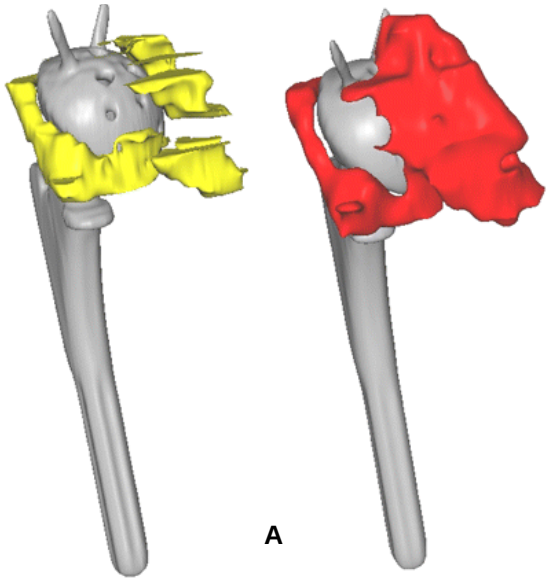

A

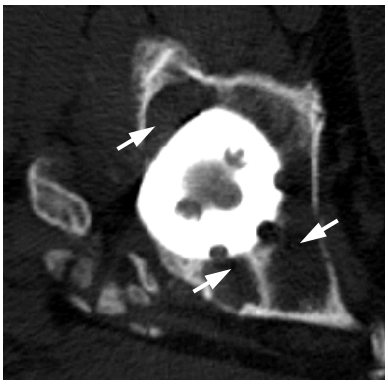

B

Fig.5.5 **A.** Three dimensional reconstructed images of CT scans of total hip replacements generated using True Life Anatomy© software (Adelaide, Australia). In this example, the total volume of acetabular osteolytic lesions measured was 26 cm^3 (yellow), increasing to 43 cm^3 (red) two years later. **B.** Selected image from the CT scan, showing areas of osteolysis around the acetabular component (arrows).

of the analysis in instances in which the edge of the head shadow was difficult to discern, automatic edge detection was disabled. Intra-observer error was 5% for linear wear measurements and 6% for volumetric wear measurements. Two of the 31 hips that were analyzed had extreme wear values (3173 and 4318 mm^3) and were confirmed as having wear-through of the acetabular liner at the time of subsequent revision surgery. These two hips were excluded from the wear analyses only.

To determine whether patient-related variables were associated with the volume of osteolytic lesions and/or progression in the size of osteolytic lesions, relevant values (patient age at the time of primary THR, gender, body mass index 28, the patient-reported Harris hip pain score 29, and the Harris hip score 29) were retrospectively obtained from data that had been prospectively entered into a joint replacement outcomes database. The patient's self-assessment of walking limitations was used to generate a Charnley classification (Charnley et al., 1972), and patient activity was assessed with use of a patient-reported 5-point activity scale (Johnston et al., 1991).

To avoid skewing of average data due to important outliers, the data in the present study was expressed as medians. Statistical analysis was performed with use of GraphPad Prism software (version 4.00 for Windows; Graph Pad Software, San Diego, California), with the level of alpha set at 0.05. Correlation analysis was undertaken with use of the Spearman rank correlation coefficient. It was determined that a minimum sample size of ten was required for correlation analyses with a power of 90% (PowerCalc). Associations between the size of the osteolytic lesions at the time of the initial CT scan and the rate of osteolysis progression as well as patient-related, clinical, and implant-related variables were examined with use of the Mann-Whitney U, Kruskal-Wallis, Fisher exact, or chi-square tests.

5.3.2 Results

PO was detectable with CT in 32 of the 35 hips, although all patients were selected for CT scans because of presumed detection of osteolysis on plain radiographs. The median volume of the lesions in hips with CT-demonstrated osteolysis was 8.1 cm^3 (mean, 12.6 cm^3; range, 0.7 to 49 cm^3). For the 31 hips, for which initial postoperative plain radiographs were available for comparison with the plain radiographs made just before the initial CT scan, the magnitude of migration was divided into two groups: acetabular components that had migrated >3 mm and those that had migrated ≤3 mm, according to the system described by Schyterz et al. (1996). Five acetabular components had migrated >3 mm (median, 5.0 mm; range, 3.6 to 7.2 mm). The median volume of osteolytic lesions as determined with CT in that group was 11.2 cm^3 (range, 0.7 to 16 cm^3). In contrast, 26 hips had migrated ≤3 mm (median, 2.0 mm; range, 0.3 to 3.0 mm); the median volume of the osteolytic lesions in that group was 5.9 cm^3 (range, 0 to 49 cm^3). The difference in size of the osteolytic lesions in the two groups was not significant ($p = 0.436$).

The results of tests of association between the size of the osteolytic lesions and patient-related, implant-related, and clinical variables are shown in Table 5.3. Good correlation was found between the size of the osteolytic lesion and the total volume of PE wear as well as the PE wear rate since implantation ($r = 0.780$ and $r = 0.760$, respectively). Hips with higher volumes of PE wear and higher PE wear rates tended to have larger osteolytic lesions ($p < 0.0001$). The presence or absence of acetabular component migration did not significantly influence this correlation ($p = 0.89$). Of interest, outliers were also identified with high wear rates (>80 mm^3/yr) but relatively small osteolytic lesions (Fig. 5.6).

Patients with higher activity scores, no walking limitations (Charnley grade A), or a larger femoral head size were also found to have significantly larger osteolytic lesions on the most recent CT scan (Table 5.3). The median volume of osteolytic lesions around acetabular components in patients with the activity categories sedentary, semi-sedentary, light labor or sports, and moderate manual labor and sports were 1.9, 7.4, 7.6, and 27 cm^3, respectively ($p = 0.009$). The median volume of osteolytic lesions in patients with no walking limitations (Charnley grade A) was 16 cm^3, compared with 5.4 cm3 in patients with walking limitations due to other joint or health problems (Charnley grade B or C) ($p = 0.006$). The median volume of osteolytic lesions around acetabular components with a 26 or 28-mm femoral head was 9.4 cm^3, as compared with a median volume of 5.1 cm^3 for lesions around acetabular components with a 22-mm femoral head ($p = 0.028$). In this cohort, the inclusion of hips with >3 mm of migration did not affect the median volumes of osteolytic lesions in any of the categories (Table 5.3).

Of the 30 hips that underwent repeat CT at a median interval of 15 months (range, 12 to 27 months), 16 (53%) had lesions that progressed in size during the study period (Fig. 5.7). The median size of the lesions in these 16 hips was 10.3 cm^3 on the initial CT scan, compared with 13.3 cm^3 on the repeat CT scan; this increase was significant ($p = 0.001$). The hips with osteolytic lesions that increased in size during the study period had significantly larger osteolytic lesions on the initial CT scan (median, 10.3 cm^3; mean, 17.2 cm^3; range, 1.9 to 45.3 cm^3) as compared with those with lesions that did not increase in size (median, 4.0 cm^3; mean, 5.3 cm^3; range, 0 to 28.2 cm^3) ($p = 0.002$). Importantly, 8 of the 9 hips with osteolytic lesions measuring >10 cm^3 on the initial CT scan had an increase in lesion size.

TABLE 5.3 Results of Tests of Association between the Volume of Osteolytic Lesions and Patient, Implant, and Clinical Variables

	All components (n=35)		
Variable	Descriptive statistics*	Correlation coefficient and p value	Test of Association
Osteolysis *(cm^3)*	7.5 (0-49)	-	-
Total volumetric PE wear *(mm^3)*	816 (170-2213)	r=0.780,p<0.0001ˆ	Linear regression analysis
Annual PE wear rate *(mm^3/yr)*	56 (11-140)	r=0.760, p<0.0001ˆ	Linear regression analysis
Age *(yrs)*	60 (35-70)	r=0.309, p=0.07ˆ	Linear regression analysis
Gender M:F ratio *(no. of hips)*	21:14	p=0.09#	Mann-Whitney U test
Body Mass Index *(<25, ≥25)*	15:20	p=0.960#	Mann-Whitney U test
Implant duration *(months)*	189 (120-225)	r=0.123, p=0.482ˆ	Linear regression analysis
Activity† (1:2:3:4:5:6)	0:7:13:10:5:0	p=0.009$	Kruskal-Wallis test
Charnley grade‡ (A:B:C)	9:4:22	p=0.006 A vs B,C)	Mann-Whitney U test
Harris Pain score§ (<40, ≥40)	15:20	p=0.582#	Mann-Whitney U test
Harris Hip score# *(points)*	82 (34-100)	r=0.130, p=0.517ˆ	Linear regression analysis
Femoral head size (22:26:28)	13:18:4	p=0.028# (22 vs 26,28)	Mann-Whitney U test

*The values are given as the median (with the range in parentheses) or as the distribution at the time of the latest computed tomography scan. †1 = bedridden or confined to wheelchair, 2 = sedentary, 3 = semi-sedentary, 4 = light labor or sports, 5 = moderate manual labor or sports, and 6 = heavy manual labor or vigorous sports (Johnston et al., 1991). ‡A = only one hip involved and with no other condition that interferes with walking, B = both hips involved but the rest of the body normal, and C = some other factor that interferes with walking ability (Charnley et al., 1972). §44 = no pain, or pain ignored; 40 = slight occasional pain, no compromise in activities; 30 = mild pain, no effect on average activities, rarely moderate pain with unusual activity; 20 = moderate pain, tolerable but with some limitations of ordinary work or activity; 10 = marked pain, severe at times, with serious limitations of activity; 0 = totally disabled, crippled, pain in bed, or bedridden (Harris et al., 1969). #90 to 100 = excellent, 80 to 89 = good, 70 to 79 = fair, and <70 = poor (Harris et al., 1969).

Relationship between the total volume of osteolytic lesions and the polyethylene wear rate

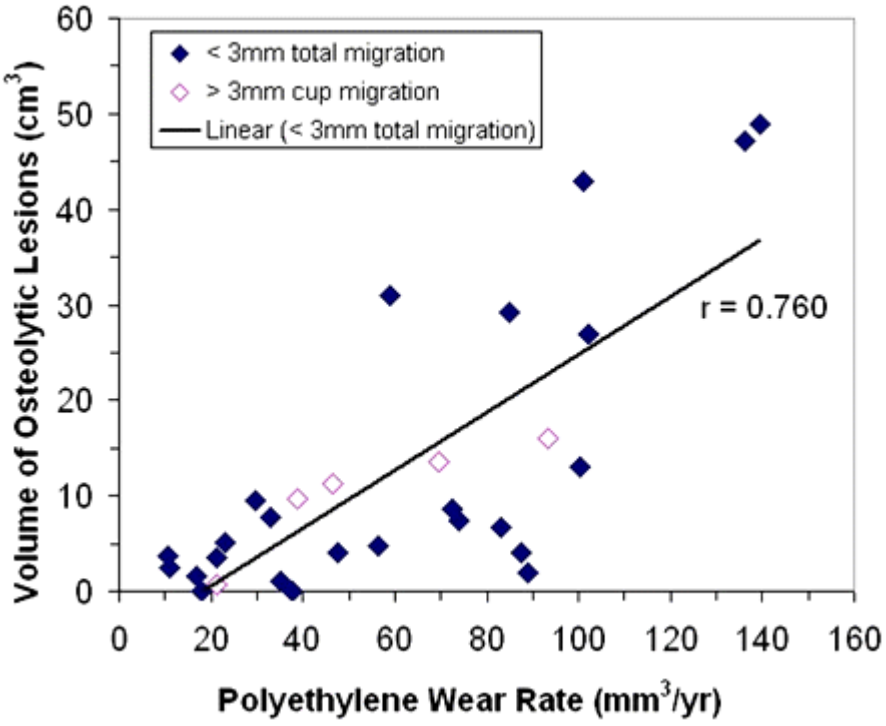

Fig.5.6 Relationship between the total volume of osteolytic lesions and the polyethylene wear rate. The polyethylene wear rate was calculated as the total wear volume divided by the time since prosthesis implantation. Components that had migrated >3 mm over the life of the implant were excluded from the regression analysis.

Osteolytic lesions measuring >10 cm^3 in volume on the initial CT scan were 2.5 times (95% confidence interval, 1.3 to 4.8 times) more likely to progress in size over one year than osteolytic lesions measuring ≤10 cm^3 in volume.

In the 16 hips with an increase in the size of osteolytic lesions between the time of the initial CT scan and the time of the repeat CT scan, the median volume of PE wear and the median PE wear rate were significantly higher than those in the 14 hips in which the osteolytic lesions did not progress in size ($p = 0.013$ and 0.009, respectively) (Table 5.4). Good correlation ($r = 0.690$) was found between the PE wear rate at the time of the initial CT scan and progression in the size of the osteolytic lesions (Fig. 5.8). In hips with a volumetric polyethylene wear rate of <40 mm^3/year, the progression in the size of acetabular osteolytic lesions was small. The presence or absence of acetabular component migration did not significantly influence this correlation ($p = 0.854$). A significant association was also found between progression in the size of the osteolytic lesions and femoral head size (Table 5.4). There were significantly more hips with osteolytic lesions that progressed in size around acetabular components with a 26 or 28-mm femoral head than around acetabular components with a smaller (22-mm) femoral head ($p = 0.019$). No other variables examined were significantly associated with the progression in the size of acetabular lesions (Table 5.4).

5.3.3 Discussion

Considerable variation was found in the size and progression of osteolytic lesions around cementless acetabular components of the same design. Most hips had relatively small osteolytic lesions adjacent to the acetabular component, even after long implantation times, and the osteolytic lesions in many of these hips were relatively quiescent. Hips with larger osteolytic lesions on the initial CT scan were

Progression in the volume of osteolytic lesions adjacent to cementless acetabular components

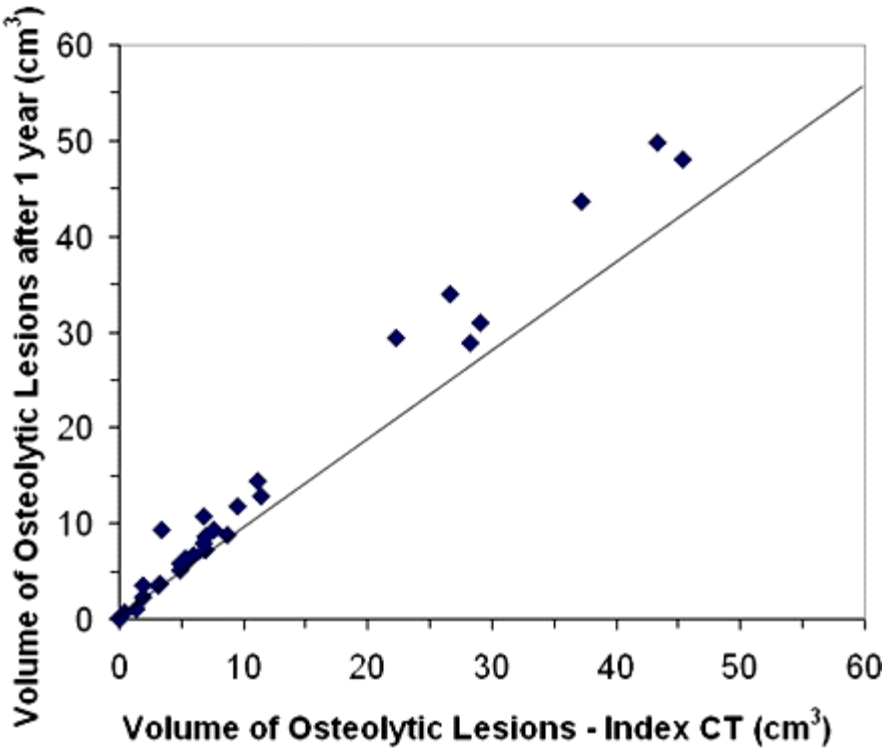

Fig.5.7 Progression in the volume of osteolytic lesions adjacent to cementless acetabular components, expressed as the increase in the volume of osteolytic lesions per year to correct for different time intervals between scans. The graph shows the progression of osteolysis measured in thirty hips. The diagonal line indicates no change in volume. Data points above the line indicate progression in the size of the osteolytic lesions.

TABLE 5.4 Results of Tests of Association between the Progression in Size of Osteolytic Lesions and Patient, Implant, and Clinical Variables

	Descriptive statistics*			
Variable	Nonprogressive Osteolytic Lesions(N=14)	Progressive Osteolytic Lesions(N=16)	P value	Tests of Association
Osteolysis *(cm^3)*	4.0 (0 - 28.2)	10.3 (1.9 - 45.3)	0.002	Mann-Whitney U test
Total volumetric PE wear *(mm^3)*	662 (175 -1326)	1339 (395 - 2128)	0.013	Mann-Whitney U test
Annual PE wear rate*(mm^3/yr)*	42 (12 - 91)	93 (28 - 151)	0.009	Mann-Whitney U test
Age *(yrs)*	60 (49 - 69)	58 (43 - 67)	0.279	Mann-Whitney U test
Gender M:F ratio *(no.of hips)*	8:6	11:5	0.707	Fisher exact test
Body Mass Index *(<25, ≥25)*	4:10	8:8	0.284	Fisher exact test
Implant duration *(months)*	177 (134 - 212)	166 (149 - 186)	0.088	Mann-Whitney U test
Activity† (1:2:3:4:5:6)	0:3:7:3:1:0	0:1:7:5:3:0	0.498	Chi-square test
Charnley grade‡ (A:B:C)	2:1:11	7:2:7	0.103	Fisher exact test
Harris Pain score§ (<40, ≥40)	6:8	7:9	1.00;	Fisher exact test
			0.933	Mann-Whitney U test
Harris Hip score# *(points)*	80 (47 - 97)	88 (34 - 97)	0.506	Mann-Whitney U test
Femoral head size (22:26:28)	8:6:0	2:11:3	0.019	Fisher exact test

*The values are given as the median (with the range in parentheses) or as the distribution at the time of the initial computed tomography scan. † 1= bedridden or confined to wheelchair, 2= sedentary, 3=semi-sedentary, 4=labor or sports, 5= moderate manual labor or sports, and 6=heavy manual labor or vigorous sports (Johnston et al., 1991). ‡ A= only one hip involved and with no other condition that interferes with walking, B=both hips involved but rest of the body normal, and C= some other factor that interferes with walking ability (Charnley et al., 1972). §44= no pain, or pain ignored; 40=slight occasional pain, no compromise in activities; 30= mild pain, no effect on average activities, rarely moderate pain with unusual activity; 20= moderate pain, tolerable but with some limitations of ordinary work or activity, 10= marked pain, severe at times, with serious limitations of activity; and 0= totally disabled, crippled, pain in bed, or bedridden (Harris et al., 1969). # 90 to 100= exellent, 80 to 89= good, 70 to 79=fair, and <70=poor (Harris et al., 1969).

Relationship between progression in the size of osteolytic lesions and the polyethylene wear rate

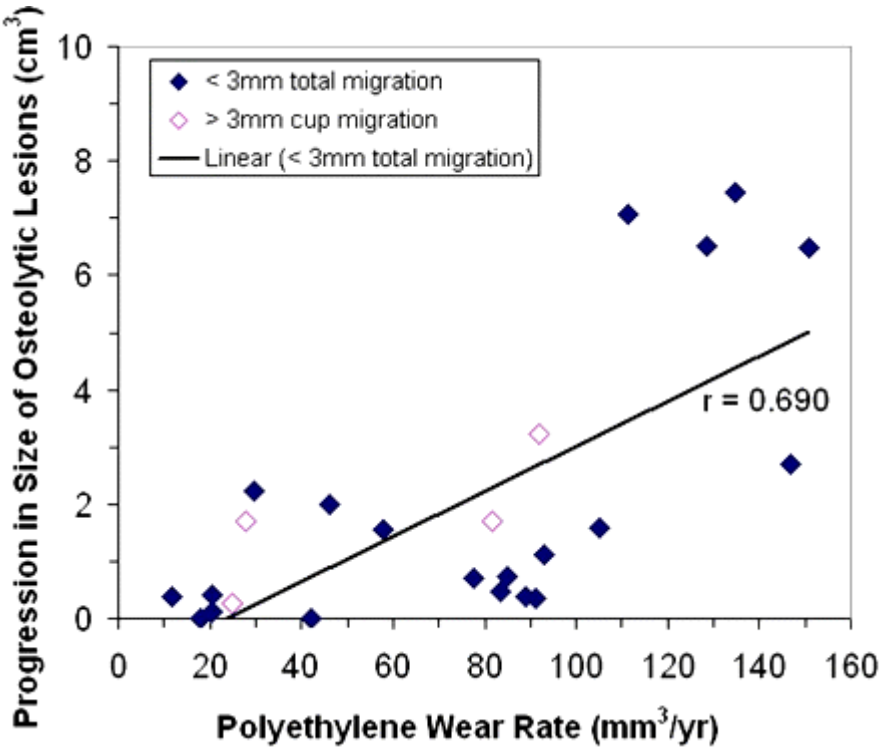

Fig.5.8 Relationship between progression in the size of osteolytic lesions and the polyethylene wear rate. The polyethylene wear rate was calculated as the total wear volume divided by the time since prosthesis implantation. Components that had migrated >3 mm over the life of the implant were excluded from the regression analysis.

most likely to show progression. Lesions with a total size of >10 cm^3 were 2.5 times more likely to progress over one year when compared with smaller lesions. These results agree with those of Schwarz et al., (2003) who reported progression of osteolysis over one year in a mixed population of 20 patients with established periacetabular osteolysis, also with use of CT imaging but with no measure of migration. A direct correlation was found between the volume of PE wear and the size of the osteolytic lesion: the greater the volume of PE wear, the larger the size of the osteolytic lesion. The wear rates that we found were slightly higher than, but consistent with, previously reported rates (Dumbleton et al., 2002) and reflected the duration of implantation and the fact that we chose to selectively make CT scans for hips with signs of osteolysis on plain radiographs. Importantly, there were some hips with large amounts of PE wear but only small osteolytic lesions (Fig. 5.6). In those instances, the acetabular component was stable and so the osteolytic lesions were in fact small and not just apparently so because of migration of the acetabular component into the osteolytic region. No evidence was obtained that migration of the acetabular component increased the size of osteolytic lesions or that migration of the acetabular component into the osteolytic lesion caused us to underestimate osteolysis.

The presence of outliers (i.e., hips with large volumes of PE wear but without large osteolytic lesions) suggests that, despite controlling for many variables such as implant type and surgeon, factors other than wear and migration may determine the extent and progression of PO. It is generally accepted that, in order for wear particle-induced PO to occur, access of wear particles to periprosthetic bone is required. As already described above, lesions were commonly found in close association with screws and screw holes, and further studies to determine the importance of screw holes may point to the need to provide better sealing of these holes. Progression of

>1 cm^3 per year was the amount chosen as being clearly greater than the error of measurement and an amount considered to be a clinically important increase in osteolysis. In the present study, patient activity, walking limitations, and femoral head size were all found to be positively associated with the size of the osteolytic lesions around a stable acetabular component. This is not surprising, given that positive associations between PE wear and patient activity and femoral head size have been reported previously (Livermore et al., 1990, Devane et al., 1997, Eggli et al., 2002). Interestingly, other than PE wear, femoral head size was the only patient or implant-related variable that was found to be positively associated with the progression of osteolysis. However, any associations that may exist between these variables and the progression of osteolysis in a one-year period may be difficult to establish because of the relatively short monitoring period. With longer periods of monitoring of osteolysis progression in more patients, the ability to detect associations will strengthen.

Importantly, the PE wear rate was highly correlated with the progression of osteolysis, suggesting that, in the majority of hips, the PE wear rate is a good indicator of osteolysis progression. At this time, it is not possible to make recommendations about when or how frequently to undertake quantitative CT analyses of osteolysis as the wear rate may not be linear over time. One approach may be that, because patients with an overall wear rate of < 40 mm^3 per year tended to have little or no increase in the size of the lesion, patients with small osteolytic lesions and a low PE wear rate on plain radiographs could be followed with radiographic analyses of wear alone. An increase in the wear rate may then be an indication for additional CT analysis. In contrast, patients with large osteolytic lesions and a PE wear rate of 40 mm^3 per year may warrant closer monitoring with CT. Further studies over longer time-periods at a number of orthopaedic centers will be

required to better define the place for screening plain radiographs and CT in the evaluation of osteolysis.

The present study focused on the evaluation and management of patients who had periacetabular osteolysis without clinically important pain or other symptoms. While findings may be different for symptomatic patients, it is more likely that symptomatic patients warrant imminent revision surgery and are less likely to be candidates for prospective monitoring. Importantly, newer CT technology, such as that used in the present study, may provide a means of evaluating the outcomes of medical treatments such as the use of antiresorptive agents to treat peri-prosthetic osteolysis, particularly bisphosphonates, which have emerged as potential pharmacological treatments (Singer et al., 1995, Fleisch et al., 2003).

In summary, this study demonstrates that sensitive, validated CT measurement of osteolysis combined with accurate measurement of component migration and wear demonstrates considerable variation in the progression of PO around stable acetabular components. While the PE wear rate was a relatively good indicator of osteolysis progression, there was substantial variation among individuals, implying multiple factors that influence this parameter. Importantly, while small lesions may demonstrate some progression, osteolytic lesions measuring >10 cm^3 in size were associated with a high risk of progression.

5.3.4 Conclusions: There is considerable variation in the rates of progression of the size of osteolytic lesions around stable acetabular components. Lesion size and the progression of lesion size are generally related to PE wear rate, higher patient activity levels, and a larger diameter femoral heads. Osteolytic lesions measuring >10 cm^3 in volume are associated with a high rate of progression.

This study has been published, as listed on page vii, and was performed in collaboration with the authors listed under the study.

Chapter 6

General Discussion, Conclusions and Future Directions

6.1 Introduction

As was evident from the literature review, PO following THR is a serious long-term clinical complication and its detection, measurement and monitoring is a significant challenge in radiology. Well known is the limited efficiency of plain radiography to provide reliable and accurate information. The main aim of this thesis was to develop a valid and reliable CT technique for detection and quantification of acetabular PO following THR surgery.

6.2 General Discussion

The work of this thesis resulted in the development of an *in-vitro* validated CT technique using customised CT scanning protocols that demonstrated excellent sensitivity and specificity of the detection and very good to excellent accuracy and precision of the measuring of simulated PO. The results demonstrate the capability of the last two generations of spiral multi-slice CT scanners (with limited and with extended CT scale).

In the first *in-vitro* validation study, a CT protocol was developed using a conventional CT scanner with limited CT scale (up to 4000 Hounsfield units [HU]). The CT operating conditions were determined that enabled volumetric measurements that were accurate to within 96% for small and large defects and precise to greater than 98% for small and large defects. Since the ilium is the most commonly affected site by PO, and is an area almost free of metal artifact, this technique is applicable for use with conventional CT scanners. The findings showed that, in experimental models of THR-associated bone loss, it is feasible to use CT scanning with limited

CT scale to measure the volume of defects in the cancellous bone superior (cranial) to metal-backed acetabular implants. Using the scanning parameters that were determined and described in the CT protocol, accurate and reliable volumetric measurements can be obtained. However, these earlier instruments were limited by metal artifact, such that scans on the level and below the metal acetabular cup were not very informative.

In the second *in-vitro* validation study a CT protocol was developed to use a multi-slice spiral CT scanner with an extended CT scale (up to 40,000 HU) for the measurement of periprosthetic bone defects in all acetabular and periacetabular areas.

A limitation of the *in-vitro* validation was that bovine acetabulum specimen models of THR-associated bone loss were used to validate this new CT technique. In the first *in-vitro* study it was used parallel with human cadaver pelvis model. This choice was made for a number of reasons. First, the use of fresh-frozen human cadaver bodies for medical research was not permitted for legal and ethical issues. Second, formalin-treated cadaver bones demonstrated poor cancellous bone radiodensity, which made small simulated bone defects of less than 1 cm^3 undetectable. Third, and more importantly, there was good anatomical similarity between human and bovine acetabular and periacetabular bone areas, including the similar size of the acetabulum. CT images of THR prosthesis *in-situ* from both the *in-vitro* and *in-vivo* studies illustrated this similarity (Fig.6.1). Another limitation of the in-vitro studies was the absence of a sclerotic border surrounding the bone lesion, which is a typical characteristic of PO osteolysis. This made the mapping of the simulated bone defects more difficult and may have reduced the accuracy and precision of CT volume measurements.

CT images
In-vitro* and *In-vivo

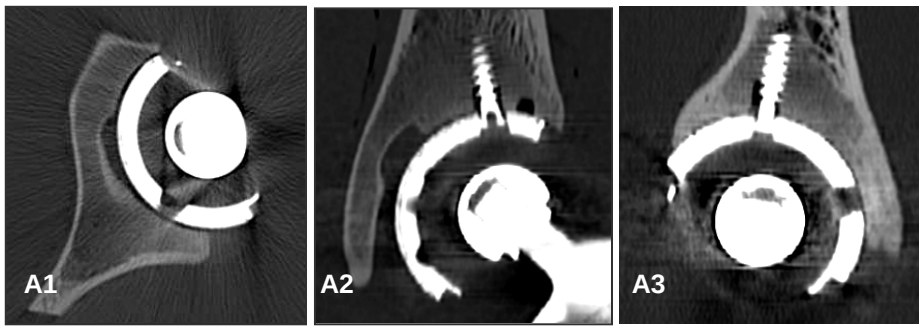

A. *In-vitro* validation study (Bovine acetabulum specimen)

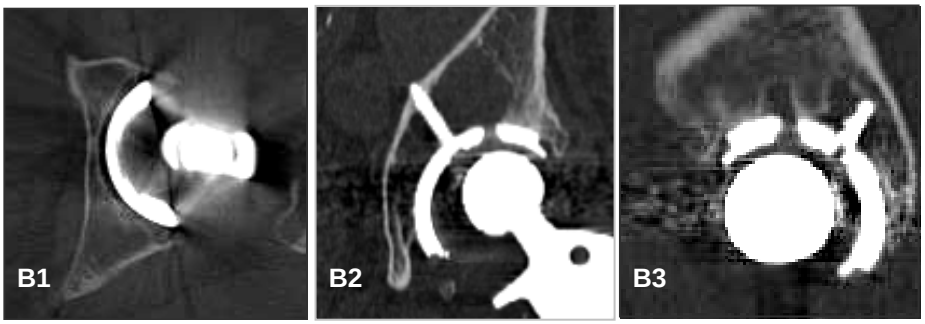

B. Clinical study (Human acetabulum-patient)

Fig.6.1 CT images of THR prosthesis *in-situ* from *in-vitro* (A) and *in-vivo* (B) studies. The corresponding CT images in axial (A~~1~~→ B1); coronal (A2→B2) and sagittal (A3→B3) planes demonstrate anatomical similarity of the acetabular and peri-acetabular bone areas between bovine and human bone.

Developments in CT instruments proceeded rapidly during the course of this work so that metal artifact is now minimal (Fig.6.2).

The CT protocols developed and described in the work of this thesis should be followed as a guideline only, and adapted for use with different CT scanners. The metal artifact suppression should not be made at the expense of unnecessarily high radiation doses to the patient.

The effective radiation dose from the CT scan protocol developed in the work of this thesis was in agreement with the International (ICRP, 1996) and Australian (ARPANSA, 2008) safety guidelines. Furthermore, when this protocol was recently adapted for use with 128-slice CT scan (Siemens SOMATOM DEFINITION AS+, Germany) with extended CT scale and automatic exposure control (AEC), the radiation dose was cut down by approximately 40% (CTDIw 10,17 mGy) without compromising the image quality (Fig.6.3).

The ultimate goal for the development of a CT measurement technique was to actually use it in clinical studies. In this thesis, two studies were described.

In the first clinical study, CT was used to determine the volume, location and number of PO lesions adjacent to 45 cementless Harris-Galante 1 (HG-1) acetabular components fixed with screws and 22 cementless porous coated anatomic (PCA) acetabular components without screws with respect to the acetabular component and to the anatomical bone sites. The findings of this study showed that, in the long term, there were differences in the distribution of osteolytic lesions between different designs of cementless acetabular components, and particularly the osteolytic

Metal artifact reduction in-vitro and in-vivo

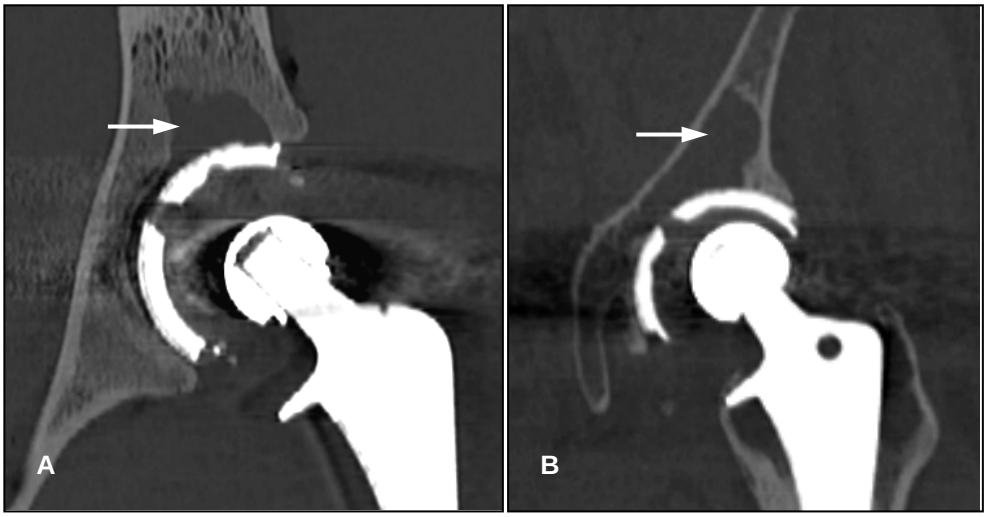

Fig.6.2. CT coronal reconstruction images showing (A) bovine acetabulum specimen model of periprosthetic osteolysis (arrow) and (B) periprosthetic osteolysis (arrow) in a clinical case. In both examples the new CT protocol provided excellent metal artefact reduction in all areas of interest: cranial, on the level of the acetabulum and caudal. Even the neck of the femoral stem is visible through the cobalt-chrome-made femoral head.

Use of 128 slice CT scanner with automatic exposure control (AEC)

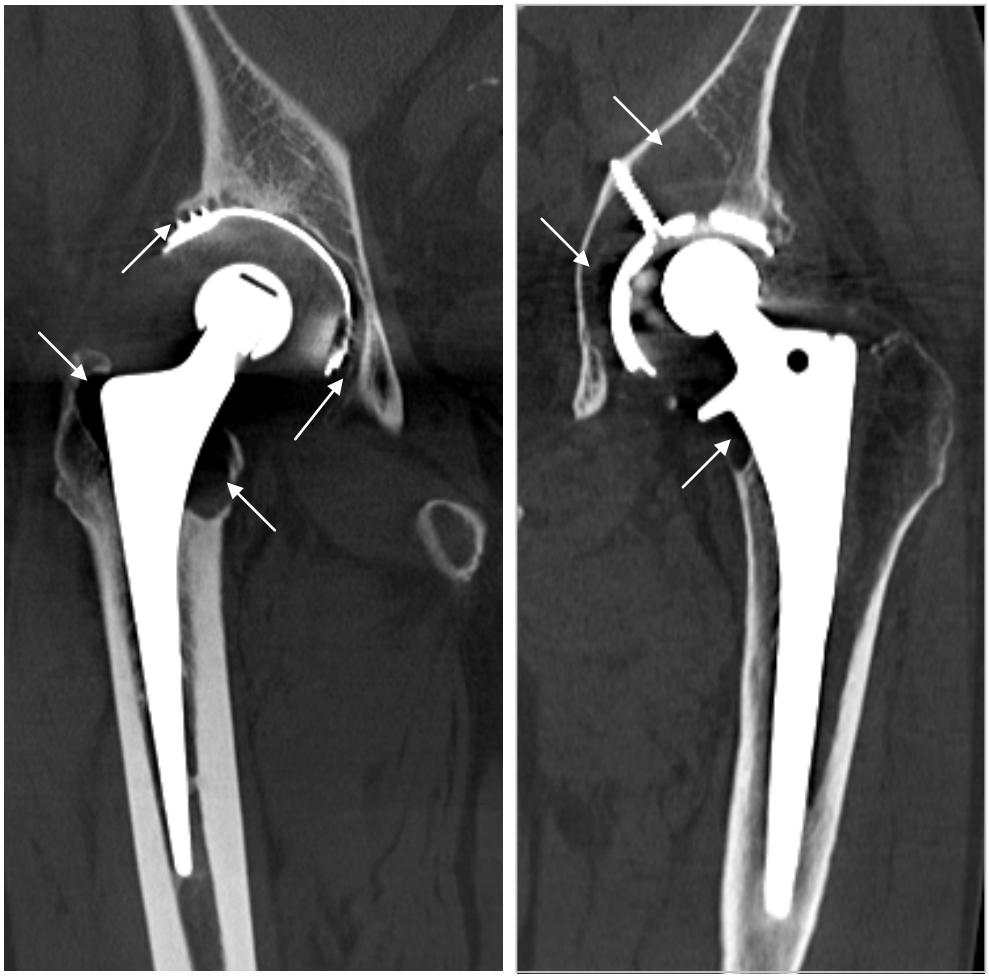

Fig.6.3 CT images derived from adapted CT protocol for use with 128-slice CT scan (Siemens SOMATOM DEFINITION AS+, Germany) with extended CT scale and automatic exposure control (AEC). The effective radiation dose was cut from 20.56 mGy down to 10.17 mGy without compromising the image quality. Shown are periprosthetic osteolytic lesions adjacent to both acetabular and femoral components (arrows).

involvement in the peripheral region of the components, where fixation is likely to be important. While many differences in design and fixation technique may have contributed, importantly, in the presence of a similar total volume of osteolysis, multi-hole acetabular components with screw fixation had less osteolysis affecting the periphery of the components.

In the second clinical study CT was used to determine the volume and progression of PO lesions around stable uncemented THR acetabular components. Considerable variation in the rates of progression of the size of osteolytic lesions around stable acetabular components was found. Lesion size and the progression of lesion size were generally related to PE wear rate, higher patient activity levels, and a larger diameter femoral heads. Osteolytic lesions measuring >10 cm3 in volume were associated with a high rate of progression. These data provided the first reliable information on the progression of osteolytic lesions around uncemented THR and confirmed, that for THR it is possible to use the annual PE wear rate as an indicator of the potential for osteolysis and as a guide to management.

6.3 General Conclusions

Despite some limitations, the CT technique described in this thesis is the first so far that quantified the sensitivity, specificity, accuracy, intra-observer and inter-observer reproducibility of the CT as a tool for detection, measurement and monitoring of THR-associated acetabular PO.

The findings of the clinical studies reported in this thesis are of important value to the orthopaedic community.

The findings showed that, in the long term, there were differences in the distribution of osteolytic lesions between different designs of cementless acetabular components,

and particularly the osteolytic involvement in the peripheral region of the components, where fixation is important.

The data provided the first reliable information on the natural history and progression of osteolytic lesions around uncemented THR and suggested that for THR it is possible to use the annual polyethylene wear rate as an indicator of the potential for osteolysis and as a guide to management.

And finally, these findings contribute to the understanding of biology and natural history of PO.

6.4 Future Directions

High-technology science and industry have made a great progress on improving the spiral multi-slice CT scanners. These instruments are increasingly flexible and provide faster scanning, better z-axis resolution and greater coverage.

A CT scanner (PICKER 6000) from the first generation with limited CT scale (up to 4 000 HU) was used in the first *in-vitro* validation study (1999-2001) of this thesis. Despite its restricted use only in the ilium (cranial to the acetabulum), excellent accuracy and precision were demonstrated in this minimally artifact-affected area.
CT scanner (SIEMENS VOLUME ZOOM) from the next generation of scanners with extended CT scale (up to 40 000 HU) was used in the second *in-vitro* validation study. The CT quantification of PO was validated in all acetabular and periacetabular areas (ilium, anterior wall, medial wall, posterior wall, pubis and ischium) and then was applied in few clinical studies. Thirty-two and 64-slice systems are now widely available, and 128-slice scanner has been introduced into the market (June 2008). CT scanners with 256-slice system are planned for the very near future.

Applications of the CT technique described in the work of this thesis are numerous. It could be used for pre-operative planning of revision hip surgery to determine:

1) The location of the osteolysis,

2) The communication between the osteolysis and the joint space,

3) Whether there are single or multiple osteolytic lesions,

4) Whether the lesion is contained or associated with a defect in the medial wall,

5) The best surgical access to approach and debride the lesion and

6) The volume of the lesion.

It could also be used to monitor PO; to monitor the effect of non-surgical treatment with the use of bisphosphonates; and to examine the completeness of the bone grafting of osteolytic cavities (Fig.6.4).

This method is applicable for assessment of PO in joint replacement in any joint- already shown in hip- now data for knee. Despite the shape and the geometry of the knee implants being more complex, test images of very good quality have been obtained from total knee replacement (TKR) clinical cases, using modified THR CT scan protocol with significantly reduced parameters and radiation dose (Fig.6.5).

Indeed, CT imaging technology has made amazing progress, providing cutting-edge image quality of the bone surrounding metal prosthetic implants. While just 15-20 years ago the presence of metal implants was a strong contraindication for CT scanning due to resulting artifacts, the way is clear for CT to become a routine tool for the assessment and monitoring of joint replacement prostheses, thanks to a number of quality technical and clinical research studies.

CT Assessment of Bone Grafting

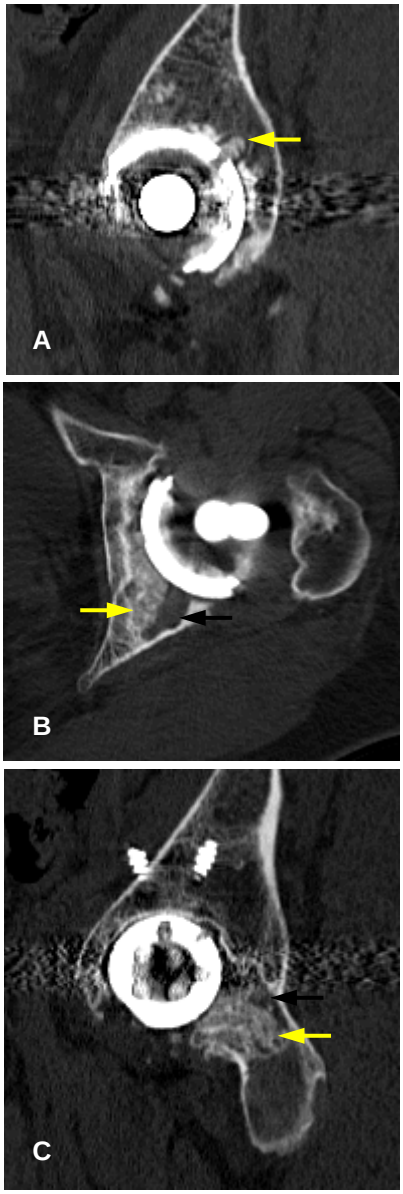

Fig.6.4 Axial and sagittal CT reconstruction images demonstrate osteolytic lesions partially filled with bone graft in: **A**, ilium, adjacent to an empty fixation screw-hole; **B**, medial and posterior walls of the acetabulum and **C**, in the ischium. Yellow arrows indicate bonegraft in place. Black arrows indicate non-grafted part of the osteolytic cavities.

CT assessment of TKR for periprosthetic osteolysis

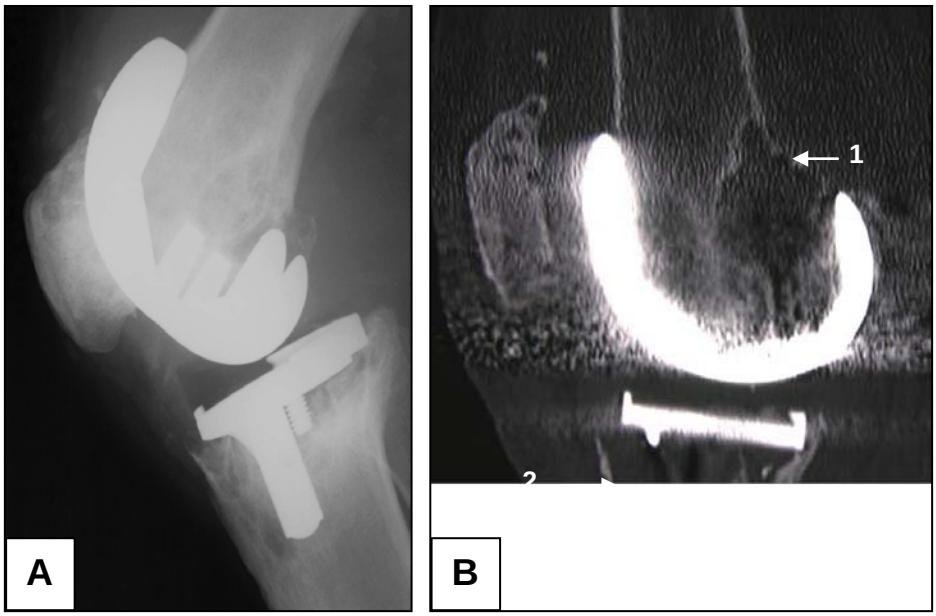

Fig.6.5 Assessment of TKR for periprosthetic osteolysis by A, plain radiography and B, computed tomography. Shown is B1, femoral and B2, tibial periprosthetic osteolysis (arrows).

Better software, more efficient metal artifact suppression, and patient's radiation dose reduction by AEC are expected to increase the clinical application and effectiveness of the quantitative CT for assessment of osteolysis, pre-operative planning of revision surgery, monitoring of the natural history of PO and the potential benefits of surgical treatment, including bone grafting without prosthesis removal (Schmalzried et al., 1998), or pharmacological treatment.

The results from *in-vitro* studies and the findings from the clinical studies suggest that the use of this CT technique allows investigation of the natural history of osteolytic lesions, and will enhance preoperative planning, improve monitoring of THR patients, and enable measurement of the outcomes of new ways to manage PO.

APPENDIX

156

Royal Adelaide Hospital

Medical Administration
Level 3, Margaret Graham Building
Royal Adelaide Hospital
North Terrace, Adelaide 5000
South Australia
Telephone: (08) 8222 5345
Facsimile: (08) 8222 5936
Web: http://www.rah.sa.gov.au

8222 4139

11 November 1999

ORTHOPAEDIC
19 NOV 1999
& TRAUMA

Prof D Howie
ORTHOPAEDIC & TRAUMA SERVICE
ROYAL ADELAIDE HOSPITAL

Dear Prof Howie,

Re: "Quantification of bone loss following total hip replacement using computed tomography: A pilot study." RAH Protocol No: 991106

I am writing to advise that ethical approval has been given to the above project. Please note that the approval is ethical only, and does not imply an approval for funding of the project.

Human Ethics Committee deliberations are guided by the Declaration of Helsinki and N.H. and M.R.C. Guidelines on Human Experimentation. Copies of these can be forwarded at your request.

Adequate record-keeping is important and you should retain at least the completed consent forms which relate to this project and a list of all those participating in the project, to enable contact with them if necessary, in the future. The Committee will seek a progress report on this project at regular intervals and would like a brief report upon its conclusion.

If the results of your project are to be published, an appropriate acknowledgment of the Hospital should be contained in the article.

157

ROYAL ADELAIDE HOSPITAL
North Terrace
Adelaide
South Australia 5000

RESEARCH ETHICS COMMITTEE
Level 3, Hanson Institute
Telephone: (08) 8222 4139
Fax: (08) 8222 3035
email: tpietraf@mail.rah.sa.gov.au

5 March 2004

Prof D Howie
Head
ORTHOPAEDIC & TRAUMA SERVICE
ROYAL ADELAIDE HOSPITAL

Dear Prof Howie,

Re: "Intraoperative measurement of volume of periprosthetic bone defects at total hip replacement revision surgery."
RAH PROTOCOL NO: 040212

I am writing to advise that ethical approval has been given to the above project.

Research Ethics Committee deliberations are guided by the NH&MRC National Statement on Ethical Conduct in Research Involving Humans. A copy of this document can be forwarded at your request.

Adequate record-keeping is important and you should retain at least the completed consent forms which relate to this project and a list of all those participating in the project, to enable contact with them if necessary, in the future. The Committee will seek a progress report on this project at regular intervals and would like a brief report upon its conclusion.

Government of South Australia
Central Northern Adelaide
Health Service

158

ROYAL ADELAIDE
HOSPITAL
North Terrace,
Adelaide, SA 5000
Tel: +61 8 8222 4000
Fax: +61 8 8222 5939
ABN 80 230 154 545
www.rah.sa.gov.au
Research Ethics Committee
Level 3, Hanson Institute
Tel: (08) 8222 4139
Fax: (08) 8222 3035

COPY

18 May 2006

Prof D Howie
Dept of Orthopaedics & Trauma
ROYAL ADELAIDE HOSPTIAL

Dear Prof Howie,

Re: "The measurement of periprosthetic osteolysis measured by computed tomography."
RAH PROTOCOL NO: 060510.

I am writing to advise that Research Ethics Committee approval has been given to the above project.

Research Ethics Committee deliberations are guided by the NHMRC National Statement on Ethical Conduct in Research Involving Humans.

The general conditions of approval follow:

- Adequate record-keeping is important. If the project involves signed consent, you should retain the completed consent forms which relate to this project and a list of all those participating in the project, to enable contact with them in the future if necessary. The duration of record retention for all research data is 15 years.
- You must notify the Research Ethics Committee of any events which might warrant review of the approval or which warrant new information being presented to research participants, including:
  (a) serious or unexpected adverse events which warrant protocol change or notification to research participants,
  (b) changes to the protocol,
  (c) premature termination of the study.
- The Committee must be notified within 72 hours of any serious adverse event occurring at this site.
- Approval is ongoing, subject to satisfactory annual review. An annual review form will be forwarded to you at the appropriate time.

Physical measurement of the volume of the simulated bone defects using
Blu-Tack adhesive (Blu-Tack®, Bostik Findley, Thomastown, Vic., Australia Pty.Ltd.)

First Specimen

Site of Lesion	First step		Second step		Third step		Fourth step		Fifth step		Sixth step	
	Mass (g)	Vol.(cm3)	Mass (g)	Vol.(cm3)	Mass (g)	Vol.(cm3)	Mass (g)	Vol.(cm3)	Mass (g)	Vol.(cm3)	Mass (g)	Vol.(cm3)
Ilium	0.027	0.015	0.141	0.078	1.402	0.779	comb 3.239	1.799	16.58	9.21	16.58	9.21
					top 0.140	0.078	top 0.140	0.078				
					med 0.133	0.074	med 0.133	0.074				
					botm 0.150	0.084	botm 0.150	0.084				
Ant.wall	0.027	0.015	0.136	0.076	0.957	0.531	0.957	0.531				
Med.wall	0.026	0.014	0.026	0.014	0.134	0.074	comb 3.239	1.799				
Ischium	0.032	0.018	0.032	0.018	0.157	0.087	0.157	0.087			5.59	3.1
Pubis											4.36	2.42

Second Specimen

Site of Lesion	First step		Second step		Third step		Fourth step		Fifth step		Sixth step	
	Mass (g)	Vol.(cm3)	Mass (g)	Vol.(cm3)	Mass (g)	Vol.(cm3)	Mass (g)	Vol.(cm3)	Mass (g)	Vol.(cm3)	Mass (g)	Vol.(cm3)
Ilium									17.37	9.65	17.37	9.65
Ant.wall	0.034	0.019	0.034	0.019	0.133	0.074	comb 2.278	1.266				
Med.wall	0.024	0.013	0.149	0.083	0.774	0.43	0.774	0.43				
Post.wall	0.031	0.017	0.111	0.062	0.926	0.514	0.926	0.514				
Pubis	0.031	0.017	0.031	0.017	0.13	0.072	comb 2.278	1.266			4.7	2.6
Ischium											5.09	2.82

Third Specimen

Site of Lesion	First step		Second step		Third step		Fourth step		Fifth step		Sixth step	
	Mass (g)	Vol.(cm3)	Mass (g)	Vol.(cm3)	Mass (g)	Vol.(cm3)	Mass (g)	Vol.(cm3)	Mass (g)	Vol.(cm3)	Mass (g)	Vol.(cm3)
Ilium	0.031	0.017	0.031	0.017	large 3.625	2.014	large 3.625	2.014	19.47	10.81	19.47	10.81
					small 0.118	0.066	small 0.118	0.066				
Post.wall	0.026	0.014	0.026	0.014	0.13	0.072	comb 3.311	1.839				
Pubis	0.036	0.02	0.148	0.082	0.868	0.482	0.868	0.482			7.5	4.16
Ischium	0.032	0.018	0.156	0.087	1.209	0.672	comb 3.311	1.839			7.28	4.04

$$\text{Volume (cm3)} = \frac{\text{Mass (gram)}}{\text{Density (gram/cm3)}}$$

Density/Specific Gravity (g/ml) : 1.8 Temperature (°C) : 20
Blu-Tack®, Bostik Findley, Thomastown, Vic., Australia Pty.Ltd.)

Reference:
1.Technology Supplies Ltd Phoenix House, Tern Hill,market Drayton, Shropshire, Tf 9 3PX, UK.
2.Harrison J, Nixon M, Fright W, Snape L. Use of hand-held laser scanning in the assessment of facial swelling:a preliminary study. *Br J Oral Maxillofac Surg* 42:8-17, 2004.

Computed Tomography Technique for the Measurement of Bone Defects Adjacent to Uncemented Acetabular Components of Total Hip Replacement

R.B.Stamenkov

CHAPTER 3

MEASUREMENT OF BONE DEFECTS ADJACENT TO ACETABULAR COMPONENTS OF HIP REPLACEMENT

R. Stamenkov, D. Howie, J. Taylor, D. Findlay, M. McGee, G. Kourlis, A. Carbone, M. Burwell

Discipline of Orthopaedics and Trauma
The University of Adelaide, Adelaide, SA. 5005 Australia
Department of Radiology
Royal Adelaide Hospital

Clin Orthop Relat Res. 2003; 412: 117-124.

161

Computed Tomography Technique for the Measurement of Bone Defects Adjacent to Uncemented Acetabular Components of Total Hip Replacement

R.B.Stamenkov

STATEMENT OF AUTORSHIP

MEASUREMENT OF BONE DEFECTS ADJACENT TO ACETABULAR COMPONENTS OF HIP REPLACEMENT

Clin Orthop Relat Res. 2003; 412: 117-124.

NOTE:
Statements of authorship appear in the print copy of the thesis held in the University of Adelaide Library.

CLINICAL ORTHOPAEDICS AND RELATED RESEARCH
Number 412, pp. 117–124

Measurement of Bone Defects Adjacent to Acetabular Components of Hip Replacement

Roumen Stamenkov, MD; Donald Howie, MBBS, PhD*; James Taylor, MBBS**; David Findlay, MSc, PhD*; Margaret McGee, BSc, MPH*; George Kourlis, BSc**; Angelo Carbone, BSc*; and Matthew Burwell, MBBS**

Stamenkov, R., Howie, D., Taylor, J., Findlay, D., McGee, M., Kourlis, G., Carbone, A. & Burwell, M. (2003) Measurement of bone defects adjacent to acetabular components of hip replacement.
Clinical orthopaedics and related research, v. 412, pp. 117-124

Computed Tomography Technique for the Measurement of Bone Defects Adjacent to Uncemented Acetabular Components of Total Hip Replacement

R.B.Stamenkov

THE CORRELATION OF RANK, RANKL AND TNFα EXPRESSION WITH BONE LOSS VOLUME AND POLYETHYLENE WEAR DEBRIS AROUND HIP IMPLANTS

C. Holding, D. Findlay, R. Stamenkov, S. Neale, H. Lucas, A. Dharmapatni, S. Callary, K. Shrestna, G. Atkins, D. Howie, D. Haynes.

Discipline of Pathology
And Discipline of Orthopaedics and Trauma
The University of Adelaide, Adelaide, SA. 5005 Australia

Biomaterials 2006; 27: 5215-5219.

Computed Tomography Technique for the Measurement of Bone Defects Adjacent to Uncemented Acetabular Components of Total Hip Replacement

R.B.Stamenkov

STATEMENT OF AUTORSHIP

THE CORRELATION OF RANK, RANKL AND TNFα EXPRESSION WITH BONE LOSS VOLUME AND POLYETHYLENE WEAR DEBRIS AROUND HIP IMPLANTS

Biomaterials 2006; 27: 5215-5219.

NOTE:
Statements of authorship appear in the print copy of the thesis held in the University of Adelaide Library.

Available online at www.sciencedirect.com
SCIENCE DIRECT®
Biomaterials 27 (2006) 5212–5219
Biomaterials
www.elsevier.com/locate/biomaterials

The correlation of RANK, RANKL and TNFα expression with bone loss volume and polyethylene wear debris around hip implants

Christopher A. Holding[a], David M. Findlay[b,c], Roumen Stamenkov[b], Susan D. Neale[b], Helen Lucas[a], A.S.S.K. Dharmapatni[a], Stuart A. Callary[b], Kush R. Shrestha[a,b,c], Gerald J. Atkins[b], Donald W. Howie[b,c], David R. Haynes[a,*]

[a]*Department of Pathology, The University of Adelaide, North Terrace, Adelaide, South Australia 5000, Australia*
[b]*Department of Orthopaedics and Trauma, The University of Adelaide, North Terrace, Adelaide, South Australia 5000, Australia*
[c]*Hanson Institute, Adelaide, South Australia 5000, Australia*

Received 22 January 2006; accepted 29 May 2006
Available online 27 June 2006

Holding, C.A., Findlay, D.M., Stamenkov, R., Neala, S.D., Lucas, H., Dharmapatni, A.S.S.K., Callary, S.A., Shrestha, K.R., Atkins, G.J., Howie, D., & Haynes, D.R. (2006) The correlation of RANK, RANKL and TNFα expression with bone loss volume and ployethylene wear debris around hip implants.
Biomaterials, v. 27, pp. 5212-5219

Computed Tomography Technique for the Measurement of Bone Defects Adjacent to Uncemented Acetabular Components of Total Hip Replacement

R.B.Stamenkov

CHAPTER 5

PROGRESSION OF ACETABULAR PERIPROSTHETIC OSTEOLYTIC LESIONS MEASURED WITH COMPUTED TOMOGRAPHY

D. Howie, S. Neale, R. Stamenkov, M. McGee, D.J. Taylor, D. Findlay

Discipline of Orthopaedics and Trauma
The University of Adelaide, Adelaide, SA. 5005 Australia
Department of Radiology
Royal Adelaide Hospital

J Bone Joint Surg Am 2007; 89: 1818-1825.

Computed Tomography Technique for the Measurement of Bone Defects Adjacent to Uncemented Acetabular Components of Total Hip Replacement

R.B.Stamenkov

STATEMENT OF AUTORSHIP

PROGRESSION OF ACETABULAR PERIPROSTHETIC OSTEOLYTIC LESIONS MEASURED WITH COMPUTED TOMOGRAPHY

J Bone Joint Surg Am 2007; 89: 1818-1825.

NOTE:
Statements of authorship appear in the print copy of the thesis held in the University of Adelaide Library.

Progression of Acetabular Periprosthetic Osteolytic Lesions Measured with Computed Tomography

By Donald W. Howie, MBBS, PhD, FRACS, Susan D. Neale, MSc, Roumen Stamenkov, MD, Margaret A. McGee, BSc, MPH, David J. Taylor, MBBS, and David M. Findlay, MSc, PhD

Investigation performed at the Department of Orthopaedics and Trauma and the Department of Radiology, Royal Adelaide Hospital, and the Discipline of Orthopaedics and Trauma, University of Adelaide, Adelaide, Australia

Howie, D.W., Neale, S.D., Stamenkov, R., McGee, M.A., Taylor, D.J. & Findlay, D.M. (2007) Progression of acetabular periprosthetic osteolytic lesions measured with computed tomography.
The Journal of bone and joint surgery (American), v. 89, pp. 1818-1825

Computed Tomography Technique for the Measurement of Bone Defects Adjacent to Uncemented Acetabular Components of Total Hip Replacement

R.B.Stamenkov

CHAPTER 5

DISTRIBUTION OF PERIACETABULAR OSTEOLYTIC LESIONS VARIES ACCORDING TO COMPONENT DESIGN

R. Stamenkov, D. Howie, S. Neale, M. McGee, D.J. Taylor, D. Findlay

Discipline of Orthopaedics and Trauma
The University of Adelaide, Adelaide, SA. 5005 Australia
Department of Radiology
Royal Adelaide Hospital

J Arthroplasty 2009: Article in Press

Computed Tomography Technique for the Measurement of Bone Defects Adjacent to Uncemented Acetabular Components of Total Hip Replacement

R.B.Stamenkov

STATEMENT OF AUTORSHIP

DISTRIBUTION OF PERIACETABULAR OSTEOLYTIC LESIONS VARIES ACCORDING TO COMPONENT DESIGN

J Arthroplasty 2009: Article in Press

NOTE:
Statements of authorship appear in the print copy of the thesis held in the University of Adelaide Library.

The Journal of Arthroplasty Vol. 00 No. 0 2009

Distribution of Periacetabular Osteolytic Lesions Varies According to Component Design

Roumen B. Stamenkov, MD,* Donald W. Howie, PhD, FRACS,*†
Susan D. Neale, MSc,* Margaret A. McGee, BSc, MPH,*†
David J. Taylor, FRACR,‡ and David M. Findlay, PhD†

Stamenkov, R.B, Howie, D.W, Neale, S.D., McGee, M.A., Taylor, D.J. & Findlay, D.M. (2010) Distribution of periacetabular osteolytic lesions varies according to component design.
Journal of arthroplasty, v. 25(6), pp. 913-919

Bibliography

Adolphson P, von Sivers K, Dalen N, Jonsson U, and Dahlborn M: Bone and muscle mass after hip arthroplasty. A quantitative computed tomography study in 20 arthrosis cases. *Acta Orthop Scand* 164: 181-184, 1993.

Adolphson P, von Sivers K, Jonsson U, Dalen N, and Dahlborn M: Bone and muscle mass after hip rearthroplasty. Controlled CT study of 12 patients. *Acta Orthop Scand* 64: 282-284, 1993.

American National Institutes of Health. Consensus Development Conference on Total Hip replacement. 12: 1-3, 1994.

Amis ES, Jr., Butler PF, Applegate KE: American College of Radiology white paper on radiation dose in medicine. *J Am Coll Radiol* 4: 272-284, 2004.

Australian Radiation Protection and Nuclear Safety: Safety Guide for Radiation Protection in Diagnostic and Interventional Radiology, Radiation Protection Series 14.1, 2008. (www.arpansa.gov.au/Publications/codes/rps14_1.cfm).

Archibeck MJ, Jacobs JJ, Roebuck KA, Glant TT: The basic science of periprosthetic osteolysis. *J Bone Joint Surg* 82-A: 1478-1489, 2000.

Aubin JE, Bonnelye E: Osteoprotegerin and its ligand: a new paradigm for regulation of osteoclastogenesis and bone resorption. *Osteoporos Int* 11: 905-913, 2000.

Australian Orthopaedic Association National Joint Replacement Registry. Annual Report. Adelaide: AOA, 2006. (http://www.dmac.adelaide.edu.au/aoanjrr/documents/aoanjrrreport_2006.pdf).

Australian Orthopaedic Association National Joint Replacement Registry. Annual Report, 2008. (www.aoa.org.au/jointregistry_pub.asp).

Barmeir E, Dubowitz B, Roffman M: Computed tomography in the assessment and planning of complicated total hip replacement. *Acta Orthop Scand* 53: 597-604, 1982.

Barrett JF, Keat N: Artifacts in CT: recognition and avoidance. Radio Graphics 24: 1679–1691, 2004.

Bartel D, Bickell V, Wright T: The effect of conformity, thickness, and material on stresses in ultra-high molecular weight components for total joint replacement. *J Bone Joint Surg* 68-A: 1041-1051, 1986.

Berger RA, Kull LR, Rosenberg AG, Galante JO: Hybrid total hip arthroplasty: 7- to 10-year results. *Clin Orthop Relat Res* 333: 134-146, 1996.

Berger R, Jacobs J, Quigley L, Rosenberg A G, Galante JO: Primary cementless acetabular reconstruction in patients younger than 50 years old. 7-to 11-year results. *Clin Orthop* 344: 216-226, 1997.

Berman AT, McGovern K M, Paret R S, Yanichko Jr D R: The use of preoperative computed tomography scanning in total hip arthroplasty. *Clin Orthop* 222: 190-196, 1987.

Berry DJ: Management of osteolysis around total hip arthroplasty. *Orthopaedics* 22: 805-808, 1999.

Berry D J, Le wallen D G, H anssen A D: Pelvic discontinuity i n revision t otal hi p arthroplasty. *J Bone Joint Surg* 81-A: 1692-1702, 1999.

Berry DJ: Periprosthetic fractures associated with osteolysis: A problem on the rise. *J Arthroplasty* 18(3 Suppl 1): 107-111, 2003.

Bojescul J A, X enos JS, C allaghan JJ, S avory C G: Results of porous-coated anatomic total hip arthroplasty without cement at fifteen years. *J Bone Joint Surg* 85-A: 1079-1083, 2003.

Bono JV, Sanford L, Toussaint JT: Severe polyethylene wear in total hip arthroplasty: observations from retrieved AML PLUS hip implants with an ACS polyethylene liner. *J Arthroplasty* 9: 119-125, 1994.

Brand R, Yoder S, Pedersen D: Interobserver variability in interpreting radiographic lucencies about total hip reconstruction. *Clin Orthop* 192: 237–239, 1985.

Burt CF, Garvin KL, Otterberg ET, Jardon OM: A femoral component inserted without cement in total hip arthroplasty: a study of the Tri-Lock component with average ten-year duration of follow up. *J Bone Joint Surg* 80-A: 952-960, 1998.

Callaghan JJ, Savory C G, O 'Rourke M R, Jo hnston RC: Are al l ce mentless acetabular components created equal? *J Arthroplasty* 19: 95-98, 2004.

Carlsson A , G entz C : Radiographic versus clinical l oosening of t he ace tabular component in noninfected total hip arthroplasty. *Clin Orthop* 185: 145–150, 1984.

Chatoo M , P arfitt J, P earse M F: P eriprosthetic acetabular f racture asso ciated w ith extensive osteolysis. *J Arthroplasty* 13: 843-845, 1998.

Chiang PP Burke DW, Freiberg AA, Rubash HE: Osteolysis of the pelvis. Evaluation and treatment. *Clin Orthop Relat Res* 417: 164-74, 2003.

Childs L, Paschalis E, Xing L, Dougal W, Anderson D, Boskey A, Puzas E, Rosier R, O'Kefe R, Boyce B, Schwarz E: In-vivo RANK signalling blockade using the receptor activator o f N F-kB: F c effectively pr events and ameliorates wear debr is-induced osteolysis via ost eoclast de pletion w ithout i nhibiting ost eogenesis. *J Bone M in R es* 17 (2): 192-199, 2002.

Clarke HJ, Jinnah RH, Cox QG, Curtis MJ: Computerised templating in uncemented total hip arthroplasty to assess component fit and fill. *J Arthroplasty* 7: 235-239, 1992.

Claus AM, Engh C A Jr , S ychterz C J, X enos JS , Orishimo K F, E ngh C A S r: Radiographic definition o f pelvic osteolysis following t otal hi p arthroplasty. *J Bone Joint Surg* 85-A: 1519-1526, 2003.

Claus AM, Sychterz C J, H opper R H, E ngh C A: Pattern o f ost eolysis around two different cementless metal-backed cups. *J Arthroplasty* 16: 177-182, 2001.

Clohisy JC, Harris WH: The Harris-Galante Porous-Coated acetabular component with screw fixation: an average ten-year follow-up study. *J Bone Joint Surg* 81-A: 66-73, 1999.

De Souza AP, Trevilatto PC, Scarel-Caminaga RM. MMP-1 promoter polymorphism: association with chronic periodontitis severity in a Brazilian population. *J Clin Periodontol* 30: 154, 2003.

Dias J, Johnson G, Finlay D, Stoyle TF: Preoperative evaluation for uncemented hip arthroplasty: the role of computed tomography. *J Bone Joint Surg* 71-Br: 43–46, 1989.

Dumbleton JH, Manley MT, Edidin AA. A literature review of the association between wear rate and osteolysis in total hip arthroplasty. *J Arthroplasty* 17: 649–661, 2002.

Duncan CP, Masri BA: Fractures of the femur after hip replacement. *Instr Course Lect* 45: 293-304, 1995.

Engh CA Jr, McAuley JP, Sychterz CJ, Sacco Me, Engh CA Sr: The accuracy and reproducibility of radiographically assessing stress shielding: a postmortem analysis. *J Bone Joint Surg* 82-A: 1414-1420, 2000.

Engh CA, Sychterz CJ, Young AM, Pollock DC, Toomey SD, Engh CA: Interobserver and intraobserver variability in radiographic assessment of osteolysis. *J Arthroplasty* 17: 752-759, 2002.

European Commission. European guidelines on quality criteria for computed tomography. Report EUR 16262. Luxembourg, 1999.

Faulkner K, Moores BM: Radiation dose and somatic risk from computed tomography. *Acta Radiol* 28: 483-488, 1987.

Fiala TG, Noveline RA, Yaremchuk MJ: Comparison of CT imaging artefacts from craniomaxillofacial internal fixation devices. *Plast Reconstr Surg* 92: 1227-1232, 1993.

Fowble V, Schmalzried T, Amstutz H: Decreased morbidity with lesional treatment of pelvic osteolysis. Transactions AAOS Annual Meeting, San Francisco, 1997.

Gaffey JL, Callaghan JJ, Pedersen DR, Goetz DD, Sullivan PM, Johnston RC: Cementless acetabular fixation at fifteen years. A comparison with the same surgeon's results following acetabular fixation with cement. *J Bone Joint Surg* 86-A: 257-261, 2004.

Garsia-Cimberelo E, Madero R, Blasco-Alberdi A, Munuera L: Femoral osteolysis after low-friction arthroplasty. Aplanimetric study and volumetric estimate. *J Arthroplasty* 12: 624-634, 1997.

Garcia-Cimbrelo E, Tapia M, Martin-Hervas C: Multislice computed tomography for evaluating acetabular defects in revision THA. *Clin Orthop Relat Res* 463: 138-143, 2007.

Godoy-Santos AL, D 'Elia C O, T eixeira WJ, C abrita H B, C amanho G L: A septic loosening of total hip arthroplasty: Preliminary genetic investigation. *J Arthtroplasty* 24 (2): 297-302, 2009.

Goldring SR, Schiller AL, Roelke M, Rourke CM, O'Neil DA, Harris WH: The synovial-like membrane at the bone-cement interface in loose total hip replacements and its proposed role in bone lysis. *J Bone Joint Surg* 65-A: 575-584, 1983.

Graves, Davidson, Ingerson. Australian Orthopaedic Assoc. Natl Joint Replacement Registry Ann Report, 2008.

Haramati N, S taron RB, M azel-Sperling K : CT sca ns through m etal sca nning technique versus hardware composition. *Comput Med Imaging Graph* 18: 429–434, 1994.

Harley JM, W ilkinson JA: Hip r eplacement for a dults with u nreduced co ngenital dislocation. *J Bone Joint Surg* 69-Br: 752–755, 1987.

Harris WH: The problem is osteolysis. *Clin Orthop* 311: 46-53, 1995.

Heekin RD, Engh CA, Herzwurm PJ: Fractures through cystic lesions of the greater trochanter: a cause of late pain after cementless total hip arthroplasty. *J Arthroplasty* 11: 757-760, 1996.

Hegemann N, Kohn B, Brunnberg L: Biomarkers of joint tissue metabolism in canine osteoarthritic and arthritic joint disorders. *Osteoarthritis Cartilage* 10: 714, 2002.

Hidajat N, Maurer J, Schro¨der RJ, Wolf M, Vogl T, Felix R: Radiation exposure in spiral computed tomography: dose reduction and dose distribution. *Invest Radiol* 34: 51–57, 1999.

Hofbauer: The roles of osteoprotegerin and osteoprotegerin ligand in the paracrine regulation of bone resorption. *J Bone Min Res* 15: 2-12, 2000.

Holding C, Findlay D, Stamenkov R, Neale SD, Lucas H, Dharmapatni ASSK, Callary SA, Shrestha KR, Atkins GJ, Howie D W, Haynes DR: The correlation of RANK, RANKL and TNFa expression with bone loss volume and polyethylene wear debris around hip implants. *Biomaterials* 27: 5212-5219, 2006.

Hopper KD, King SH, Lobell M H: In plane x-ray protection during diagnostic CT-shielding with bismuth radioprotective garments. *Radiology* 205: 853-858, 1997.

Horowitz S M, Gautsch TL, Frondoza C G, Riley L Jr : Macrophage exposure to polymethylmethacrylate leads to mediator release and injury. *J Orthop Res* 9: 496-513, 1991.

Horowitz SM, Doty SB, Lane JM, Burstein AH: Studies of the mechanism by which the mechanical failure of polymethylmethacrylate leads to bone resorption. *J Bone Joint Surg 75*-A: 802-813, 1993.

Howie D W: Tissue response in relation to type of wear particles around failed hip arthroplasties. *J Arthroplasty* 5: 337-348, 1990.

Howie D W, V ernon-Roberts B, C ornish B L: Resurfacing hi p ar throplasty. Classification of loosening and the role of prosthesis wear particles. *Clin Orthop Relat Res* 255: 144-159, 1990.

Howie DW, Neale SD, Stamenkov R, McGee MA, Taylor DJ, Findlay DM: Progression of acetabular periprosthetic osteolytic lesions measured by computed tomography. *J Bone Joint Surg* 89-A: 1818-1825, 2007.

Hozack W, Mesa J, Rothman R: Total hip revision for pelvic osteolysis—the value of early intervention. *J Arthroplasty* 11: 229-235, 1996.

Hubbard L, McDermott J, Garret G: Computed axial tomography in musculoskeletal trauma. *J Trauma* 22: 388-394, 1982.

Illgen R 2nd, R ubash H E: The opt imal f ixation o f the cementless acetabular component in primary total hip arthroplasty. *J Am Acad Orthop Surg* 10: 43-56, 2002.

International Commission on Radiological Protection. 1990 Recommendations of the International C ommission on R adiological P rotection. Publication 6 0. Annals of t he ICRP 21 (1-3), Pergamon Press, Oxford, 1991.

International C ommission o n R adiological P rotection. Radiological Protection and safety i n M edicine. Publication 73. Annals of t he I CRP 26 (2), Pergamon P ress, Oxford, 1996.

Jasty M , F loyd WE, Schiller A L, G oldring S R, H arris WH: Loc alized ost eolysis in stable, non-septic total hip replacement. *J Bone Joint Surg* 68-A: 912-919, 1986.

Jerosch J, Steinbeck J, Fuchs S, Kirchhoff C: Radiologic evaluation of acetabular defects on acetabular loosening of hip alloarthroplasty. *Unfallchirurg* 99: 727-733, 1996.

Jones LC, Hungerford DS: Cement disease. *Clin Ortop Relat Res* 225: 192-206, 1987.

Kadoya Y, Kobayashi A, Ohashi H: Wear and osteolysis in total joint replacements. *Acta Orthop Scand* Suppl 278: 1-16, 1998.

Kalender W, Klotz E, Sokiranski R, Felsenberg D. Algorithm for the reconstruction of CT artifacts caused by metallic implants. *SPIE Med Imag* 1234: 642-40, 1990.

Kalender WA, Seissler W, Klotz E, Vock P: Spiral volumetric CT with single-breathhold technique, continuous transport, and continuous scanner rotation. *Radiology* 176: 181–183, 1990.

Kalra MK, Maher M M, Toth TL: Comparison of z-axis automatic tube current modulation technique with fixed tube current CT scanning of the abdomen and pelvis. *Radiology* 232: 347-353, 2004.

Kanamori Y, Mitsushima M, Minaguchi T et al: Correlation between expression of the matrix metalloproteinase-1 gene in ovarian cancers and an insertion/deletion polymorphism in its promoter region. *Cancer Res* 59: 4225, 1999.

Kim YH: Long-term results of the cementless porous-coated anatomic total hip prosthesis. *J Bone Joint Surg* 87-Br: 623-627, 2005.

Kim K J, K otake S, Udagawa N , I da H , Ishii M , T akei I , Kubo T, Takagi M : Osteoprotegerin i nhibits *in-vitro* mouse osteoclast formation i nduced by j oint f luid from failed total hip arthroplasty. *J Biomed Mater Res* 58 (4): 393-400, 2001.

Kiralti BJ, Heiner JP, McBeat AA, Wilson MA: Determination of bone mineral density by dual x-ray abso rptiometry i n pat ients with unce mented t otal hi p ar throplasty. *J Orthop Res* 10: 836-844, 1992.

Kitamura N, L euing SB, E ngh CA: Characteristics of pelvic osteolysis on co mputed tomography after total hip replacement. *Clin Orthop Relat Res* 441: 291-297, 2005.

Kitamura N, Na udie DDR, L eung S B, H opper R H, E ngh C A: Diagnostic features of pelvic osteolysis on co mputed t omography: T he i mportance o f co mmunication pathways. *J Bone Joint Surg* 87-A: 1542-1550, 2005.

Konttinen YT, Zhao D, Beklen A, Ma G, Takagi M, Kivelä-Rajamäki M, Ashammakhi N, Santavirta S. The microenvironment around total hip replacement prostheses. *Clin Orthop Relat Res* 430: 28-38, 2005.

Lam J , Takeshita S : TNF-alpha i nduces osteoclastogenesis by di rect st imulation o f macrophages exposed to permissive levels of RANK ligand. *J Clin Invest* 106: 1481-1488, 2000.

Lapaucis A, Bourne RB, Rorabeck CH: The effect of elective THR on health related quality of life. *J Bone Joint Surg* 75-A: 1619-1626, 1993.

Learmonth I D, H ussell JG , G robler G P: U npredictable pr ogression o f osteolysis following ce mentless hip ar throplasty. 2 4 femoral co mponents followed f or 6 -10 years. *Acta Orthop Scand* 67: 245-248, 1996.

Learmonth I D, S mith EJ, C unningham J L: The pathogenesis of osteolysis in t wo different cementless hip replacements. *Proc Inst Mech Eng* 211: 59-63, 1997.

Leung S , N audie D, K itamura N , Walde T, E ngh C A: Computed t omography i n t he assessment of periacetabular osteolysis. *J Bone Joint Surg* 87-A: 592-597, 2005.

Lewallen D G, B erry D J: P eriprosthetic fracture o f t he femur af ter t otal hi p arthroplasty: treatment and results to date. *J Bone Joint Surg* 79-A: 1881-1886, 1997.

Link TM, Berning W, Scherf S: CT of metal implants: Reduction of artefacts using an extended CT scale technique. *J Comput Assist Tomogr* 24: 165-172, 2000.

Little BS, Wixson R L, S tulberg S D: Total Hip A rthroplasty w ith t he porous-coated anatomic hip prosthesis results at 11 to 18 Years. *J Arthroplasty* 21: 338-343, 2006.

Looney R , B oyd A ,Totterman S , Seo G, Tamez-Pena J, C ampbell D , N ovothny L, Olcott C , M artell J, H ayes FA, O'Keefe R J. S chwarz E M: Volumetric computerized tomography as a m easurement o f per i-prosthetic acetabular ost eolysis and i ts correlation with wear. *Arthritis Res* 4: 59-63, 2002.

Mack L, H arley J, Winquist R : CT o f a cetabular fractures: a nalysis of fracture patterns. *Am J Roentgenol* 138: 407–412, 1982.

Magid D , F ishman E , B rooker A: Multiplanar co mputed tomography o f ac etabular fractures. *J Computer Assist Tomogr* 10: 778–783, 1986.

Malchau H, Herberts P, Eisler T, Garellick G, Söderman P: The Swedish Total Hip Replacement Register. J Bone Joint Surg 84-A: Suppl 2: 2-20, 2002.

Maloney WJ, Ja sty M , R osenberg A , H arris WH: B one l ysis in w ell-fixed ce mented femoral components. *J Bone Joint Surg* 72-Br: 966-970, 1990.

Maloney WJ, G alante JO , A nderson M : F ixation, pol yethylene wear, and p elvic osteolysis in primary total hip replacement. *Clin Orthop* 369: 157-164, 1999.

Maloney WJ, H erzwurm P , P aprosky W, R ubash H E, E ngh C : Treatment o f p elvic osteolysis associated with a stable acetabular component inserted without cement as part of a total hip replacement. *J Bone Joint Surg* 79-A: 1628-1634, 1997.

Maloney W, P eters P, E ngh C : S evere ost eolysis of t he pelvis in asso ciation w ith acetabular replacement without cement. *J Bone Joint Surg* 75-A: 1627-1634, 1993.

Manley MT, D'Antonio JA, Capello WN, Edidin AA: Osteolysis: A disease of access to fixation interfaces. *Clin Orthop Relat Res* 450: 129-137, 2002.

McGee MA, Howie DW, Costi K, Haynes DR, Wildenauer CI, Pearcy MJ, McLean JD: Implant r etrieval st udies of t he w ear a nd l oosening o f pr osthetic j oints: a r eview. *Wear* 241: 158-165, 2000.

Mian S, Truchly G, Pflum F: Computed tomography measurement of acetabular cup anteversion and retroversion in total hip arthroplasty. *Clin Orthop* 276: 206-209, 1992.

Murray DW: The definition and measurement of acetabular orientation. *J Bone Joint Surg* 75-Br: 228-232, 1993.

Nayak N, Mulliken B, Rorabeck C: Osteolysis in cemented versus cementless acetabular components. *J Arthroplasty* 11: 135-142, 1996.

Neale SD, Haynes DR, Howie DW, Murray DW, Athanasou NA: The effect of particle phagocytosis and metallic wear particles on osteoclast formation and bone resorption in vitro. *J Arthroplasty* 15: 654-662, 2000.

Neander G, von Silvers K, Adolphson P, Dahlborn M, Dalen N: An evaluation of bone loss after total hip arthroplasty for femoral head necrosis after femoral neck fracture: a quantitative CT study in 16 patients. *J Arthroplasty* 14: 64-70, 1999.

Oparaugo PC, Clarke IC: Correlation of wear debris-induced osteolysis and revision with volumetric wear-rates of polyethylene: a survey of 8 reports in the literature. *Acta Othop Scand* 72: 22-28, 2001.

O'Sullivan G, Goodman S, Jones H: Computerized tomographic evaluation of acetabular anatomy. *Clin Orthop* 277: 175–181, 1992.

Paprosky WG, Perona PG, Lawrence JM: Acetabular defect classification and surgical reconstruction in revision arthroplasty. A 6-year follow-up evaluation. *J Arthroplasty* 9: 34-44, 1994.

Parvizi J, Sullivan T, Duffy G, Cabanela ME: Fifteen-year clinical survivorship of Harris-Galante total hip arthroplasty. *J Arthroplasty* 19: 672-677, 2004.

Perez RE, Rodriguez JA, Deshmukh RG, Ranawat CS: Polyethylene wear and periprosthetic osteolysis in metal backed acetabular components with cylindrical liners. *J Arthroplasty* 13 (1): 1-7, 1998.

Portney LG, Watkins MP. Foundations of clinical research. Applications to practice. 2nd ed. Upper Saddle River, New Jersey; Prentice Hall Health, 2000.

Puri L, Wixson R, Stern S, Kohli J, Hendrix R, Stulberg D: Use of helical computed tomography for the assessment of acetabular osteolysis after total hip arthroplasty. *J Bone Joint Surg* 84-A: 609-614, 2002.

Rasquinha VJ, Dua V, Rodriguez JA: Fifteen year survivorship of a collarless, cemented, normalized femoral stem in primary hybrid total hip arthroplasty with a modified third-generation cement technique. *J Arthroplasty* 18: 86, 2003.

Reiner BI, Siegel EL, Hooper FJ: Accuracy of interpretation of CT scans: comparing PACS monitor displays and hard-copy images. *Am J Roentgenol* 179: 1407–1410, 2002.

Rizzo S, Kalra M, Schmidt B: Comparison of angular and combined automatic tube current modulation techniques with constant tube current CT of the abdomen and pelvis. *Am J Roentgenol* 186: 673-679, 2006.

Robertson DD, Sutherland CJ, Lopes T, Yuan J: Preoperative description of severe acetabular defects caused by failed total hip replacement. *J Comput Assist Tomogr* 22: 444-449, 1998.

Robertson DD, Yuan J, Wang G, Vannier MW: Total hip prosthesis metal-artefact suppression using iterative deblurring reconstruction. *J Comput Assist Tomogr* 21: 293-298, 1997.

Rogers SD, Howie DW, Graves SE, Pearcy MJ, Haynes DR: In vitro human monocyte response to wear particles of titanium alloy containing vanadium or niobium. *J Bone Joint Surg* 79-B: 311-315, 1997.

Sa´nchez-Sotello J, McGrory BC, Berry DJ: Acute periprosthetic fracture of the acetabulum associated with osteolytic pelvic lesions: a report of 3 cases. *J Arthroplasty* 15: 126-130, 2000.

Santos MCLG, Campos MIG, Souza AP: Analysis of MMP-1 and MMP-9 promoter polymorphism in early osseointegrated implant failure. *Int J Oral Maxillofac Implants* (19): 38, 2004.

Scott W, Fishman E, Magid D: Acetabular fractures: optimal imaging. *Radiology* 165: 537–539, 1987.

Schmalzried T P, F owble V A, Amstutz H C: T he fate of pel vic osteolysis after reoperation. No recurrence with lesional treatment. *Clin Orthop* 350: 128-137, 1998.

Schmalzried T P, K wong LM , Ja sty M , Sedlacek RC, Ha ire TC, O 'Connor DO , Bragdon C R, K abo JM , M alcolm A J, H arris WH: The m echanism o f l oosening o f cemented ace tabular co mponents in t otal h ip ar throplasty. A nalysis of sp ecimens retrieved at autopsy. *Clin Orthop* 274: 60-78, 1992.

Schmalzried T P, J asty M , H arris WH: Periprosthetic bone l oss in t otal hi p arthroplasty. T he r ole o f pol yethylene w ear debr is and co ncept o f e ffective j oint space. *J Bone Joint Surg* 74-A: 849-863, 1992.

Schmalzried T , G uttman D , G recula M , A mstutz H C: T he r elationship between t he design, posi tion, an d ar ticular w ear of ac etabular co mponents i nserted w ithout cement and the development of pelvic osteolysis. *J Bone Joint Surg* 76-A: 677-688, 1994.

Schmalzried T , Akizuki KH, F edenko AN, Mirra J: The role of access of joint fluid to bone in periarticular osteolysis. A report of four cases. *J Bone Joint Surg* 79-A: 447-452, 1997.

Schmalzried T , B roun I, A mstutz H , E ngh C , H arris W: The r ole o f ace tabular component screw holes and/or screws in the development of pelvic osteolysis. *Proc Inst Mech Eng* 213: 147-153, 1999.

Schwarz EM, C ampbell D , T otterman S , B oyd A , O 'Keefe R J, L ooney R J, Looney RJ: U se of volumetric computerizied tomography as a primary outcome measure to

evaluate drug efficacy in the prevention of peri-prosthetic osteolysis: a 1-year clinical pilot of etanercept vs. placebo. *J Orthop Res* 21 (6): 1049-55, 2003.

Shirkhoda A, Brashear H, Staab E: Computed tomography of acetabular fractures. *Radiology* 134: 683–688, 1980.

Smith S, Fehring T, Braun E: Liner motion in modular acetabular components: a comparative study. *J Arthroplasty* 11: 230-237, 1996.

Soto MO, Rodriguez JA, Ranawat CS: Clinical and radiographic evaluation of the Harris-Galante cup: incidence of wear and osteolysis at 7 to 9 years follow–up. *J Arthroplasty* 15: 139-145, 2000.

Stamenkov R, Howie D, Taylor J, Findlay D, McGee M, Kourlis G, Carbone A, Burwell M: Measurement of bone defects adjacent to acetabular components of hip replacement. *Clin Orthop Relat Res* 412: 117-124, 2003.

Swedish Hip Arthroplasty Register. An Report, 2006. (http://www.jru.orthop.gu.se).

Takagi M, Santavitra S, Ida H, Ishii M, Takei I, Niissalo S, Ogino T, Konttinen YT: High-turnover periprosthetic bone remodelling and immature bone formation around loose cemented total hip joints. *J Bone Miner Res* 16 (1): 79-88, 2001.

Thanner J, Karrholm J, Malchau H, and Herberts P: Poor outcome of PCA and Harris-Galante hip prostheses. Randomised study of 171 arthroplasties with 9-year follow-up. *Acta Orthop Scand* 70: 155-162, 1999.

Thompson MW, McInnes RR, Willard HF: Genetics in medicine. 5th ed. Philadelphia: Thompson & Thompson, 1991.

Vernon-Roberts B, Freeman MAR: The tissue response to total joint replacement prostheses. In: Swanson SAV, Freeman MAR, eds. The scientific basis of joint replacement. London: Pitman Medical: 86-129, 1997.

Walde TA, Weland DE, Leung SB, Kitamura N, Sychterz CJ, Engh CA Jr, Claus AM, Potter HG, Engh CA Sr: Comparison of CT, MRI and radiographs in assessing pelvic osteolysis: a cadaveric study. *Clin Orthop Relat Res* 437: 138-144, 2005.

Wan Z, Dorr LD: Natural history of femoral focal osteolysis with proximal ingrowth smooth stem implant. *J Arthroplasty* 11: 718-725, 1996.

Wang G, Frei T, Vannier MW: Fast iterative algorithm for metal artifact reduction in x-ray CT. *Acta Radiol* 7: 607–614, 2000.

Wellings RM, Davies AM, Pyncent PB, Carter SR, Grimer RJ: The value of computed tomographic measurements in osteosarcoma as a predictor of response to adjuvant chemotherapy. *Clin Radiol* 49: 19-23, 1994.

Willert HG, Semlitsch M: Reactions of the articular capsule to wear products of artifitial joint prostheses. *J Biomed Mater Res* 11: 157-164, 1997.

Willert HG, Buchhorn GH, Hess T: The significance of wear and material fatigue in loosening of hip prostheses. *Orthopaede* 18: 350-369, 1989.

Xenos JS, Hopkinson WJ, Callagan JJ: Osteolysis around an uncemented cobalt chrome total hip arthroplasty. *Clin Orthop* 317: 29-36, 1995.

Xenos JS, Callaghan JJ, Heekin RD: The porous coated anatomic total hip prosthesis, inserted without cement: a prospective study with a minimum of ten years of follow up. *J Bone Joint Surg* 81-A: 74-80, 1999.

Yasuda H, Shima N, Nakagawa N, Yamaguchi K, Kinosaki M, Mochizuki S, Tomoyasu A, Yano K, Goto M, Murakami A, Tsuda E, Morinaga T, Higashio K, Udagawa N, Takahashi N, Suda T: Osteoclast differentiation factor is a ligand for osteoprotegerin/osteoclastogenesis-inhibitory factor and is identical to TRANCE/RANKL. *Proc Natl Acad Sci USA* 95 (7): 3597-3602, 1998.

Young J, Resnik C: Fracture of the pelvis: current concepts of classification. *Am J Radiol* 155: 1169–1175, 1990.

Zicat B, Engh CE, Gokcen E: Patterns of osteolysis around total hip replacements inserted with and without cement. *J Bone Joint Surg* 77-A: 432-439, 1995.

Zimlich RH, Fehring TK: Underestimation of pelvic osteolysis: the value of the iliac oblique radiograph. *J Arthroplasty* 6: 796-801, 2000.